Mathematical Modeling of *Neisseria meningitidis*: A Case Study of Nigeria

©2019

Mayowa Micheal Ojo

B.Tech. Mathematics, Ladoke Akintola University of Technology, 2015

Submitted to the graduate degree program in Ecology and Evolutionary Biology and the Graduate Faculty of the University of Kansas in partial fulfillment of the requirements for the degree of Master of Arts.

Folashade B. Agusto, Chairperson

Committee members

Maria E. Orive, Co-Chair

A. Townsend Peterson

Daniel Reuman

Date defended: December 09, 2019

The thesis committee for Mayowa Micheal Ojo certifies
that this is the approved version of the following thesis:

Mathematical Modeling of *Neisseria meningitidis*:
A Case Study of Nigeria

Folashade B. Agusto, Chairperson

Maria E. Orive, Co-Chair

Date approved: December 16, 2019

Abstract

Bacterial meningitis remains one of the deadliest infectious diseases in the African meningitis belt. It is defined as an acute inflammation of the meninges, the protective membranes that cover the brain and spinal cord. This deadly disease has different serogroups with geographical distribution and epidemic potential varying amongst each serogroup. To date, six of these serogroups have been identified as causative agents of epidemics. The effect of this disease cannot be ignored due to its high morbidity and mortality; however, vaccination has played a major role in preventing the spread of the disease in the population. The work presented here was therefore designed to study the effect of constant and pulse vaccination in controlling the disease in the population using a non-impulsive model and an impulsive models. The two models were analyzed qualitatively to determine the conditions for eradicating the disease. Numerical simulation of the non-impulsive model showed that meningitis can be effectively controlled in the population using an imperfect vaccine with an efficacy greater than 75% and high vaccine coverage rate of at least 85%. For the impulsive model, we obtain the disease-free periodic solution, and the model is locally asymptotically stable when the threshold quantity, $\mathcal{R}_p$, is less than one. Furthermore, numerical simulations showed that final infected population size is lower when applying the impulsive vaccination strategy compared with the scenario without vaccination. Thus, disease burden in the population decreases with increasing vaccination pulses. Lastly, we present a deterministic model to study the dynamics of co-infection of multiple strains (serogroup A and serogroup C) in the presence of vaccination. For the scenario in which we set the transmission probability of a strain to zero, our results show that the co-infection model exhibits competitive exclusion (a strain driving the other strain into extinction when both are at endemic equilibrium). However, for the scenario in which we set the transmission probability of one strain greater than

that of the other (transmission probability of neither strain is equal to zero), we observed a trade-off mechanism which enables co-existence of the two strains. In this case, regardless of the greatest reproduction number value of each strain, the strain with the highest transmission probability in co-infected individuals will dominate in the population without driving the other strain into extinction. We further analyzed and simulated the model without co-infection. The model exhibit competitive exclusion when $\mathcal{R}_{0A} > \mathcal{R}_{0C} > 1$ (strain A drives out strain C) or when $\mathcal{R}_{0C} > \mathcal{R}_{0A} > 1$ (strain C drives out strain A). Additionally, our results show that when the two strains have the same reproduction number at their endemic state, the two strains will co-exist but the dominance of a strain will depend on the initial size of its population.

Acknowledgements

My deep gratitude goes to Him who is able to do exceedingly abundantly above all that we ask or think, according to the power that worketh in us. I am grateful to God for sustaining me this far, no one can replace His place in my life.

Special thanks goes to my supervisors Professor Folashade B. Agusto and Maria E. Orive, without whom this thesis wouldn't exist. Thank you for your endless supports, tremendous contributions, and for providing me with abundant help. I will also like to appreciate my committee members, Professor A. Townsend Peterson and Daniel Reuman for making themselves available always. Your contributions, advice and mentorship is immeasurable.

My sincere appreciation goes to all the staffs and faculty members of the department of Ecology and Evolutionary Biology for their supports throughout my program. Special thanks to Professor Paulyn Cartwright for her continous supports and encouragements. Also, I want to say a big thanks to Ms. Aagje Ashe for her continous help. My sincerest gratitude goes to my fellow graduate students for making this season a memorable one for me. Special thanks to Rebekah and Richard Wagner, Benjamin Kerbs for their encouragements and for all the fun moments we had together, you are more than just a friend to me.

I am grateful to all who God has placed in my life as a support. Thanks to Professor F. O Akinpelu for your role as a mentor and mother in my life. I appreciate all my Professors back home in Nigeria, Professor Daniel Okuonghae, B. Gbadamosi, S. Olaniyi and R. Oderinu. I thank the Ninth Street Missionary Baptist Church members for their supports, prayers and encouragements. Specially, I say thank you to Pastor Dr. Eric Galbreath for his spiritual guidance and mentoship, indeed this is my home far away from home. I must say thank you

to the family of Mr and Mrs Monroe, Aunty Rita and Bolin William for their continous love, and thanks for making me part of the loving family.

Finally, this acknowledgement will be incomplete if I don't appreciate those that have been, and will forever be part of my life. I am grateful to my parents, Mr. James Ojo and my dearest mother Mrs. Yemisi Ojo, for their prayers, advice, and continous supports in every stage of my life. My prayer is that, you will live long with good health to eat the fruit of your labor. Also, to all my seven siblings, words cannot express how grateful I am for having you all. You are the best!. Big thanks goes to my fiancée Latavia Hill, for her continous supports, advice and deeper understanding of who I am. I am grateful to all God has sent to me through you all, I say thank you all for believing in me.

Contents

List of Figures

List of Tables

Chapter 1

General Introduction

1.1 Background

A disease is an abnormal condition that negatively affects the structure or function of an organism. Diseases can be caused by pathogens or by internal dysfunctions. In humans, disease often refers to any condition that causes pain, distress, dysfunction or death to the person affected. Diseases can be classified into two main types: infectious or non-infectious diseases (World Health Organization, 2018a). The focus of my work is on the modeling of infectious diseases. Infectious diseases, also known as transmissible diseases, are diseases caused by microorganisms such as bacteria, viruses, fungi or parasites. Infectious diseases can be spread directly or indirectly from one person to another. Various types of infectious diseases include but are not limited to meningitis, influenza, malaria, measles, tuberculosis, and human immunodeficiency virus / acquired immunodeficiency syndrome (HIV/AIDS).

Infectious diseases are a leading cause of illness and death worldwide. Globally, infections cause over a fifth of all deaths and a quarter of all illnesses, and this has a high burden on poorer communities and poor countries (Bartlett et al., 2006). Developing models of infectious disease transmission and dynamics is important in order to further enhance our understanding of the mechanisms by which diseases spread and also to predict the future course of an outbreak. In addition, developing such models allows us to test our understanding of the disease epidemiology (incidence, distribution, and control of the disease) by comparing different model results and observed patterns, since the formulation of transmission models are based on the current understanding of the natural history of infection and

immunity against the disease (Huppert & Katriel, 2013; May, 2004).

1.1.1 Meningitis

Meningitis is a devastating disease which remains a major public health challenge (World Health Organization, 2018b). It is defined as an acute inflammation (swelling) of the protective membrane which covers the brain and spinal cord collectively known as the meninges (Centers for Disease Control and Prevention (CDC), 2017; Merck Manual, 2018; Sáez-Llorens & McCracken Jr, 2003). This deadly disease can be caused by an infection with various microorganisms such as bacteria, viruses, fungi, or protozoa. In addition, it may also result from various non-infectious causes, such as cancers, certain medicines, head injury and brain surgery (Centers for Disease Control and Prevention (CDC), 2017; Ginsberg, 2004; Gleissner & Chamberlain, 2006; Mayo Clinic, 2018; Merck Manual, 2018). However, the highest global burden among all these causes arises from bacterial meningitis (World Health Organization, 2018b). Bacterial meningitis is of significant public health importance because of its high morbidity and mortality globally and it can give rise to epidemics depending on the type of bacteria causing the disease (Oordt-Speets et al., 2018). As reported by Oordt-Speets et al. (2018), bacterial meningitis can be fatal in 50% of cases if untreated. Even when diagnosed early and treated adequately, $8-15\%$ of patients die, typically within 24 and 48 hours of symptom onset. Furthermore, $10-20\%$ of the survivors are prone to permanent sequelae (a condition which is the consequence of a previous disease or injury); these include brain damage, hearing loss, and learning disabilities.

Bacterial meningitis can be caused by several different types of bacteria. These include *Haemophilus influenzae (H. influenzae)*, *Streptococcus pneumoniae (S. pneumonia)*, *Listeria monocytogenes (L. monocytogenes)*, Group B *Streptococcus*, and *Neisseria meningitidis (N. meningitidis)*. Among all these types of bacteria, *N. meningitidis* is responsible for causing meningococcal meningitis (Centers for Disease Control and Prevention (CDC), 2019; Rouphael & Stephens, 2012; World Health Organization (WHO), 2018). The agents respon-

sible for bacteria meningitis vary by age group. Among neonates (new born children), most cases of bacterial meningitis are due to Group B *Streptococcus* and *L. monocytogenes*, while most cases in children and adults are caused by *Streptococcus pneumoniae* and *Neisseria meningitidis* (Brouwer et al., 2010; Oordt-Speets et al., 2018). Three predominant bacterial types are responsible for more than 70% of bacterial meningitis cases, namely, *Neisseria meningitidis*, *Haemophilus influenzae* and *Streptococcus pneumoniae* (Centre for Disease Control, 2019). In this study, our focus will be on meningococcal meningitis.

1.1.2 Meningococcal Meningitis

Meningococcal meningitis caused by *N. meningitidis* bacteria is of public health importance because of its potential to cause large epidemics. *N. meningitidis* has 12 different serogroups, out of which six have been identified as capable of causing an epidemic (serogroups A, B, C, W, X and Y) (Rouphael & Stephens, 2012; World Health Organization (WHO), 2018). It is important to note that geographical distribution and epidemic potential differs according to each serogroup. Chapter 3 of this thesis will discuss this further.

N. meningitidis can only be found in humans and can be transmitted between humans through throat secretions from carriers (people who carry the bacterial in their throat or nose but are not showing symptoms) (Agier et al., 2017; Tartof et al., 2013). Close and prolonged contact such as kissing, sneezing or coughing on someone facilitates the spread of the disease. The incubation period ranges between 2 to 10 days (World Health Organization (WHO), 2018). Symptoms of infections include fever, headache, appearance of rashes and neck stiffness; if not properly managed, complications can result in deafness, vomiting, inability to tolerate light and noise, and epilepsy (Van de Beek et al., 2006; World Health Organization (WHO), 2018). Meningococcal meningitis is treatable with antibiotics such as penicillin, ampicillin and ceftriaxone (World Health Organization (WHO), 2018); it is also preventable via vaccination and chemoprophylaxis (World Health Organization (WHO), 2018, 2019b).

Figure 1.1: The meningitis belt of Africa (World Health Organization, 2018b), show the regions in the sub-Saharan Africa, with the highest rate of incidence of meningitis

Meningococcal meningitis disease was first reported in the 16^{th} century and it was discovered in Switzerland Geneva by physician Gaspard Vieusseux, in the year 1805. Anton Weichselbaum, an Austrian pathologist and bacteriologist first identified the bacterium in the spinal fluid of a patients in 1887 Greenwood (2006); Rouphael & Stephens (2012). Identification of the disease has increased globally over the years. Meningococcal meningitis is distributed globally with the highest burden in the meningitis belt of Africa, which stretches from Senegal to Ethiopia (Agier et al., 2017; Molesworth et al., 2002; Tartof et al., 2013) (see Figure 1.1). During the dry season in this region between December to June, there is always an increase in the risk of meningococcal disease due to damage of the nasopharyngeal mucosa by dust winds, cold weather and upper respiratory tract infections. In addition to these, increased transmission of *N. meningitidis* may be caused by overcrowded housing. These factors explain the large epidemics which occur during the dry season in the meningitis belt of Africa (World Health Organization (WHO), 2019b).

1.1.3 Literature Review

Modeling of infectious diseases

In the field of epidemiology, researchers have employed the use of mathematical modeling to successfully reproduce the observed incidence and prevalence of many diseases, including meningitis (Weston et al., 2018). Mathematical models allow us to infer the dynamics of an outbreak from the current information, to forecast the future and, most importantly, to measure the uncertainty in these predictions. In addition, mathematical models have played a very significant role in understanding the dynamics of infectious diseases with the major role of better exploring the effect of control strategies to mitigate diseases.

Daniel Bernoulli, a trained physician, was the first to utilize mathematical modeling for the spread of a disease. In 1766, he created a mathematical model to analyze mortality due to smallpox in England, which at that time was 1 in 14 infected individuals. This study showed that inoculation against the virus would increase the life expectancy at birth by about three years (Hethcote, 2000; Siettos & Russo, 2013).

Following Bernoulli, many physicians have contributed to modern mathematical epidemiology, such as Lambert and Laplace in 1772, who followed up the work of Bernoulli by extending his model to incorporate age-dependent parameters (Lambert, 1772; Laplace, 1812; Siettos & Russo, 2013). However, as mentioned by Siettos & Russo (2013), modeling of infectious disease had not been developed systematically until the paper of Ross in 1911 which established modern mathematical epidemiology (Wiratsudakul et al., 2016). Ross utilized the mechanistic modeling approach using a set of differential equations to estimate the discrete-time dynamics of malaria through mosquito-borne pathogen transmission (Smith et al., 2012). After the work of Ross, the number of models developed to describe the spread of disease in populations has been rapidly increasing. Among the most acclaimed of these were McKendrick and Kermack, whose paper titled *"A contribution to the Mathematical Theory of Epidemics"* published in 1927, founded deterministic compartmental epidemic

modeling (Kermack & McKendrick, 1927, 1932, 1933). Models in which the values of the dependent variables of the system are determined by the parameters of the model are called deterministic model. The authors present a simple deterministic compartmental model which successfully mimics the dynamics of many recorded epidemics (Brauer et al., 2001).

Over the years, mathematicians, biologists, physicians, epidemiologists, and others have contributed to the maturing discipline of mathematical epidemiology. This includes the use of a mathematical modeling approach in studying the effect of different control measures such as vaccination, treatments, and isolation, just to mention a few, on eradicating disease in the population. Numerous researchers have explored different methodologies and several approaches have been proposed for studying and answering different questions on the dynamics of diseases. As mentioned by Siettos & Russo (2013), these encompass three general categories of mathematical models, namely: (1) statistical methods for surveillance of outbreaks and identification of spatial patterns in real epidemics, (2) mathematical models within the context of dynamical systems (also called state-space models) used to forecast the evolution of a "hypothetical" or on-going epidemic spread, and (3) machine learning or expert methods for the forecasting of the evolution of an ongoing epidemic (Siettos & Russo, 2013). The above three categories also have different sub-models which have been used by many researchers in various studies. For instance, sub-models of state-space models include deterministics models, stochastic models, complex networked models and agent-based models (Siettos & Russo, 2013).

In this thesis, I focus on the use of deterministic models. These describe the dynamics of epidemics within human populations. Generally, deterministic models have been used in various epidemiological studies, including models with age-structures where the population is stratified into age groups in order to investigate the effect of control measures on the most infected groups in the population (Agusto et al., 2016; Del Valle et al., 2013; Forouzannia & Gumel, 2014; Hogan et al., 2016; Zibolenová et al., 2016). Also, some studies have explored the use of deterministic models in investigating the dynamics of co-infection of different dis-

eases such as tuberculosis - HIV, malaria-HIV, malaria-meningitis, to mention a few (Aldila & Agustin, 2018; Awoke & Kassa, 2018; Mutua et al., 2015; Osman & Makinde, 2018; Slater et al., 2013). In addition, co-infection of multiple strains of the same pathogen has been studied using deterministic models, for example Agyingi et al. (2016); Ahn et al. (2014); Garmer et al. (2015); Orwa et al. (2019); Qiu et al. (2013). The next sub-section focuses specifically on a review of the literature for the mathematical modeling of meningitis.

Modeling of Meningitis

Mathematical models have helped in understanding the spread and control of many infectious diseases, including meningitis. Over the years, many researchers have worked on the deadly disease *Neisseria meningitidis*, using various approaches to explore disease dynamics and the control measure suitable for mitigating the disease in populations. I focus here on a few examples of these studies.

Irving et al. (2012) employed deterministic compartmental models to investigate how well simple compartmental models can qualitatively capture the patterns of disease observed in the meningitis belt of Africa. Their results showed that seasonal variation of transmission is capable of accounting for the complex and irregular epidemics of meningococcal meningitis. This indicates that the frequent but irregular epidemics could be the result of interaction between temporary immunity and seasonal variation in disease transmissibility. In addition, their results suggest that population immunity is an important factor to include in models trying to predict meningitis epidemics.

Another study of the dynamics of meningococcal meningitis in this region is that of Broutin et al. (2007). The authors present a comparative study of the dynamics of meningococcal meningitis across nine African countries, by utilizing some mathematical tools to time series analysis and wavelet method to better understand meningococcal meningitis evolution in time and space. Their results highlight the strong interest and the necessity of a global survey of meningococcal meningitis in order to predict and prevent large epidemics by adapted

vaccination strategy. In addition, they further suggest the possibility of controlling the infectious disease by international cooperation in public health and cross disciplinary studies.

An age-structured deterministic model was formulated by Martcheva & Crispino-O'Connell (2003), to better understand the dynamics of meningococcal infection. The authors used the model to study the conditions for the stability of the disease-free steady state which implies an extinction of the disease in the population. They further established the condition for the existence of an endemic state (the persistence of a disease in a given population). The study results are applied to identify the contribution of the carriers to the transmission of meningococcal disease in the population. Similarly, Coen et al. (2000) employed deterministic compartmental models to fit age-structured data sets of nasopharyngeal carriage of meningococci, *Neisseria lactamica* (LC) and meningococcal disease. Their results show that the model most consistent with the available data sets is the one where LC inhibits meningococcal disease. This model is also consistent with the hypothesis that *Neisseria lactamica* acts as a natural immunogen against meningococcal disease.

Deterministic modeling has also been used in studying the effect of control measures for mitigating diseases in a given population. Among many other studies is a study by Asamoah et al. (2018). The authors presents a nonlinear deterministic model with time-dependent controls to describe the dynamics of bacteria meningitis in a population. Their results show that carrier individuals have a higher chance of spreading the infection than infected individuals with clinical symptoms because of restriction to bed during the acute phase of infection. In addition, numerical simulation of their optimal control problem demonstrates that combination of both vaccination and other intervention such as treatment and public health education are the best control strategies to control bacterial meningitis in the population. Similarly, Agusto & Leite (2019) presents a deterministic model for *Neisseria meningitidis* with an imperfect vaccine. In this study, sensitivity analysis suggests facial masks and vaccination as the parameters whose variability has the strongest impact on the disease reproduction number (the number of cases one infected individual generates on av-

erage over the course of the infectious period in a susceptible population). Using these two parameters as time-dependent control variables, Agusto & Leite (2019) shows that the two controls prevent more infections at low costs. In addition, their results show an inverse relationship between the use of facial masks and vaccine (meaning that, when the use of vaccine is high, the use of facial masks is low and vice versa).

Miller & Shahab (2005) carried out a review on the cost effectiveness of immunization strategies for the control of epidemic meningococcal meningitis. They access seven economic studies on the use of polysaccharide vaccination strategies in order to highlight the relevant epidemiological and economical issues surrounding the decisions for their use. Five of the seven studies were based in Africa, the region with the highest annual incidence rates. Their studies established that vaccination against meningococcal disease during outbreaks is suboptimal due to inability to rapidly immunize populations in the poor areas. Their results further show that economic analyses of mass immunization campaigns and routine vaccination suggest that routine use of meningococcal vaccines for preventive strategies could be within the range of cost-effective public health interventions in areas where the disease is endemic.

Among many studies that have considered the use of vaccination in controlling *Neisseria meningitidis*, to the best of our knowledge no studies have explored the use of pulse vaccination in the eradication of this disease in the population. Pulse vaccination strategy involves repeated vaccination at specific times of at-risk groups of certain age in order to eradicate an epidemic (Gao et al., 2006b; Nokes & Swinton, 1995, 1997). Over the years, this is gaining prominence as a strategy for the elimination of childhood viral infectious diseases such as parotitis, smallpox, measles, hepatitis and phthisis (Agur et al., 1993; Ramsay et al., 1994; Shulgin et al., 1998; Zou et al., 2009). Pulse vaccination remains an effective way of controlling the transmission of diseases with some practical advantages, (Agur et al., 1993; d'Onofrio, 2005; Gao & Chen, 2005; Shulgin et al., 1998; Stone et al., 2000; Zou et al., 2009). For example, the use of annual immunization days was found to be successful in eradicat-

ing measles in the Gambia between the year 1967 and 1972 (Moneim & Greenhalgh, 2005; Williams & Hull, 1983). South and Central America have successfully applied pulse vaccination strategy to poliomyelitis (Moneim & Greenhalgh, 2005; Sabin, 1991), and this method is now used in Brazil and is easier to arrange and more effective than constant vaccination strategy (Moneim & Greenhalgh, 2005). Pulse vaccination is sometimes more effective than constant vaccination (Li & Yang, 2011; Li & Cui, 2009; Röst & Vizi, 2014; Shulgin et al., 1998), hence our goal in this thesis include the investigation of the dynamics of an impulsive model with pulse vaccination. Impulsive models are models which allows impulsive effects such as time delay. Chapter two of this thesis focuses on the use of an impulsive model in studying the effect of pulse vaccination in controlling meningitis in the population. To the best of our knowledge, this study is the first work to consider pulse vaccination strategy on meningitis in Nigeria.

A study by Maseno (2011) developed a mathematical model to study the dynamic behavior of malaria-meningitis co-infection among children under the age of five years, with an assumption of no simultaneous infection of host with the two diseases. Their results deduce that a reduction in malaria infection cases would reduce the number of new co-infection cases.

While several studies such as that by Maseno (2011) have been done on co-infection of other diseases, no work has been done on the modeling of multiple strains of *Neisseria meningitidis* in Nigeria. Due to the existence of multiple invasive strains in the meningitis belt of Africa, we develop a mathematical model to study the dynamic of multiple strain in the presence of vaccination. This is presented in the third chapter of this thesis.

1.1.4 Research Aim and Objectives

The main aim of this thesis is to study the effect of vaccination in controlling meningitis, specifically utilizing data from Nigeria to parameterize the model. This includes the role of

vaccination in the strain replacement of meningitis A by meningitis C in Nigeria. To help us achieve the main aim of this study, the following objectives were sought:

(i) To study the effect of constant and pulse vaccination in controlling meningitis using an ordinary differential equation model (which we will refer to as the non-impulsive model) and an impulsive differential equation model (which we will refer to as the impulsive model). We use the non-impulsive model to study the effect of vaccination when a fixed proportion of the susceptible individuals are vaccinated, while the impulsive model is used when vaccination is administered impulsively at other regular or irregular times.

(ii) To study the dynamics of meningitis A and meningitis C in the presence of vaccination under different scenarios. The scenarios considered in this thesis include the more generalized model with co-infected individuals of strain A and C. Since there is no data on the ability of individuals to be infected with the two strain at the same time, we consider the case whereby assumed co-infected individuals can only transmit the strain with the highest transmission probability. Also, we considered the model without individuals co-infected with the two strains.

1.1.5 Research questions

The above aim and objectives are channeled to answer the following questions:

(i) What are the conditions for controlling meningitis in the population, in the presence of imperfect vaccine (Chapter 2) ?.

(ii) In the presence of multiple strains (serogroup A and serogroup C) in the population, does competitive exclusion occur (will a strain drive out the other strain when both are endemic) (Chapter 3) ?

(iii) Under what conditions will the two strains co-exist (if there is co-existence of strain A and strain C in the population), and which strain will dominate in the presence of

co-existence of the two strains (Chapter 3) ?

Chapter 2

Modeling the Effect of Vaccination on *Neisseria meningitidis* in Nigeria

2.1 Introduction

Meningitis is an acute inflammation of the protective membrane covering the spinal cord and the brain which is collectively known as the meninges (Centers for Disease Control and Prevention (CDC), 2017; Sáez-Llorens & McCracken Jr, 2003). Meningitis is caused by an infection with microorganisms such as bacteria, viruses, fungi and protozoa and it may also result from various non-infectious causes (Centers for Disease Control and Prevention (CDC), 2017; Ginsberg, 2004; Gleissner & Chamberlain, 2006; Mayo Clinic, 2018). Several different bacteria are capable of causing meningitis, these include *Neisseria meningitidis* which causes Meningococcal Meningitis (Rouphael & Stephens, 2012; World Health Organization (WHO), 2018). *N. meningitidis* has 12 different serotypes, out of which six has been identified capable of causing an epidemic namely serotypes A, B, C, W, X and Y (Rouphael & Stephens, 2012; World Health Organization (WHO), 2018).

N. meningitidis can only be found in humans, and can be transmitted from human to human through throat secretions from carriers (people who carry the bacterial in their throat or nose but are not showing symptoms) (Agier et al., 2017; Tartof et al., 2013). Also, close and prolonged contact such as kissing, sneezing or coughing on someone, facilitates the spread of the disease. The incubation period ranges between 2 to 10 days (World Health Organization (WHO), 2018). The symptoms are often characterized by fever, headache, appearance of

rashes and neck stiffness, but if not properly managed, complications can result in deafness, vomiting, inability to tolerate light and noise and epilepsy (Van de Beek et al., 2006; World Health Organization (WHO), 2018). Meningococcal meningitis is treatable with antibiotics such as penicillin, ampicillin and ceftriaxone (World Health Organization (WHO), 2018); it is also preventable *via* vaccination and chemoprophylaxis (World Health Organization (WHO), 2018).

The first outbreak of meningococcal meningitis was discovered in Switzerland Geneva in 1805 (Greenwood, 2006; Rouphael & Stephens, 2012). The disease has since spread globally with the highest burden in the meningitis belt in Africa, which stretches from Senegal to Ethiopia (Agier et al., 2017; Molesworth et al., 2002; Tartof et al., 2013). The disease outbreaks usually occur during dry season with no rain; in Nigeria, outbreaks occur during the Harmanttan season when dry wind from the Sahara Desert blows downward to the Gulf of Guinea. However disease incidence often declines with the onset of rains in the raining season (Agier et al., 2013; Moore, 1992). Between January 1996 to June 1996 a severe meningitis A outbreak occurred in Nigeria with 109,580 cases and 11,717 deaths, with 10.69% case fatality rate (World Health Organization (WHO), 2017). Since 2010 Nigeria has been carrying out mass immunization campaigns with MenAfriVac against meningitis A serogroup. However, since 2013 Nigeria has been experiencing large outbreaks of meningitis C. In 2015, over 2500 cases of the disease were reported in the country (World Health Organization (WHO), 2017). Another outbreak occurred in 2017 in Nigeria with over 9,902 cases and 602 deaths (Nigeria Centre for Disease Control (NCDC), 2017).

Early detection of cases and emergency mass vaccination of the population have been the approach for controlling meningitis epidemic (LaForce et al., 2007). Provision of vaccine against this disease has been shown to be effective in preventing the disease in adult and children. There are two types of vaccine currently used in Africa, these are conjugate and polysaccharide vaccines. The conjugate vaccines are used for routine immunization schedules, preventive campaign and outbreak response (World Health Organization (WHO), 2018).

These type of vaccine include monovalent A, monovalent C and tetravalent A, C, Y, W. Conjugate vaccines confer long-lasting immunity, they prevent carriage and also induce herd immunity (World Health Organization (WHO), 2018). Polysaccharide vaccines on the other hand are either bivalent which prevents against (serogroups A and C), trivalent vaccine which prevents against (serogroups A, C, and W) or a tetravalent vaccine which prevents against (serogroups A, C, Y, and W) (World Health Organization (WHO), 2018). They have been available and in use since the 1970s (Centers for Disease Control and Prevention and others, 2012) and they have limited efficacy (LaForce et al., 2007; Reingold et al., 1985) they do not decrease carriage and they do not confer herd immunity (Hassan-King et al., 1988; LaForce et al., 2007). Recently, a first-in-man phase 1 single-centre, double-blind, randomised, controlled study in healthy adults was carried out to assess the effects of NmCV-5 pentavalent meningococcal conjugate vaccine which targets the A, C, Y, W, and X serogroups (Chen et al., 2018).

In this study, we present a mathematical model to study the effect of constant and pulse vaccination in controlling meningitis in the population using an ordinary differential equation and an impulsive differential equation respectively. Pulse vaccination strategy involves repeated vaccination at specific times of at risk groups say of certain age in order to eradicate an epidemic (Gao et al., 2006a; Nokes & Swinton, 1995, 1997). This is gaining prominence as a strategy for the elimination of childhood viral infectious diseases such as parotitis, smallpox, measles, hepatitis and phthisis (Agur et al., 1993; Ramsay et al., 1994; Shulgin et al., 1998; Zou et al., 2009).

Pulse vaccination remains an effective way of controlling the transmission of diseases with some practical advantages (Agur et al., 1993; d'Onofrio, 2005; Gao & Chen, 2005; Shulgin et al., 1998; Stone et al., 2000; Zou et al., 2009). For instance, the use of annual immunization days was found to be successful in eradicating measles in the Gambia between 1967 and 1972 (Moneim & Greenhalgh, 2005; Williams & Hull, 1983). South and Central America have

successfully applied pulse vaccination strategy to poliomyelitis (Moneim & Greenhalgh, 2005; Sabin, 1991), and this method is now used in Brazil and is easier to arrange and more effective than constant vaccination strategy (Moneim & Greenhalgh, 2005). Pulse vaccination has been used in Africa recently although with only partial success (Moneim & Greenhalgh, 2005). Pulse vaccination sometimes is more effective than constant vaccination (Li & Yang, 2011; Li & Cui, 2009; Röst & Vizi, 2014; Shulgin et al., 1998) hence our goal in this chapter is to investigate the dynamics of the impulsive model with pulse vaccination. To the best of our knowledge, this study is the first work to consider pulse vaccination strategy on meningitis in Nigeria.

This chapter is organized as follows: the model formulation with constant vaccination strategy is presented in Section 2.2. In Section 2.3, we analyze the stability of model with constant vaccination and determined the reproduction number. The sensitivity analysis of the model with constant vaccination is investigated in Section 2.3.4. The impulsive model, existence of a periodic solution, and the stability of the model are presented in Section 2.4. We illustrate the result of the impulsive model using numerical simulations in Section 2.5. The results of the study are discussed in Section 2.6.

2.2 Formulation of model with constant vaccination

First, we study the effect of constant vaccination strategy using the *N. meningitidis* model developed by Agusto & Leite (2019). The population is divided into Susceptible (S), Vaccinated (V), Carrier (C), Infected (I), and Recovered (R) classes, where the total population is given as

$$N = S + V + C + I + R.$$

Nigeria is Africa's most populous country. The Nigerian population since the 1950s has been trending exponentially up due to very high birth rates Wikipedia (2019). The susceptible class is populated by birth at rate πN since the population is growing exponentially. Alos,

the population increase in number by vaccine waning at rate ω from the vaccinated class, and by loss of immunity of the recovered individuals at the rate κ. The susceptible population is reduced by natural death at rate μ, by constant vaccination to the vaccinated class at rate ν and by infection to the carrier class λ. The quantity λ is the infection function of the susceptible by both carrier and infected classes and it is given as

$$\lambda = \frac{\beta(\eta C + I)}{N}.$$

Hence, the rate of change of the susceptible population at any time t is given as:

$$\frac{dS}{dt} = \pi N + \omega V + \kappa R - \lambda S - (\nu + \mu)S. \tag{2.1}$$

The vaccinated population is obtained as a result of vaccination of the susceptible class at a rate ν. Although, there are various types of vaccine, namely conjugate, polysaccharide, and pentavalent (in trial) vaccines with different efficacy and waning, we assume in this study a generic vaccine with generic efficacy and waning since all the vaccines protect the population with different efficacies and waning which our model is able to capture by using the appropriate values for the parameters corresponding to vaccine efficacy and vaccine waning. However, since the vaccine is imperfect, a fraction $(1 - \varepsilon)$ of the vaccinated class is infected, where ε is the vaccine efficacy. $\varepsilon = 1$ implies the vaccine is 100% effective at preventing infection. Therefore, the vaccinated class is depopulated *via* natural death at rate μ and as a result of vaccine waning at rate ω. Thus, the vaccinated population is as follows

$$\frac{dV}{dt} = \nu S - (1 - \varepsilon)\lambda V - (\omega + \mu)V. \tag{2.2}$$

Carrier class derived its population from infection coming from both susceptible and vaccinated classes and depopulated by disease progression to the infected class at rate σ, by

recovery to the recovered class at rate γ_C, and by natural death at rate μ. The carrier population is given below as

$$\frac{dC}{dt} = \lambda S + (1-\varepsilon)\lambda V - (\sigma + \gamma_C + \mu)C. \tag{2.3}$$

The infected population is generated following the progression from the carrier class. This class is reduced by recovery at rate γ_I to the recovered class, by natural death at rate μ, and by death resulting from complication of infection at rate δ. The infected population is given as

$$\frac{dI}{dt} = \sigma C - (\gamma_I + \mu + \delta)I. \tag{2.4}$$

The recovered class gets its population as a result of recoveries from both carrier and infected classes at rate γ_C and γ_I respectively. Depopulation of this class result from loss of immunity at rate κ and by natural death at rate μ. The recovered population is given as

$$\frac{dR}{dt} = \gamma_C C + \gamma_I I - (\mu + \kappa)R. \tag{2.5}$$

The overall processes explained above transforms into the following systems of ordinary differential equation given as:

$$\begin{aligned}
\frac{dS}{dt} &= \pi N + \omega V + \kappa R - \lambda S - (\nu + \mu)S \\
\frac{dV}{dt} &= \nu S - (1-\varepsilon)\lambda V - (\omega + \mu)V \\
\frac{dC}{dt} &= \lambda S + (1-\varepsilon)\lambda V - (\sigma + \gamma_C + \mu)C \\
\frac{dI}{dt} &= \sigma C - (\gamma_I + \mu + \delta)I \\
\frac{dR}{dt} &= \gamma_C C + \gamma_I I - (\mu + \kappa)R.
\end{aligned} \tag{2.6}$$

The model flow-diagram is given in Figure 2.1 and model the variables and parameters

descriptions are given in Table 2.1.

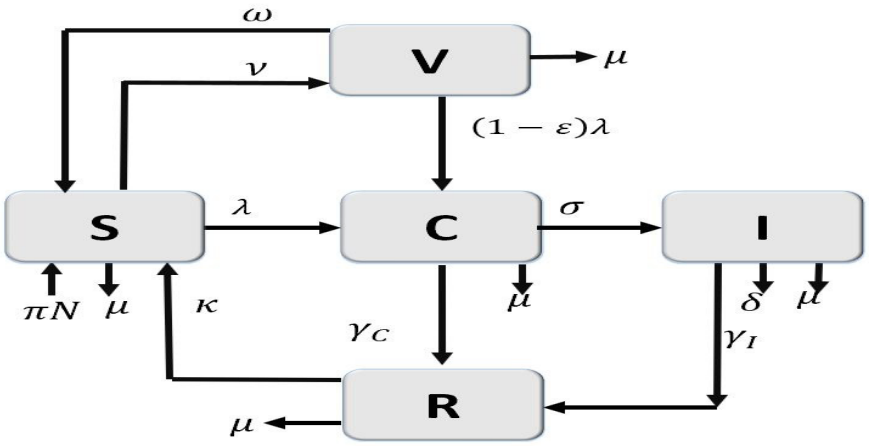

Figure 2.1: Flow diagram of the meningitis model (2.6).

Adding components of the meningitis model (2.6) gives

$$\frac{dN(t)}{dt} = (\pi - \mu)N - \delta I \tag{2.7}$$

Given nonnegative initial numbers of individuals in each class with $N(0) > 0$, Equation (2.7) shows that $N(t)$ remains positive and bounded for all finite $t > 0$.

Variable	Description
$S(t)$	Susceptible individuals
$V(t)$	Vaccinated individuals
$C(t)$	Carrier individuals
$I(t)$	Infected individuals
$R(t)$	Recovered individuals
Parameter	**Description**
π	Recruitment rate
ν	Vaccination rate
ε	Vaccine efficacy
ω	Vaccine waning rate
β	Transmission probability
η	Disease modification parameter
γ_C	Recovery rate of carrier
γ_I	Recovery rate of infected
σ	Progression rate of carrier to infected
κ	Immunity waning rate
μ	Natural death rate
δ	Disease induced death rate

Table 2.1: Description of the variables and parameters of the meningitis model (2.6).

2.3 Analysis of the meningitis model

It is easier to analyze the model in terms of proportions, so we make the following transformation $S = sN$, $V = vN$, $C = cN$, $I = iN$, and $R = rN$, leading to the system (2.8) below while still using the same variable names as model (2.6) above.

$$\begin{aligned}
\frac{dS}{dt} &= \pi - \pi S + \omega V + \kappa R - \beta(\eta C + I)S - \nu S + \delta SI \\
\frac{dV}{dt} &= \nu S - \beta(1-\varepsilon)(\eta C + I)V - (\pi + \omega)V + \delta VI \\
\frac{dC}{dt} &= \beta(\eta C + I)[S + (1-\varepsilon)V] - (\pi + \sigma + \gamma_C)C + \delta CI \qquad (2.8) \\
\frac{dI}{dt} &= \sigma C - (\pi + \gamma_I + \delta)I + \delta I^2 \\
\frac{dR}{dt} &= \gamma_C C + \gamma_I I - (\pi + \kappa)R + \delta RI.
\end{aligned}$$

The total population in (2.7) is now given as

$$\frac{dN(t)}{dt} = (\pi - \mu - \delta i)N \tag{2.9}$$

The meningitis model (2.8) will be analyzed in the biologically-feasible region defined as

$$\Omega \subset \mathbb{R}^5_+$$

where,

$$\Omega = \left\{ (S(t), V(t), C(t), I(t), R(t)) \in \mathbb{R}^5_+ \ : \ 0 \leq S(t), V(t), C(t), I(t), R(t) \leq 1 \right\}.$$

The region Ω is positively invariant.

2.3.1 Stability of the disease-free equilibrium (DFE)

The meningitis model (2.6) has a disease free equilibrium obtained by setting the right-hand sides of the equations in the model to zero when $C = I = R = 0$. Thus, the disease free equilibrium is given by

$$\mathcal{E}_0 = (S^*, V^*, C^*, I^*, R^*) = \left(\frac{\pi + \omega}{\pi + \nu + \omega}, \frac{\nu}{\pi + \nu + \omega}, 0, 0, 0 \right). \tag{2.10}$$

The stability of the dfe $\mathcal{E}_0$ can be established using the next generation operator method (P. Van den Driessche and J. Watmough, 2002) with C and I as the infected compartment.

The F and V matrices for the transmission matrix (new infection) and the transition matrix

(remaining transfer terms) are given respectively by

$$F = \begin{pmatrix} \frac{\beta\eta\left[S^* + (1-\varepsilon)V^*\right]}{N^*} & \frac{\beta\left[S^* + (1-\varepsilon)V^*\right]}{N^*} \\ 0 & 0 \end{pmatrix} \qquad V = \begin{pmatrix} k_3 & 0 \\ -\sigma & k_4 \end{pmatrix}$$

where $k_3 = \pi + \sigma + \gamma_C + \mu$ and $k_4 = \pi + \gamma_I + \mu + \delta$. Thus, the reproduction number is given as

$$\mathcal{R}_0 \quad = \quad \rho(FV^{-1}) = \frac{\beta[S^* + (1-\varepsilon)V^*](\eta k_4 + \sigma)}{k_3 k_4} \tag{2.11}$$

where ρ is the spectral radius (highest eigenvalue) of the matrix FV^{-1}.

Hence, the following result is established.

Theorem 1 *The meningitis model* (2.8) *disease-free equilibrium* $\mathcal{E}_0$ *is locally-asymptotically stable (LAS) if* $\mathcal{R}_0 < 1$ *and unstable if* $\mathcal{R}_0 > 1$.

The basic reproduction number $\mathcal{R}_0$ measures the average number of new infections generated by a single infected person during his or her infectious period in a population that is fully susceptible. Thus, the epidemiological implication of Theorem 1 is that meningitis will be controlled in the population whenever $\mathcal{R}_0 < 1$ if the initial sizes of the population of the model are in the basin of attraction of the DFE ($\mathcal{E}_0$).

2.3.2 Existence and stability of boundary equilibria (EEP)

Here we will establish the conditions for the existence of an equilibrium for which the disease is endemic in the population. Let

$$\mathcal{E}_1 = (S^{**}, V^{**}, C^{**}, I^{**}, R^{**})$$

denote the infection equilibria of the meningitis model (2.8). Setting the right-hand side of Equation (2.8) to zero and solving for $S^{**}, V^{**}, C^{**}, R^{**}$ in terms of I^{**} we have

$$\begin{aligned}
S^{**} &= -(\kappa\gamma_C\delta(I^{**})^2 + \pi\sigma\delta I^{**} - \kappa\gamma_C k_3 I^{**} - \kappa\gamma_I\sigma I^{**} - \pi\sigma k_4)(-EE\beta\eta k_3 I^{**} \\
&\quad + EE\beta\eta\delta(I^{**})^2 - EE\beta\sigma I^{**} - k_1\sigma + \sigma\delta I^{**})/[(\delta I^{**} - k_4)(\sigma\delta^2(I^{**})^3 EE\beta\eta \\
&\quad - \sigma\delta EE\beta\eta k_3(I^{**})^2 - \sigma^2\delta EE\beta(I^{**})^2 - \sigma^2\delta k_1 I^{**} - \beta\eta k_3\delta\sigma(I^{**})^2 + \beta\eta\delta^2\sigma \\
&\quad - \omega\sigma^2\nu(I^{**})^3 - \beta\sigma^2\delta(I^{**})^2 - \nu\sigma^2\delta I^{**} + 2\beta^2\eta k3 EE\sigma(I^{**})^2 + \beta\eta k_3 k_1\sigma I^{**} \\
&\quad + \beta^2\eta^2\delta^2 EE(I^{**})^4 + \beta^2\eta^2 k_3^2 EE(I^{**})^2 - 2\beta^2\eta^2 k_3 EE\delta(I^{**})^3 \\
&\quad - 2\beta^2\eta\delta EE\sigma(I^{**})^3 + \beta^2\sigma^2 EE(I^{**})^2 + \beta\sigma^2 k_1 I^{**} - \beta\eta\delta k_1\sigma(I^{**})^2 \\
&\quad + \nu\sigma EE\beta\eta k_3 I^{**} - \nu\sigma EE\beta\eta\delta(I^{**})^2 + \nu\sigma^2 EE\beta I^{**} - \pi\sigma^2\delta I^{**} \\
&\quad + \pi\sigma EE\beta\eta k_3 I^{**} - \pi\sigma EE\beta\eta\delta(I^{**})^2 + \pi\sigma^2 EE\beta I^{**} + \pi\sigma^2 k_1 + \nu\sigma^2 k_1 + \sigma^2\delta^2(I^{**})^2)]
\end{aligned}$$

$$\begin{aligned}
V^{**} &= \nu\sigma(\pi\sigma\delta I^{**} - \kappa\gamma_C k3 I^{**} + \kappa\gamma_C\delta(I^{**})^2 - \kappa\gamma_I\sigma I^{**} - \pi\sigma k_4) \\
&\quad /[(\delta I^{**} - k_4)(-EE\sigma\delta\beta\eta k_3(I^{**})^2 + \sigma\delta^2 EE\beta\eta(I^{**})^3 - \sigma^2\delta EE\beta(I^{**})^2 \\
&\quad - \sigma^2\delta k_1 I^{**} - \beta\eta k_3\delta\sigma(I^{**})^2 + \beta\eta\delta^2\sigma(I^{**})^3 - \omega\sigma^2\nu - \beta\sigma^2\delta(I^{**})^2 \\
&\quad - \nu\sigma^2\delta I^{**} + 2\beta^2\eta k_3 EE\sigma(I^{**})^2 + \beta\eta k_3 k_1\sigma I^{**} + \beta^2\eta^2\delta^2 EE(I^{**})^4 + \beta^2\eta^2 k_3^2 EE(I^{**})^2 \\
&\quad - 2\beta^2\eta^2 k_3 EE\delta(I^{**})^3 - 2\beta^2\eta\delta EE\sigma(I^{**})^3 + \beta^2\sigma^2 EE(I^{**})^2 + \beta\sigma^2 k_1 I^{**} - \beta\eta\delta k_1\sigma(I^{**})^2 \\
&\quad + \nu\sigma EE\beta\eta k_3 I^{**} - \nu\sigma EE\beta\eta\delta(I^{**})^2 + \nu\sigma^2 EE\beta I^{**} - \pi\sigma^2\delta I^{**} + \pi\sigma EE\beta\eta k_3 I^{**} \\
&\quad - \pi\sigma EE\beta\eta\delta(I^{**})^2 + \pi\sigma^2 EE\beta I^{**} + \pi\sigma^2 k_1 + \nu\sigma^2 k_1 + \sigma^2\delta^2(I^{**})^2)] \\
C^{**} &= (k_3 - \delta I^{**})I^{**}/\sigma \\
R^{**} &= (\gamma_C k_3 + \gamma_I\sigma - \gamma_C\delta I^{**})I^{**}/(\sigma(k_4 - \delta I^{**})),
\end{aligned}$$

where $EE = 1 - \varepsilon$. Substituting these into the fourth equation of (2.8) and equating to zero yields a seventh-order polynomial in I^{**} of the form

$$I^{**}[A_7(I^{**})^7 + A_6(I^{**})^6 + A_5(I^{**})^5 + A_4(I^{**})^4 + A_3(I^{**})^3 + A_2(I^{**})^2 + A_1 I^{**} + A_0] = 0. \quad (2.12)$$

The coefficients $A_0, \cdots, A_7$ of the polynomials are given in Appendix A.1. Clearly, $I^{**} = 0$ is a solution. The coefficient A_7 is positive while the sign of A_0 coincides with that of $(1 - \mathcal{R}_0)$, so that if $\mathcal{R}_0 > 1$, $A_0 > 0$, in which case, there is at least one sign change in the sequence of coefficients $(A_7, \cdots, A_0)$. Hence, by Descartes Rule of signs, there exists at least one positive real root for (2.12) aside from the root $I^{**} = 0$, whenever $\mathcal{R}_0 > 1$. This leads to the following lemma.

Lemma 1 *The meningitis model* (2.8) *has at least one endemic equilibrium whenever* $\mathcal{R}_0 > 1$.

2.3.3 Parameter estimation

The parameter values used in this study are taken from Agusto & Leite (2019). They employed three strategies for estimating the model parameter values. These include gathering of parameter values from literature such as vaccine efficacy 85%, vaccine waning rate 1/5 day^{-1}, and disease induced death rate 0.1923 year^{-1}. For parameters not found in the literature, the authors estimated their values when possible. For instance, natural death rate μ is estimated as $\mu = 1/56$ per year, where 56 years is the life expectancy in Nigeria. Lastly, for the parameters that could not be obtained by neither of the two strategies (literature and estimation), the authors fitted the parameters based on the 2017 Nigerian meningitis outbreak data which was obtained from the Nigeria Centre for Disease Control (NCDC) for weeks 5-27. It was noted that, since the data set has no public health interventions such as vaccination, the authors used the model Equation(2.6) (without implementation of public health interventions such as vaccination or facial masks) to reflect these conditions in

other to proceed with the parameterization. The parameters fitted are given as $\beta = 0.3345$, $\gamma_C = 0.1118$, $\gamma_I = 0.128$, $\sigma = 0.0438$ and $\kappa = 0.0032$. Nigeria's growth rate per year is 0.025, that is $\pi - \mu = 0.025$ from (2.7). Unlike Agusto & Leite (2019), we estimate the recruitment rate π as $\pi = 0.025 + \mu = 0.02505$ per year.

The cumulative number of cases for the 2017 meningitis outbreak in Nigeria from week 5 through 27 as presented by Agusto & Leite (2019) is depicted in Figure 2.2. The authors used these data to parameterize the model.

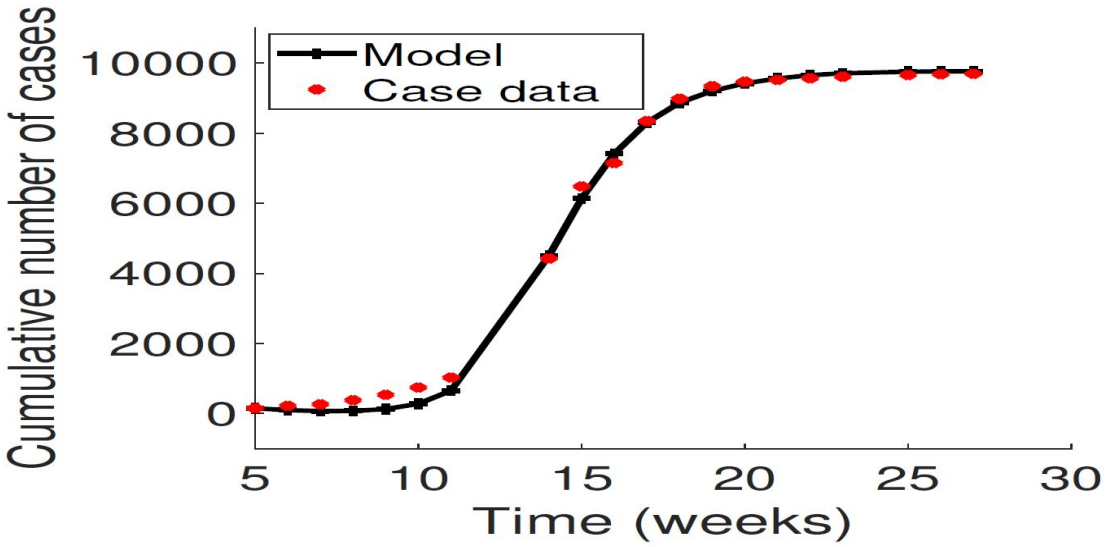

Figure 2.2: Cumulative number of cases for the 2017 meningitis outbreaks in Nigeria as presented in Agusto & Leite (2019).

2.3.4 Sensitivity analysis of the model with constant vaccination

Next, we carry out a sensitivity analysis of the model in order to determine the influence of each parameters on the reproduction number $\mathcal{R}_0$. Following McLeod et al. (2006), we use the normalized forward sensitivity index. The normalized forward sensitivity index of the reproduction number $\mathcal{R}_0$ with respect to the parameter p is defined as:

$$Z_p^{\mathcal{R}_0} = \frac{\partial \mathcal{R}_0}{\partial p} \times \frac{p}{\mathcal{R}_0} \tag{2.13}$$

where p is respective parameters in the reproduction number $\mathcal{R}_0$. The parameter values used are presented in Table 2.2. The parameters value were determined by fitting the data from the 2017 meningitis outbreak in Nigeria. The results from the analysis depicted in Figure 2.2 shows that the transmission probability (β), disease modification parameter (η), recovery rate of carrier (γ_C) and vaccine efficacy (ε) have the most impact on the reproduction number $\mathcal{R}_0$, and can be used as means to control disease burden in the community.

Parameter	Values	Sensitivity index
π	0.02505 year^{-1}	-0.0980
ν	0.4868 day^{-1}	-0.439
ε	0.85	-1.388
ω	0.200 day^{-1}	0.390
β	0.3345 day^{-1}	1.000
η	1	0.887
γ_C	0.1118 day^{-1}	-0.619
γ_I	0.1128 day^{-1}	-0.042
σ	0.0438 day^{-1}	-0.130
κ	0.0032 day^{-1}	N/A
μ	0.0179 year^{-1}	N/A
δ	0.1923 year^{-1}	-0.063

Table 2.2: Parameter values of the model meningitis and respective sensitivity index (2.6). All parameter values are taken from Agusto & Leite (2019).

For instance, the transmission probability (β) which has a sensitivity index of 1.00 has a positive impact on the reproduction number and 10% increase in β will lead to a 10% increase in disease burden. While vaccine efficacy (ε) with sensitivity index of -1.388 will reduce the disease burden to about 14% if the vaccine efficacy was increased by 10%. Similarly, the disease burden will decrease by 6.2% if the recovery rate, γ_C, among the carrier population with sensitivity index -0.619 was increased by 10%. See Figure 2.3 for the bar plot of the sensitivity indices showing the effect of the various model parameters on the reproduction number.

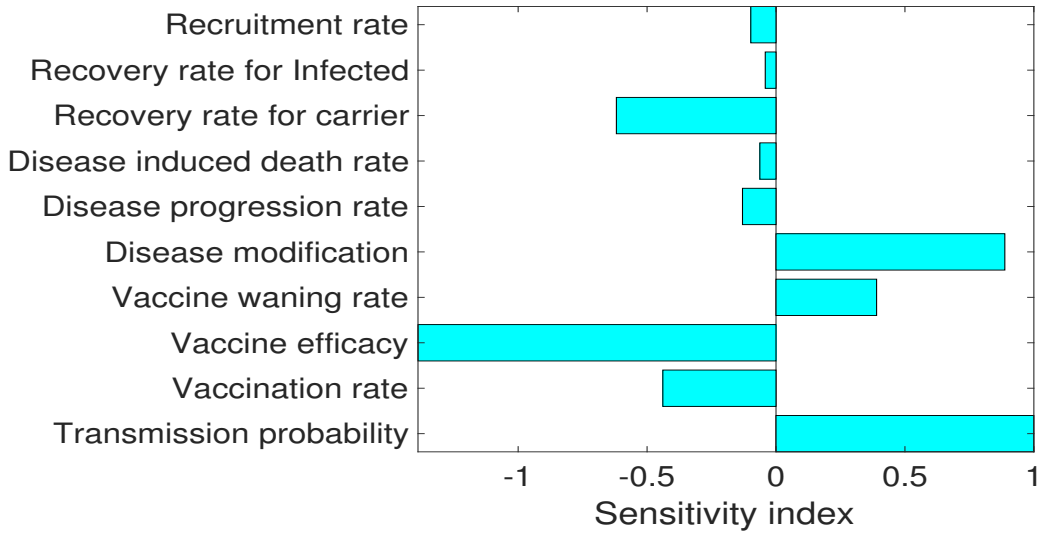

Figure 2.3: Sensitivity index of the model (2.6) using the baseline parameter value in Table 2.2.

Next, we vary in Figures 2.4 and 2.5 the values of the three vital parameters with the highest sensitivity indices, namely the transmission probability (β), recovery rate of carrier (γ_C) and vaccine efficacy (ε). This enables us to further explore their impact on the reproduction number.

We observed in Figure 2.4(a) that as the values of β increases the disease burden increase as the values of $\mathcal{R}_0$ increases. It might be difficult to curtail the disease at high values of $\beta > 0.33$ since the values of $\mathcal{R}_0$ are above one. Similarly in Figure 2.4(b), we see an increase in $\mathcal{R}_0$ values; however, curtailing the disease might be difficult at low values of $\gamma_C < 0.11$. On the other hand we see in Figure 2.4(c) that increasing values of vaccine efficacy, ε, will reduce disease burden, that is lower $\mathcal{R}_0$ values. In fact very low values of ε (say 0.25) will reduce $\mathcal{R}_0$ values.

Next, we access the impact of vaccine efficacy and its coverage in eradicating the disease in a population. Figure 2.5 shows the effect of vaccine efficacy (ε) with respect to low and high vaccine coverage (P) respectively. From Figure 2.5(a) we observed that the reproduction number $\mathcal{R}_0$ remain below one even for very low vaccine efficacy 25% at low vaccine coverage (P) of 25%. Note that even though these values are below one, they are close to one and

might not necessary guarantee disease elimination if we factor in backward bifurcation, a phenomenon common in most disease models with vaccination. Under this phenomenon, two stable equilibria co-exist at the disease-free equilibrium. We explore this possibility at a later date.

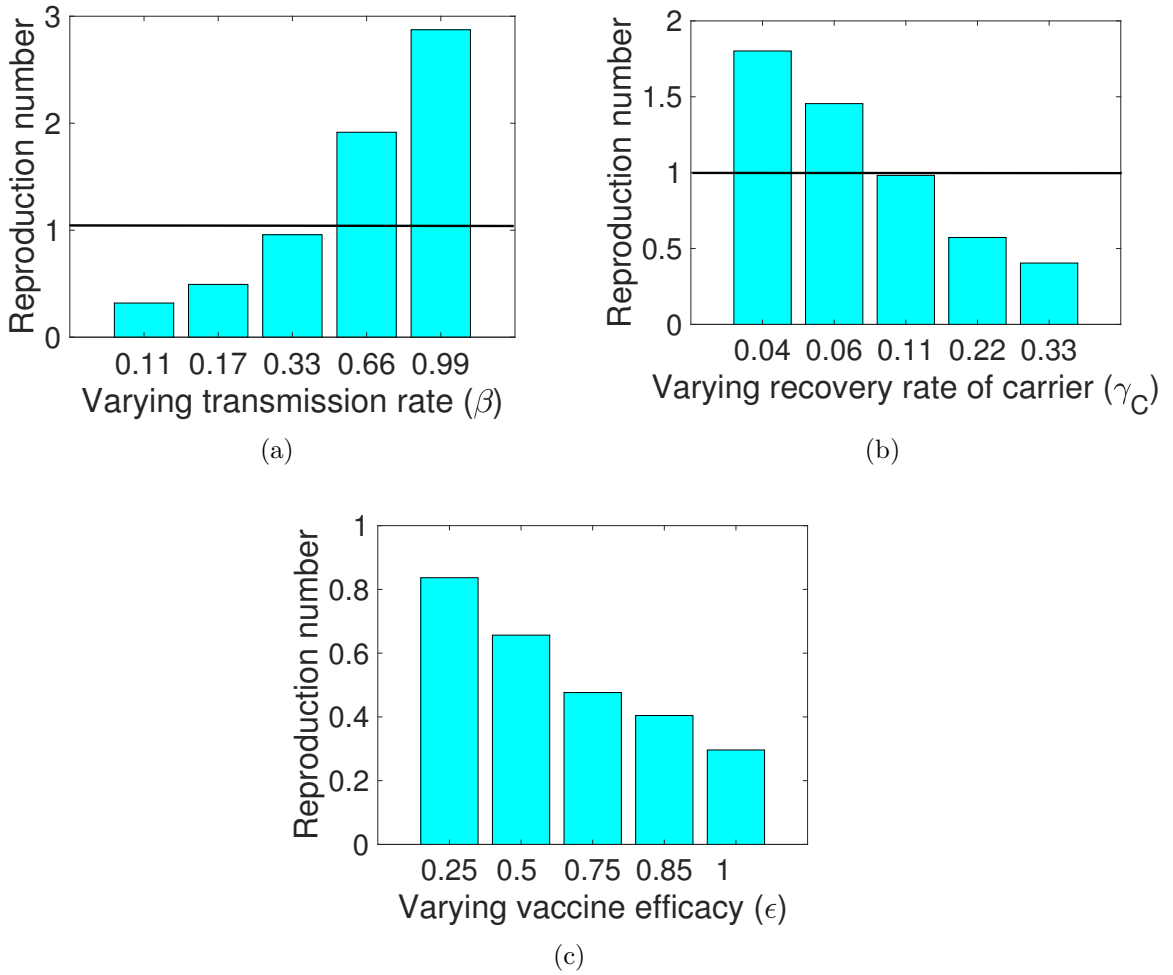

Figure 2.4: Bar plot showing the effect of the most sensitive parameters on reproduction number $\mathcal{R}_0$ using: (a) The transmission probability β; (b) Vaccine efficacy ε; (c) The recovery rate of the carrier population γ_C. Parameter values (ranges) used are as given in Table 2.2.

When the proportion vaccinated are increased to 85%, the values of the reproduction numbers $\mathcal{R}_0$ are below one for all values of the vaccine efficacy (see Figure 2.5(b)). However, the values are well below one $\mathcal{R}_0$ for higher values of the vaccine efficacy; for instance, with $\varepsilon = 75\%$ we see a strong reduction in $\mathcal{R}_0$.

In Figure 2.5(c) we vary the proportion vaccinated from 25% to 100% and keep vaccine efficacy low at $\varepsilon = 25\%$; we observed in Figure 2.5(b) high $\mathcal{R}_0$ values which are close to one. On the other hand in Figure 2.5(d), when we set the vaccine efficacy high ($\varepsilon = 85\%$), $\mathcal{R}_0$ values are below one. We observed further that we are able to bring the reproduction number all well below one with a vaccine efficacy of 75% and a coverage of 85%. Thus, this aspect of the study shows the possibilities of effectively controlling the disease in the population using an imperfect vaccine with an efficacy of $> 75\%$ and high vaccine coverage rate of at least 85%.

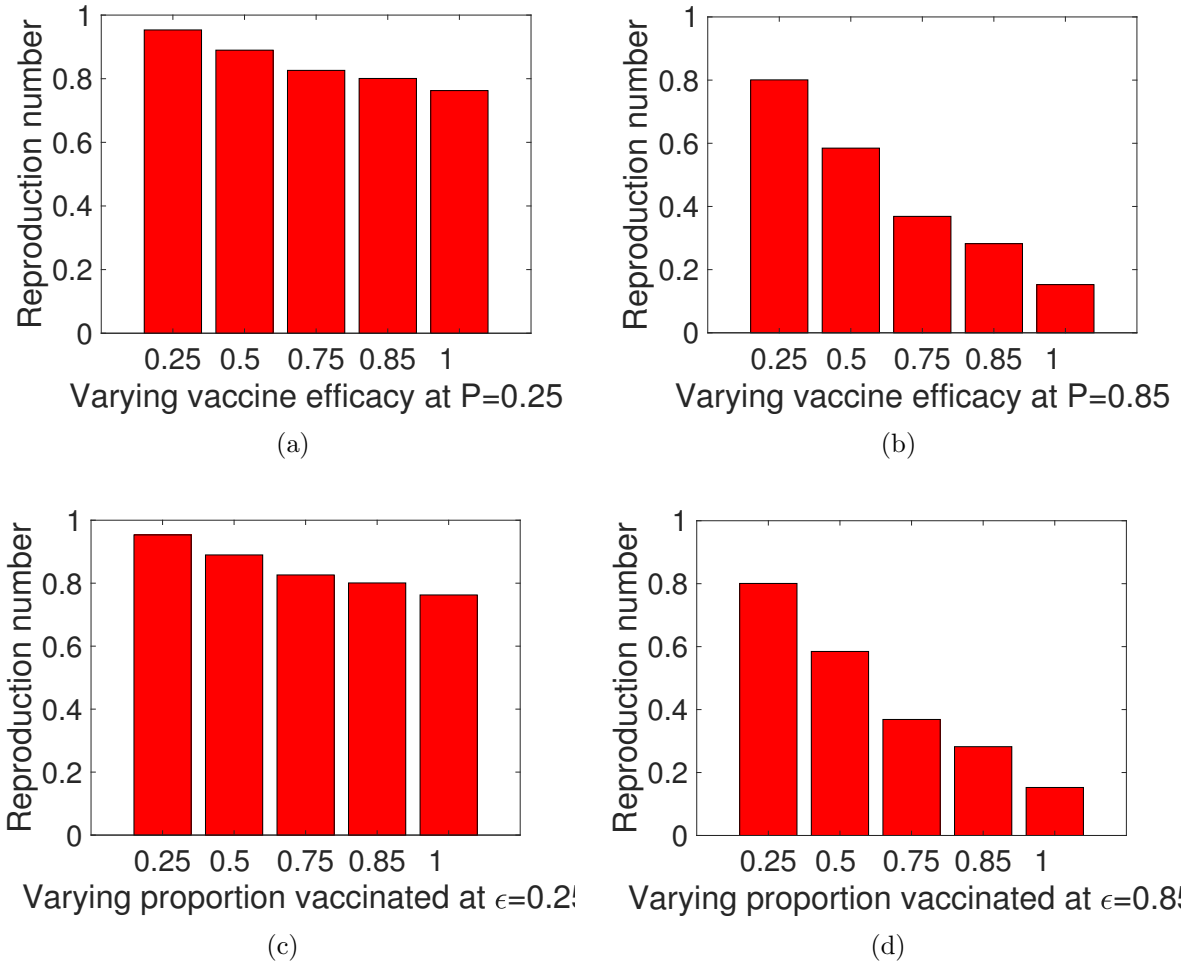

Figure 2.5: Bar plot showing the effect of vaccine efficacy (ε) with respect to coverage on the reproduction number $\mathcal{R}_0$: (a) Varying vaccine efficacy at 25% coverage; (b) Varying vaccine efficacy at 85% coverage; (c) Varying coverage at 25% vaccine efficacy; (d) Varying coverage at 85% vaccine efficacy. Parameter values used are as given in Table 2.2.

Thus, we conclude from these results that, having a high vaccine efficacy alone is not sufficient to reduce the reproduction number below one but having a high vaccine efficacy together with high coverage is sufficient to reduce the reproduction number well below one.

2.4 The Meningitis model with impulse control

In the previous section, we considered a constant vaccination where a fixed proportion of the susceptible individuals are vaccinated. However, vaccination may be administered impulsively at either regular or irregular times in order to curtail disease outbreak. Thus leading to an impulsive system described by a system of non-autonomous impulsive differential equations (Bainov & Simeonov, 1995; Lakshmikantham et al., 1989; Smith et al., 2017). Hence, impulsively vaccinating the individuals in the community, the meningitis model (2.6) becomes

$$\left.\begin{aligned}
\frac{dS}{dt} &= \pi N + \omega V + \kappa R - \lambda S - \mu S \\
\frac{dV}{dt} &= -(1-\varepsilon)\lambda V - (\omega + \mu)V \\
\frac{dC}{dt} &= \lambda[S + (1-\varepsilon)]V - (\sigma + \gamma_C + \mu)C \\
\frac{dI}{dt} &= \sigma C - (\gamma_I + \mu + \delta)I \\
\frac{dR}{dt} &= \gamma_C C + \gamma_I I - (\mu + \kappa)R
\end{aligned}\right\} \quad t \neq nT,\ n \in \mathbb{N} \tag{2.14}$$

subject to the impulse condition

$$S^+ = (1-\nu)S^-, \quad V^+ = V^- + \nu S^- \qquad t = nT,\ n \in \mathbb{N} \tag{2.15}$$

where t_k is the vaccination times which may be fixed or non-fixed; in this study we will consider the case with fixed times. As with model (2.8) in Section 2.3, we analyze the model in terms of proportions, using the same previous transformation $S = sN$, $V = vN$, $C = cN$, $I = iN$, and $R = rN$, leading to the impulsive system (2.16) below while still using the same variable names as model (2.14) above.

$$\left.\begin{aligned}
\frac{dS}{dt} &= \pi - \pi S + \omega V + \kappa R - \beta(\eta C + I)S + \delta SI \\
\frac{dV}{dt} &= -\beta(1-\varepsilon)(\eta C + I)V - (\pi + \omega)V + \delta VI \\
\frac{dC}{dt} &= \beta(\eta C + I)[S + (1-\varepsilon)V] - (\pi + \sigma + \gamma_C)C + \delta CI \\
\frac{dI}{dt} &= \sigma C - (\pi + \gamma_I + \delta)I + \delta I^2 \\
\frac{dR}{dt} &= \gamma_C C + \gamma_I I - (\pi + \kappa)R + \delta RI.
\end{aligned}\right\} \quad t \neq nT,\ n \in \mathbb{N} \qquad (2.16)$$

We will study (2.16) in the region

$$\Gamma = \left\{ (S(t), V(t), C(t), I(t), R(t)) \in \mathbb{R}^5_+ \ :\ 0 \leq S(t), V(t), C(t), I(t), R(t) \leq 1 \right\}.$$

The region Γ is positively invariant which can be seen from the right-hand side of (2.16).

2.4.1 Existence and stability of disease free periodic solution

To determine the disease-free periodic solution, assume $C(t) = I(t) = R(t) = 0$, for $t \geq 0$ system (2.16) simplifies to

$$\left.\begin{array}{rcl} \dfrac{dS}{dt} &=& \pi - \pi S + \omega V \\ \\ \dfrac{dV}{dt} &=& -(\pi+\omega)V \end{array}\right\} \quad t \neq nT,\ n \in \mathbb{N} \tag{2.17}$$

$$S^+ = (1-\nu)S^-, \qquad V^+ = V^- + \nu S^- \qquad t = nT,\ n \in \mathbb{N}.$$

Using the fact that $S(t) + V(t) = 1$, system (2.17) becomes

$$\frac{dS}{dt} = (\pi+\omega) - (\pi+\omega)S \tag{2.18}$$

In the time interval $nT \leq t \leq (n+1)T$, system (2.18) has the solution

$$S(t) = 1 + e^{-(\pi+\omega)(t-nT)}(S(nT^+) - 1) \tag{2.19}$$

Let S_{n+1} be the size of susceptible population after the $(n+1)$-th pulse, i.e. $S_{n+1} = S((n+1)T^+)$. From (2.18) we have

$$S_{n+1} = (1-\nu)(1 + e^{-(\pi+\omega)T}(S_n - 1)) := \psi(S_n).$$

The map ψ has a unique positive fixed point

$$S^* = \frac{(1-\nu)(1-e^{-(\pi+\omega)t})}{(1-(1-\nu)e^{-\mu t})};$$

If $t \neq nT$

$$\begin{aligned}\bar{S}(t) &= 1 + e^{-(\pi+\omega)(t+T-(n+1)T)}\left[\frac{(1-\nu)(1-e^{-\mu T})}{(1-(1-\nu)e^{-(\pi+\omega)T})} - 1\right] \\ &= 1 + e^{-(\pi+\omega)(t-nT)}\left[\frac{(1-\nu)(1-e^{-(\pi+\omega)T})}{(1-(1-\nu)e^{-\mu T})} - 1\right] \\ &= \bar{S}(t+1),\end{aligned}$$

and in case $t = nT$, $\bar{S}(t) = S^* = \bar{S}((n+1)T)$, so (2.18) is periodic with period T. Thus, the solution of (2.18) is a solution not only in the time interval $[0, T)$, but also for all $t \geq 0$. Hence, the solution of (2.18) in the time interval $[0, T)$ is

$$\bar{S}(t) = 1 + e^{-(\pi+\omega)(t-nT)}\left[\frac{(1-\nu)(1-e^{-(\pi+\omega)T})}{(1-(1-\nu)e^{-(\pi+\omega)T})} - 1\right],$$

Since $V(t) = 1 - S(t)$, it follows that $\bar{V}(t) = e^{-(\pi+\omega)T}\left[1 - \frac{(1-\nu)(1-e^{-(\pi+\omega)T})}{1-(1-\nu)e^{-(\pi+\omega)T}}\right]$. Further, similar to Lemma 2.2 of Gao et al. (2006a), it can be shown that $(\bar{S}(t), \bar{V}(t))$ is globally asymptotically stable by using stroboscopic map. Hence, we summarize this results below as

Lemma 2 *The model* (2.16) *has a unique disease-free periodic solution given as*

$$\begin{aligned}\bar{S}(t) &= 1 + e^{-(\pi+\omega)T}\left[\frac{(1-\nu)(1-e^{-(\pi+\omega)T})}{(1-(1-\nu)e^{-(\pi+\omega)T})} - 1\right] \\ \bar{V}(t) &= e^{-(\pi+\omega)T}\left[1 - \frac{(1-\nu)(1-e^{-(\pi+\omega)T})}{1-(1-\nu)e^{-(\pi+\omega)T}}\right] \\ \bar{C}(t) &= 0, \quad \bar{I}(t) = 0, \quad \bar{R}(t) = 0.\end{aligned}$$

From Lemma 2, system (2.16), admits the disease-free periodic solution (DFPS) $(\bar{S}(t), \bar{V}(t), 0, 0, 0)$ on every impulsive interval $[nT, (n+1)T]$. To determine the stability of DFPS of system

(2.16), we follow the approach in Xu et al. (2015) and define the following matrices

$$F = \begin{pmatrix} \beta\eta[\bar{S} + (1-\varepsilon)\bar{V}] & \beta[\bar{S} + (1-\varepsilon)\bar{V}] \\ 0 & 0 \end{pmatrix}, \quad V = \begin{pmatrix} g_2 & 0 \\ -\sigma & g_3 \end{pmatrix}$$

Let A be a $n \times n$ matrix, $\Phi_{A(.)}(t)$ be the fundamental solution matrix of the linear ordinary differential system $x' = Ax$, and $\rho(\Phi_{A(.)}(w))$ be the spectral radius of $\Phi_{A(.)}(w)$. Let $S = s(t) + \bar{S}(t),\ V = v(t) + \bar{V}(t),\ C = c(t), I = i(t), R = r(t)$. Then system (2.16) becomes

$$\begin{cases} x'(t) &= Qx(t), & t \neq nT,\ n \in \mathbb{N} \\ x(t) &= Px(t), & t = nT,\ n \in \mathbb{N} \end{cases} \tag{2.20}$$

where

$$Q(t) = \begin{pmatrix} U & B \\ 0 & F - V \end{pmatrix}, \qquad P = \begin{pmatrix} P_1 & 0 \\ 0 & P_2 \end{pmatrix}$$

with

$$U = \begin{pmatrix} -\pi & \omega & \kappa \\ 0 & -g_1 & 0 \\ 0 & 0 & -g_4 \end{pmatrix}, \quad B = \begin{pmatrix} -\beta\eta\bar{S} & -\beta\bar{S} + \delta\bar{S} \\ -(1-\varepsilon)\beta\eta\bar{V} & -(1-\varepsilon)\beta\bar{V} + \delta\bar{V} \\ \gamma_C & \gamma_I \end{pmatrix}$$

$$P_1 = \begin{pmatrix} 1-\nu & 0 & 0 \\ \nu & 1 & 0 \\ 0 & 0 & 1 \end{pmatrix}, \quad P_2 = \begin{pmatrix} 1 & 0 \\ 0 & 1 \end{pmatrix},$$

and $g_1 = (\pi + \omega),\ g_2 = (\pi + \sigma + \gamma_C),\ g_3 = (\pi + \gamma_I + \delta),\ g_4 = (\pi + \kappa)$.

Let $\Phi_Q(t) = (Q_{ij})_{1 \leq i,j \leq 2}$ be the fundamental matrix of $x'(t) = Qx(t)$. Then $\Phi'_Q(t) = Q\Phi_Q(t)$ with the initial value $\Phi_Q(0) = I$, the identity matrix. Solving the equation gives

$$\Phi_Q(t) = \begin{pmatrix} e^{Ut} & \Phi_{12}(t) \\ 0 & \Phi_{(F-V)}(t) \end{pmatrix},$$

then we have

$$P\Phi_Q(T) = \begin{pmatrix} P_1 e^{UT} & P_1\Phi_{12}(T) \\ 0 & P_2\Phi_{(F-V)}(T) \end{pmatrix}.$$

Therefore, the stability DFPS is dependent on eigenvalues of $P_1 e^{UT}$ and $P_2\Phi_{(F-V)}(T)$.

The eigenvalues of $P_1 e^{UT}$ are $e^{-\int_0^\tau g_4 dt} < 1$ and the eigenvalues of $P_1 e^{U_1 T}$, where

$$U_1 = \begin{pmatrix} -\pi & \omega \\ 0 & -g_2 \end{pmatrix}$$

and

$$\begin{aligned} \rho(P_1 e^{U_1 T}) &= \frac{1}{2}\nu e^{\int_0^\tau \omega d\tau} + \frac{1}{2}(1-\nu)e^{-\int_0^\tau \pi d\tau} + \frac{1}{2}e^{-\int_0^\tau g_1 d\tau} \\ &\quad + \frac{1}{2}\Bigg\{ \left(\nu e^{\int_0^\tau \omega d\tau} + (1-\nu)e^{-\int_0^\tau \pi d\tau} + e^{-\int_0^\tau g_1 d\tau} \right)^2 \\ &\quad - 4(1-\nu)e^{-\int_0^\tau g_1 d\tau} e^{-\int_0^\tau \pi d\tau} \Bigg\}^{\frac{1}{2}} \end{aligned}$$

We can show that $\rho(P_1 e^{U_1 T}) < 1$. Thus, the following theorem holds.

Theorem 2 *If $\rho(P_2\Phi_{(F-V)}(T)) < 1$ holds true, then the disease-free periodic solution $(\bar{S}(t), \bar{V}(t), 0, 0, 0)$ of system 2.16 is locally asymptotically stable.*

$$\begin{aligned}\rho(P_2\Phi_{(F-V)}(T)) &= \frac{1}{2}e^{\int_0^\tau[\beta\eta(\bar{S}-(1-\varepsilon)\bar{V})-g_2]d\tau}+\frac{1}{2}e^{\int_0^\tau -g_3 d\tau}\\ &\quad+\frac{1}{2}\Bigg\{\left(e^{\int_0^\tau[\beta\eta(\bar{S}+(1-\varepsilon)\bar{V})-g_2]d\tau}-e^{-\int_0^\tau g_3 d\tau}\right)^2\\ &\quad+4e^{-\int_0^\tau \sigma d\tau}e^{\int_0^\tau[\beta(\bar{S}+(1-\varepsilon)\bar{V})]d\tau}\Bigg\}^{\frac{1}{2}}\end{aligned}$$

We denote the spectral radius as $\mathcal{R}_p = \rho(P_2\Phi_{(F-V)}(T))$. Note, $\mathcal{R}_p$ does not produce the number of individual infected by a single infected carrier or infectious individual. Namely it does not produce the average number of secondary infections Xu et al. (2015). However, it works as a threshold such that the disease persists as $\mathcal{R}_p > 1$ (Xu et al., 2015).

2.4.2 Persistence of the disease

Theorem 3 *If $\mathcal{R}_p = \rho(P_2\Phi_{(F-V)}(T)) > 1$, the disease persists; namely, there exists $L > 0$ such that $\lim_{t\to\infty} C(t) \geq L > 0$, $\lim_{t\to\infty} I(t) \geq L > 0$, and $\lim_{t\to\infty} R(t) \geq L > 0$.*

Proof From $\mathcal{R}_p = \rho(P_2\Phi_{(F-V)}(T)) > 1$, we can choose small enough positive constants L, ζ_1 and ζ_2 such that

$$\rho(P_2\Phi_{(F_{(L,\zeta_1,\zeta_2)}-V)}(T)) > 1,$$

where

$$F = \begin{pmatrix} \beta\eta[\bar{S}+(1-\varepsilon)\bar{V}] & \beta[\bar{S}+(1-\varepsilon)\bar{V}] \\ 0 & 0 \end{pmatrix},$$

and $\bar{S}$ and $\bar{V}$ are given by Section 2.4.1.

First we prove there exists a positive constant L such that $\sup_{t\to\infty} C(t) \geq L > 0$, $\sup_{t\to\infty} I(t) \geq L > 0$ and $\lim_{t\to\infty} R(t) \geq L > 0$. Otherwise, there exists a $t_1 > 0$ such that $C(t) < L$, $I(t) <$

L, for all $t \geq t_1$. By the first two equations of system (2.16), we have

$$\left.\begin{array}{rcl} \dfrac{dS}{dt} & \geq & \pi + \omega V + \kappa L - \beta(\eta L + L)S - \pi S + \delta S L \\ \dfrac{dV}{dt} & \geq & -\beta(1-\varepsilon)(\eta L + L)V - (\omega + \pi)V + \delta V L \end{array}\right\} \quad t \neq nT,\ n \in \mathbb{N} \tag{2.21}$$

$$S^+ = (1-\nu)S^-, \qquad V^+ = V^- + \nu S^-, \qquad t = nT,\ n \in \mathbb{N}$$

Consider the auxiliary system

$$\left.\begin{array}{rcl} \dfrac{dx_1}{dt} & = & \pi + \omega V + \kappa L - \beta(\eta L + L)x_1 - \pi x_1 + \delta x_1 L \\ \dfrac{dx_2}{dt} & = & -\beta(1-\varepsilon)(\eta L + L)x_2 - (\omega + \pi)x_2 + \delta x_2 L \end{array}\right\} \quad t \neq nT,\ n \in \mathbb{N} \tag{2.22}$$

$$x_1^+ = (1-\nu)x_1^-, \qquad x_2^+ = x_2^- + \nu x_1^-, \qquad t = nT,\ n \in \mathbb{N}$$

Using the same method as system (2.17) and the fact that $x_1(t) + x_2(t) = 1$, we obtain that system (2.22) admits a locally asymptotically stable positive periodic solution $\bar{x} = (\bar{x}_1, \bar{x}_2)$, meanwhile $\lim_{L \to 0}(\bar{x}_1, \bar{x}_2) = (\bar{S}, \bar{V})$.

Thus, there exists a positive constant L_1 small enough and for any $\zeta_1 > 0$, such that $\bar{x}_1 \geq \bar{S} - \zeta_1$ and $\bar{x}_2 \geq \bar{V} - \zeta_1$ for $L < L_1$. By the comparison theorem, there exists $t_2 \geq t_1$ and $\zeta_2 > 0$, such that $S(t) \geq x_1(t) \geq \bar{S} - \zeta_1 - \zeta_2$, and $V(t) \geq x_2(t) \geq \bar{V} - \zeta_1 - \zeta_2$ for $t \geq t_2$.

From the infected components of system (2.16), we have

$$\left.\begin{aligned} \frac{dC}{dt} &= \beta(\eta C + I)[(\bar{S} - \zeta_1 - \zeta_2) + (1-\varepsilon)(\bar{V} - \zeta_1 - \zeta_2)] \\ &\quad -g_2 C + \delta C I \\ \frac{dI}{dt} &= \sigma C - g_3 I \\ \frac{dR}{dt} &= \gamma_C C + \gamma_I I - g_4 R \end{aligned}\right\} \quad t \neq nT,\ n \in \mathbb{N} \qquad (2.23)$$

where $g_2 = (\pi + \sigma + \gamma_C),\ g_3 = (\pi + \gamma_I + \delta),\ g_4 = (\pi + \kappa)$. Consider the auxiliary system

$$u'(t) = (F - V)u(t), \qquad t \neq nT,\ n \in \mathbb{N} \qquad (2.24)$$

where $u = (u_1, u_2)^T$. The solution of system (2.24) can be expressed as $u(t, nT, u(nT^+)) = \Phi_{(F-V)}(t - nT)u(nT^+)$. Then $u((n+1)T^+) = P_2\Phi_{(F-V)}(T)u(nT^+)$. While $\mathcal{R}_p = \rho(P_2\Phi_{(F-V)}(T)) > 1,\ u_1 \to \infty$ and $u_2 \to \infty$ as $t \to \infty$. Then $\lim_{t\to\infty} C = \infty$ and $\lim_{t\to\infty} I = \infty$, which contradicts with the boundedness of (C, I). Thus the claim is proved; that is, $\limsup_{t\to\infty} C(t) \geq L$ and $\limsup_{t\to\infty} I(t) \geq L$, which implies $\limsup_{t\to\infty} R(t) \geq L$. From the claim, we discuss the following two possibilities.

(I) $C(t) \geq L$ and $I(t) \geq L$ for all large t;

(II) $C(t)$ and $I(t)$ oscillates about L for all large t.

If condition (I) holds, then the proof is complete. Next we consider the possibility of condition (II). Since $\limsup_{t\to\infty} C(t) \geq L$ and $\limsup_{t\to\infty} I(t) \geq L$, there exists a $t_1 \in (n_1T, (n_1+1)T]$ and $t_2 \in (n_2T, (n_2+1)T]$ such that $C(t_1) \geq L$, $I(t_1) \geq L$ and $C(t_2) \geq L$, $I(t_2) \geq L$, where $n_2 - n_1 \geq 0$ is finite. Then we will consider the solution of the following equation from system (2.16) in the time interval $[t_1, t_2]$. Then from the infected component of system (2.16), we

have

$$\begin{aligned}\frac{dC}{dt} &= \beta(\eta C + I)[\bar{S} + (1-\varepsilon)\bar{V}] - k_3 C + \delta C I \geq -k_3 C \\ \frac{dI}{dt} &= \sigma C - k_4 I + \delta I^2 \geq -k_4 I.\end{aligned}$$

Integrating the above equation from t_1 to t, we have

$$\begin{aligned}C(t) &\geq C(t_1)e^{-g_2(t-t_1)} \geq Le^{-g_2(t_2-t_1)} \geq Le^{-g_2(n_2-n_1+1)T} \\ I(t) &\geq I(t_1)e^{-g_3(t-t_1)} \geq Le^{-g_3(t_2-t_1)} \geq Le^{-g_3(n_2-n_1+1)T}\end{aligned}$$

Let $L_1 = \min\{Le^{-g_2(n_2-n_1)T}), Le^{-g_3(n_2-n_1)T}), \}$, then $L_1 > 0$ cannot be infinitely small since $n_2 - n_1 \geq 0$ is finite. We have $C(t) \geq L_1 > 0$ and $I(t) \geq L_1 > 0$.

For $t > t_2$, the same arguments can be continued. We similarly get non-infinitesimal positive L_2. Therefore, we can get the sequence $\{L_k\}$ where

$$L_k = \min\{Le^{-g_2(n_{k+1}-n_k)T}, Le^{-g_3(n_{k+1}-n_k)T}\}, \quad k = 1, 2 \cdots j \cdots .$$

is non-infinitesimal since $n_{k+1} - n_k \geq 0$ is finite. Thus, solution of system (2.16) satisfies $C(t) \geq L_k > 0$ and $I(t) \geq L_k > 0$ holds true in the time interval $[t_k, t_{k+1}]$, where $t_k \in (n_k T, (n_k + 1)T]$, and $t_{k+1} \in (n_{k+1}T, (n_{k+1} + 1)T]$. Let $L^* = \min_k\{L_k\} = L_l > 0, l \in \mathbb{N}, L_l \in \{L_k\}, k = 1, 2, \cdots$. Thus, from the above discuss, we have that $C(t) \geq L^* > 0$ and $I(t) \geq L^* > 0$ for all $t \geq t_1$. Hence, the proof is complete.

2.5 Numerical simulation of the impulsive model

In this section, we present the numerical results of the impulsive model using 85% vaccine efficacy along with the parameter values in Table 2.2. In order to assess the impact of impulsive vaccination on the population, we implemented 15 vaccination pulses periodically

for a month with vaccination rate $\nu = 0.48681$. We observed from Figure 2.6 the number of vaccinated individuals increasing with increasing pulses which leads to a decrease in the number of infected and increase in the recovered individuals. We see similar dynamics when a lower vaccination rate, $\nu = 0.14868$, is used; in this case susceptible and vaccinated are $S(t) = 630$ and $V(t) = 1173$ at 10 days (see Figure 2.6(a)). However, when a higher vaccination rate was used, susceptible and vaccination at 10 days are $S(t) = 120$ and $V(t) = 2140$ respectively. This result is in line with the result obtained from the sensitivity analysis in Section 2.3.4. Thus, higher vaccination rate protect more people in the community than a lower vaccination rate.

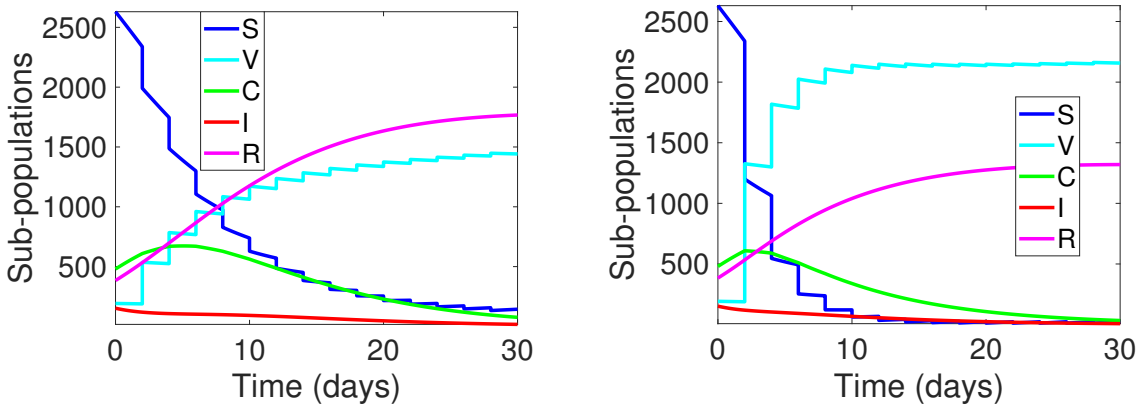

Figure 2.6: Numerical simulation of the sub-population using (a) A low vaccination rate $\nu \approx 0.1$; (b) A higher vaccination rate $\nu \approx 0.5$. Other parameter values used are as given in Table 2.2.

Furthermore, in Figure 2.7 we observed in absence of vaccination more susceptible individuals at the final time who can be infected with the disease compared to when there is vaccination (see Figures 2.7(a) and 2.7(b)). Similar, results holds at the final time for the carrier and infected individuals in the absence of vaccination compared to when the population is vaccinated.

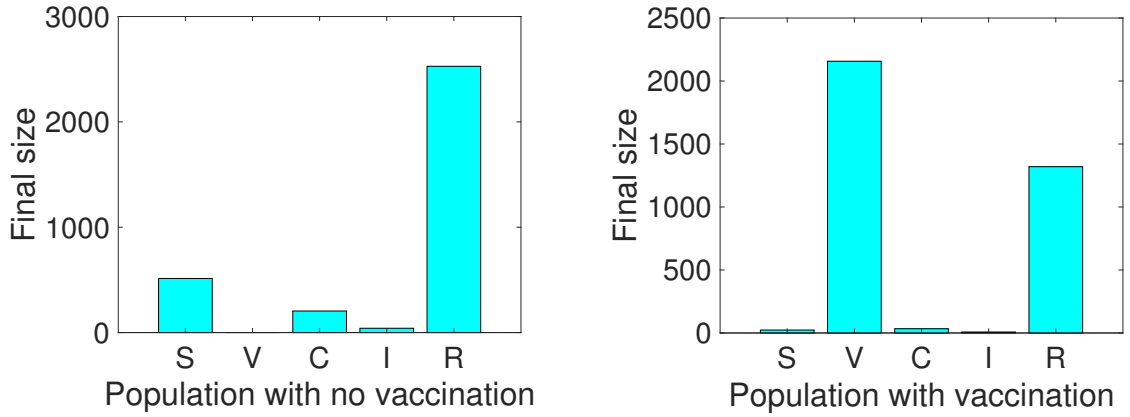

(a) (b)

Figure 2.7: Bar plot for the final size of each sub-population. (a) Final size of the population without vaccination; (b) Final size of the population with 85% vaccination coverage. Parameter values used are as given in Table 2.2.

Next, we explore the impact of different vaccination pulses on disease burden in the community on the final size at the final time of 30 days. We observed from Figures 2.8(a) and 2.8(b) with low and high vaccination rate that as the number of pulses increase, the vaccinated population increases leading to a decrease in the infected individuals in the community. It should be noted that as we increase the number of vaccine pulses within a month, the pulse period reduces. That is, our pulse vaccine period decreases from 5 days to 2 days, and the number of pulses increase from 6 pulses to 15 pulses as the days decreases.

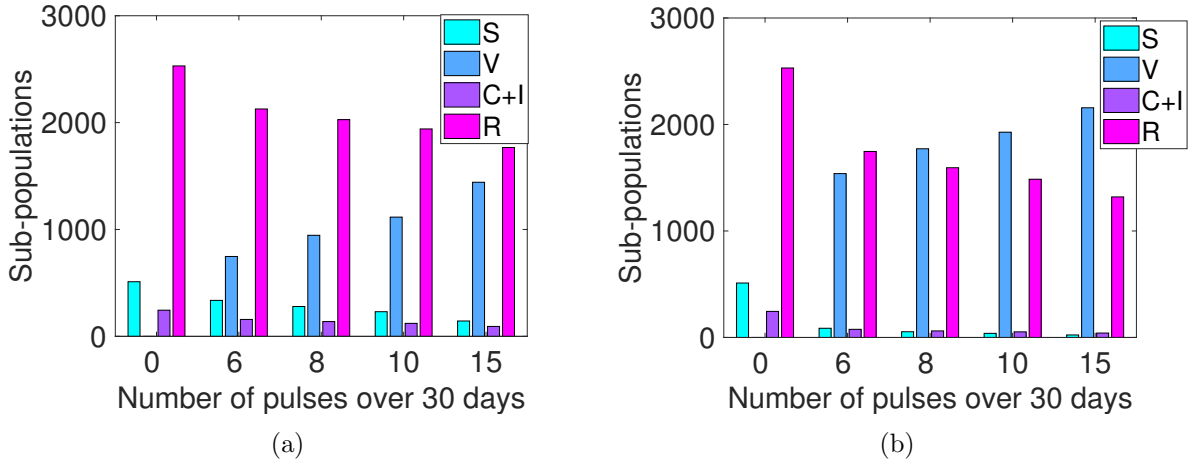

Figure 2.8: Numerical simulation of the sub-population final size. (a) A low vaccination rate $\nu \approx 0.1$; (b) A higher vaccination rate $\nu \approx 0.5$. Parameter values used are as given in Table 2.2.

2.6 Discussion and conclusions

2.6.1 Discussion

Neisseria meningitis is a bacteria responsible for causing *meningococcal meningitis* with a potential of causing epidemics mostly from six of the twelve different serotypes, namely the serotypes A, B, C, W, X and Y (Rouphael & Stephens, 2012; World Health Organization (WHO), 2018). In 2017, an outbreak of meningitis C occurred in Nigeria with over 9,902 cases and 602 deaths in 31 states of the country (Nigeria Centre for Disease Control (NCDC), 2017). The outbreak was exacerbated by the shortage of vaccine (British Broascasting Co-operation (BBC), 2017; News24, 2017; Nigeria Centre for Disease Control, 2017; Voice of America (VOA), 2017). This is due to the fact that the meningitis C polysaccharide vaccines are currently being phased out in other parts of the world (World Health Organization (WHO), 2017). Unfortunately, the more effective and long-lasting conjugate vaccines are not readily and promptly available (World Health Organization (WHO), 2017).

In this study, we developed two types of mathematical models, ordinary differential equation

model (which we will call non-impulsive model (2.6)) and impulsive differential equation model (which we will refer to as impulsive model (2.16)) respectively. Theoretical analysis of the two models showed that the disease free equilibrium of non-impulsive model is locally asymptotically stable if the reproduction number, $\mathcal{R}_0$, is less than one. While the disease free periodic solution of the impulsive model is locally asymptotically stable if the threshold quantity $\mathcal{R}_p$ is less than one. The biological implication of these results is that we will be able to control the disease in the community whenever these quantities ($\mathcal{R}_0$ and $\mathcal{R}_p$) are less that one. Note that $\mathcal{R}_p$ is not the reproduction number of the impulsive system, it is just a threshold that guarantees the stability of the equilibrium solutions.

Next, we carried out sensitivity analysis of the non-impulsive model (2.6) using the basic reproduction number as the response function. The results shown with the bar plot of the sensitivity indices in Figure 2.3 reveals that the transmission probability (β), disease modification parameter (η), recovery rate of carrier (γ_C) and vaccine efficacy (ε) are the parameters with most influence on the basic reproduction number. The implication of these results is that whenever we increase the transmission probability (β) by 10% there will be a corresponding 10% increase in disease burden since the sensitivity index is 1.00. Similarly, a 10% increase in recovery rate among the carrier population (γ_C) and vaccine efficacy (ε) will lead respectively to a 6.2% and 14% decrease in disease burden since their respective sensitivity indices are -0.619 and -1.388.

We then assess the impact of vaccine efficacy and its coverage in eradicating the disease in the population using the non-impulsive model (2.6) since we can easily assess the impact of vaccine efficacy (ε) unlike the transmission probability (β) and the recovery rate of the carrier population, γ_C. Agusto & Leite (2019) investigated the effect of controlling meningitis in Nigeria using optimal control with two time-dependent controls on vaccination and facial masks. The use of facial masks act to reduce the transmission probability (β). We observed from the bar plot showing the effect of vaccine efficacy and vaccine coverage using the

reproduction number in Figures 2.4 and 2.5 that meningitis can effectively be controlled in the population using an imperfect vaccine with an efficacy above 75% and high vaccine coverage rate of at least 85%.

Vaccine is a highly effective control strategy against the disease, and "can drastically reduce the magnitude of the epidemic" (World Health Organization (WHO), 2017). Individuals in the meningitis belt have mostly been protected against meningitis A by the use of Men A conjugate vaccine (MACV) which was introduced in 2010 (World Health Organization (WHO), 2017). Nineteen countries have administered the vaccine with over 260 million people been vaccinated leading to over 57% reduction in meningitis cases. Unfortunately, this is not the case with Men C (United Nations Children's Fund (UNICEF), 2017; World Health Organization (WHO), 2017) as observed in the 2017 meningitis C outbreak in Nigeria, most of the population are not protected against this serogroup. In a future study we will investigate the effect of vaccination in the strain replacement of meningitis A by meningitis C in Nigeria.

Hence, to ensure the protection of the population, particularly people living in hard-to-reach areas of the region, we propose the use of pulse vaccination which is an effective way of controlling disease transmission with some practical advantages (Agur et al., 1993; d'Onofrio, 2005; Gao & Chen, 2005; Shulgin et al., 1998; Stone et al., 2000; Zou et al., 2009). It is sometimes more effective than constant vaccination (Li & Yang, 2011; Li & Cui, 2009; Röst & Vizi, 2014; Shulgin et al., 1998). In a different study we will access the impact of using an optimal vs impulse control in curtailing the transmission of the disease.

In this study, we use the impulsive model (2.16) to assess the impact of vaccinating the populace. Our results shows that vaccinating with a lower rate slowly protects and prevent the disease transmission unlike when a high vaccination rate is used (see Figure 2.6) more people are protected at a faster rate. Furthermore, we observed in Figure 2.7 that vaccina-

tion, regardless of the rate, offers protection against the disease. We observed further that as we increase the vaccination pulses over a 30 days period (see Figure 2.8) more and more people in the population are protected. We expect that this vaccination strategy will help increase the herd immunity of the community particularly those in hard-to-reach places of the country where the disease is endemic.

2.6.2 Conclusions

In this study, we developed two mathematical models, an ordinary differential equation model with constant vaccination and an impulsive differential equation model with impulsive vaccination. The main results obtained from the theoretical analysis of two mathematical models, non-impulsive model (2.6) and impulsive model (2.16) developed in this study, the results obtained from the determination of a minimum vaccine efficacy and coverage needed for effective control of meningitis, and the results from the numerical exploration are summarized below.

(i) The non-impulsive meningitis model has a locally asymptotically stable disease free equilibrium whenever $\mathcal{R}_0 < 1$ and unstable if $\mathcal{R}_0 > 1$;

(ii) Sensitivity analysis reveals transmission probability β, recovery rate of carrier γ_C and vaccine efficacy ε as the important parameter impacting the reproduction number;

(iii) Meningitis can be effectively controlled in the population using an imperfect vaccine with an efficacy $> 75\%$ and high vaccine coverage rate of at least 85%;

(iv) The impulsive model is locally asymptotically stable if the threshold $\mathcal{R}_p < 1$;

(v) Numerical simulations of the impulsive model shows that meningitis can be curtailed by the use of impulsive vaccine in the population.

(vi) Infection decreases with the number of vaccination pulses.

Chapter 3

Modeling Co-infection of Meningitis A and C

3.1 Introduction

In the previous chapter, we focused on the control of meningitis in the population, by accessing the effect of vaccination in eradicating the disease. This entails the use of both constant and impulsive vaccination schemes. However, since meningitis is a disease with multiple strains, it should be noted that geographical distribution and epidemic potential of this disease differs according to each serogroup. For example, as mentioned by Peterson et al. (2019), *Neisseria meningitis* W (NmW) was the predominant serogroup in most of Africa except Algeria, Cameroon, Chad, Guinea and Nigeria. In addition, *Neisseria meningitis* A (NmA) was reported as the most prevalent in Cameroon, Chad and Guinea, while *Neisseria meningitis* C (NmC) is the most prevalent serogroup in Nigeria. In the Americas, *Neisseria meningitis* B (NmB) was reported as the most prevalent serogroup, while the second most prevalent serogroup is *Neisseria meningitis* Y (NmY) within North America. Peterson et al. (2019) stated NmB as the predominated serogroup within Europe. In their study, India was the only country where reported cases were identified as NmA.

In the African meningitis belt, serogroup A was responsible for the large majority of epidemics prior to 2010. However, the progressive introduction of a meningococcal A conjugate vaccine (MenAfriVac) to the epidemic prone areas in the African meningitis belt has brought about a dramatic reduction in cases of this serogroup and the elimination of its epidemics in these areas. On the other hand, the relative proportion of cases due to other serogroups (W, X and C) and *Streptococcus pneumoniae* has increased, thus replacing the dominant

strain A in the population (World Health Organization (WHO), 2019a). For instance, between January 1996 to June 1996 a severe meningitis serogroup A outbreak occurred in Nigeria with 109,580 cases and 11,717 deaths, with a 10.69% fatality rate (World Health Organization (WHO), 2017). Since 2010, Nigeria has been carrying out mass immunization campaigns with MenAfriVac against the meningitis A serogroup. This has led to a decline in the incidence of meningitis A serogroup in this region. However, since 2013 Nigeria has been experiencing large outbreaks of a hyper-invasive strain of meningococcal meningitis serogroup C. In 2015, over 2500 cases of the disease were reported in the country (World Health Organization (WHO), 2017). Another outbreak occurred in 2017 in Nigeria with over 9,902 cases and 602 deaths in thirty-one states of the country (Nigeria Centre for Disease Control (NCDC), 2017).

In this section, we formulate a deterministic model with multiple strains of meningococcal meningitis (serogroup A and serogroup C), to study the dynamical behavior of meningitis A and meningitis C in the presence of vaccination under different scenarios. The scenarios considered in this thesis include the more generalized model with co-infected individuals of strain A and C, and also the model with the absence of individuals co-infected with the two strains. In addition, since there is no data on the ability of individuals to be infected with the two strain at the same time, we consider the case where we assume that co-infected individuals can only transmit the strain with the highest transmission probability (due to within-host competitive advantage).

3.2 Formulation of the model

3.2.1 Formulation of the full meningitis model with co-infection

The model sub-divides the total human population at time t, denoted by $N(t)$, into susceptible individuals (S), vaccinated individuals (V), carrier individuals with strain A (C_A), infected individuals with strain A (I_A), recovered individuals from strain A (R_A), carrier

individuals with strain C (C_C), infected individuals with strain C (I_C), recovered individuals from strain C (R_c), carrier individuals with both strain A and C (C_{AC}), infected individuals with both strain A and C (I_{AC}), and recovered individuals from both strain A and C (R_{AC}). Thus, the total human population is given by

$$N(t) = S + V + C_A + I_A + R_A + C_C + I_C + R_C + C_{AC} + I_{AC} + R_{AC}$$

Flow from one class to the other is as a result of interaction with respect to the disease. The population of susceptible humans is generated by the recruitment rate which is by birth or immigration at rate π, immunity loss of vaccinated individuals ω and by vaccine waning of strain A, C and AC individuals at rate κ_A, κ_C and κ_{AC} respectively. The susceptible population is reduced by natural death at rate μ and by vaccination, at rate ν. In addition, considering that susceptible individuals can be infected by contact with strain A, or strain C carrier or infected individuals, we further consider the scenario with super-infection, where susceptibles are becoming infected through contact with the co-infected individuals. However, such individual will progress to the strain population that has the within-host competitive advantage in co-infected individuals. The susceptible population is depopulated by the infection function of the susceptible by strain A, strain C, and by strain AC carrier and infected individuals given as

$$\lambda_A = \frac{\beta_A(\eta C_A + I_A)}{N}, \lambda_C = \frac{\beta_C(\eta C_C + I_C)}{N}, \lambda_{AC} = \frac{\beta_{AC}(\eta C_{AC} + I_{AC})}{N}, \lambda_{CA} = \frac{\beta_{CA}(\eta C_{AC} + I_{AC})}{N}$$

The parameters β_A, and β_C, are transmission probabilities per contact for strain A, and strain C respectively. β_{AC} indicates that strain A is stronger in transmission in co-infected individuals while β_{CA} indicates that strain C is stronger in transmission in co-infected individuals. Thus, λ_{AC} is the force of infection which indicates when strain A have within-host advantage of over strain C, while λ_{CA} is the force of infection which indicates when strain C have within-host advantage of over strain A. Furthermore, the modification parameter $\eta < 1$

accounts for the assumed increase in the relative infectiousness of infected individuals in the I_A, I_C and I_{AC} classes compared to those in the corresponding carrier classes C_A, C_C and C_{AC}. In other words, the model employs the fact that carrier individuals can transmit infection, the rate at which this occurs is smaller than the rate at which infectious individuals transmit infection (since, in general, infectiousness is positively correlated with viral load). Hence, the susceptible population at any time t is given as

$$\frac{dS}{dt} = \pi + \omega V + \kappa_A R_A + \kappa_C R_C + \kappa_{AC} R_{AC} - (\lambda_A + \lambda_C + \lambda_{AC} + \lambda_{CA})S - (\nu + \mu)S$$

The vaccinated population is obtained as a result of vaccination on the susceptible class at a rate ν. However, owing to imperfect vaccine, the vaccinated population is reduced due to breakthrough infection *via* contact with carrier or infected individual (at a reduced rate of fraction $(1 - \varepsilon)$, where $0 < \varepsilon < 1$ is the vaccine efficacy). The vaccinated population is further depopulated via natural death at rate μ, and waning vaccine at rate ω. The vaccinated population is then given as follows

$$\frac{dV}{dt} = \nu S - (1 - \varepsilon)(\lambda_A + \lambda_C + \lambda_{AC} + \lambda_{CA})V - (\omega + \mu)V$$

Strain A carrier individuals derive from infection occuring in both the susceptible and vaccinated populations. This group is decreased by the force of infection for strain C at the rate $\theta_C \lambda_C$, disease progression to strain A infected population at rate σ_A, and natural death at rate μ. The modification parameter $0 \leq \theta_C \leq 1$ accounts for the assumed reduction of susceptibility to strain C of individuals who are already infected with strain A. Thus, the strain A carrier population is given below as

$$\frac{dC_A}{dt} = (\lambda_A + \lambda_{AC})S + (1 - \varepsilon)(\lambda_A + \lambda_{AC})V - \theta_C \lambda_C C_A - (\sigma_A + \mu)C_A$$

The strain A infected population is generated following the progression from the strain A carrier population. This population is reduced by the individual contact with strain C carrier or infected individuals $\theta_C\lambda_C$, recovery at rate γ_A, natural death μ and death resulting from complication of infection with strain A at rate δ_A. $\theta_C\lambda_C$ accounts for the assumed reduction of susceptibility to strain C of individuals who are already infected with strain A. The strain A infected population is given as

$$\frac{dI_A}{dt} = \sigma_A C_A - \theta_C\lambda_C I_A - (\gamma_A + \mu + \delta_A)I_A$$

The strain A recovered individuals increase in number as a result of recoveries from strain A infected population at rate γ_A. Depopulation of this population results from loss of immunity at rate κ_A and natural death at rate μ. The strain A recovered population is then given as

$$\frac{dR_A}{dt} = \gamma_A I_A - (\kappa_A + \mu)R_A$$

Strain C carrier individuals are derived infection coming of both susceptible and vaccinated population. This is further depopulated by the force of infection for strain A at the rate $\theta_A\lambda_A$, disease progression to strain C infected population at rate σ_C and natural death at rate μ.The modification parameter $0 \leq \theta_A \leq 1$ accounts for the assumed reduction of susceptibility to strain A of individuals who is already infected with strain C. Thus, strain C carrier population is given below as

$$\frac{dC_C}{dt} = (\lambda_C + \lambda_{CA})S + (1-\varepsilon)(\lambda_C + \lambda_{CA})V - \theta_A\lambda_A C_C - (\sigma_C + \mu)C_C$$

The strain C infected population is generated following by progression from the strain C carrier population. This population is reduced by the individual contact with strain A carrier or infected individuals $\theta_A\lambda_A$, recovery at rate γ_C, natural death μ and death resulting from complication of infection with strain C at rate δ_C. $\theta_A\lambda_A$ accounts for the assumed

reduction of susceptibility to strain A of individuals who are already infected with strain C. The strain C infected population is given as

$$\frac{dI_C}{dt} = \sigma_C C_C - \theta_A \lambda_A I_C - (\gamma_C + \mu + \delta_C) I_C$$

The strain C recovered individuals increase in number as a result of recoveries from the strain C infected population at rate γ_C. Depopulation of this population results from loss of immunity at rate κ_C and natural death at rate μ. The strain C recovered population is then given as

$$\frac{dR_C}{dt} = \gamma_C I_C - (\kappa_C + \mu) R_C$$

The coinfected strain A and C carrier individuals derive from infection in both strain A carrier and infected populations and in strain C carrier and infected populations. This is further depopulated by disease progression to coinfected strain AC infected population at rate σ_{AC}. Furthermore, the population is depopulated by natural death at rate μ. The coinfected strain AC carrier population is given below as

$$\frac{dC_{AC}}{dt} = \theta_A \lambda_A C_C + \theta_C \lambda_C C_A - (\sigma_{AC} + \mu) C_{AC}$$

The coinfected strain A and C infected population derive from infection coming of both strain A infected and strain C infected population, and from progression from the coinfected strain AC carrier population. This population is reduced by recovery at rate γ_{AC}, natural death μ and death resulting from complication of infection with strain AC at rate δ_{AC}. The coinfected strain AC infected population is then given as

$$\frac{dI_{AC}}{dt} = \sigma_{AC} C_{AC} + \theta_A \lambda_A I_C + \theta_C \lambda_C I_A - (\gamma_{AC} + \mu + \delta_{AC}) I_{AC}$$

The coinfected Strain A and C recovered individuals increase in number as a result of recoveries from the strain AC infected population at rate γ_{IAC}. Depopulation of this population

result from loss of immunity at rate κ_{AC} and natural death at rate μ. The coinfected strain AC recovered population is given as

$$\frac{dR_{AC}}{dt} = \gamma_{AC} I_{AC} - (\kappa_{AC} + \mu) R_{AC}$$

Hence, the overall process explained above leads to the model for the transmission dynamics of meningitis in a population, given by the following deterministic system of nonlinear ordinary differential equations:

$$\begin{aligned}
\frac{dS}{dt} &= \pi + \omega V + \kappa_A R_A + \kappa_C R_C + \kappa_{AC} R_{AC} - (\lambda_A + \lambda_C + \lambda_{AC} + \lambda_{CA}) S - (\nu + \mu) S \\
\frac{dV}{dt} &= \nu S - (1 - \varepsilon)(\lambda_A + \lambda_C + \lambda_{AC} + \lambda_{CA}) V - (\omega + \mu) V \\
\frac{dC_A}{dt} &= (\lambda_A + \lambda_{AC}) S + (1 - \varepsilon)(\lambda_A + \lambda_{AC}) V - \theta_C \lambda_C C_A - (\sigma_A + \mu) C_A \\
\frac{dI_A}{dt} &= \sigma_A C_A - \theta_C \lambda_C I_A - (\gamma_A + \mu + \delta_A) I_A \\
\frac{dR_A}{dt} &= \gamma_A I_A - (\kappa_A + \mu) R_A \\
\frac{dC_C}{dt} &= (\lambda_C + \lambda_{CA}) S + (1 - \varepsilon)(\lambda_C + \lambda_{CA}) V - \theta_A \lambda_A C_C - (\sigma_C + \mu) C_C \\
\frac{dI_C}{dt} &= \sigma_C C_C - \theta_A \lambda_A I_C - (\gamma_C + \mu + \delta_C) I_C \\
\frac{dR_C}{dt} &= \gamma_C I_C - (\kappa_C + \mu) R_C \\
\frac{dC_{AC}}{dt} &= \theta_A \lambda_A C_C + \theta_C \lambda_C C_A - (\sigma_{AC} + \mu) C_{AC} \\
\frac{dI_{AC}}{dt} &= \sigma_{AC} C_{AC} + \theta_A \lambda_A I_C + \theta_C \lambda_C I_A - (\gamma_{AC} + \mu + \delta_{AC}) I_{AC} \\
\frac{dR_{AC}}{dt} &= \gamma_{AC} I_{AC} - (\kappa_{AC} + \mu) R_{AC}
\end{aligned} \tag{3.1}$$

A schematic flow diagram of the model (3.1) is depicted in Figure 3.1, and the associated model variables and parameters description are presented in Table 3.1.

Variable	Description
S	Susceptible individuals
V	Vaccinated individuals
C_A, C_C, C_{AC}	Carrier individuals with strain A, C, A and C
I_A, I_C, I_{AC}	Infected individuals with strain A, C, A and C
R_A, R_C, R_{AC}	Recovered individuals from strain A, C, A and C
Parameter	**Description**
π	Recruitment rate
ν	Vaccination rate
ε	Vaccine efficacy
ω	Vaccine waning rate
β_i	Transmission probability
η, θ_A, θ_C	Disease modification parameter
μ	Natural death rate
$\gamma_A, \gamma_C, \gamma_{AC}$	Recovery rate of infected individuals with strain A, C, A and C
$\sigma_A, \sigma_C, \sigma_{AC}$	Progression rate of carrier individuals with strain A, C, A and C to infected
$\kappa_A, \kappa_C, \kappa_{AC}$	Immunity waning rate of recovered individuals from strain A, C, A and C
δ_A, δ_c, δ_{Ac}	Disease induced death rate

Table 3.1: Description of the variables and parameters of the full meningitis model (3.1).

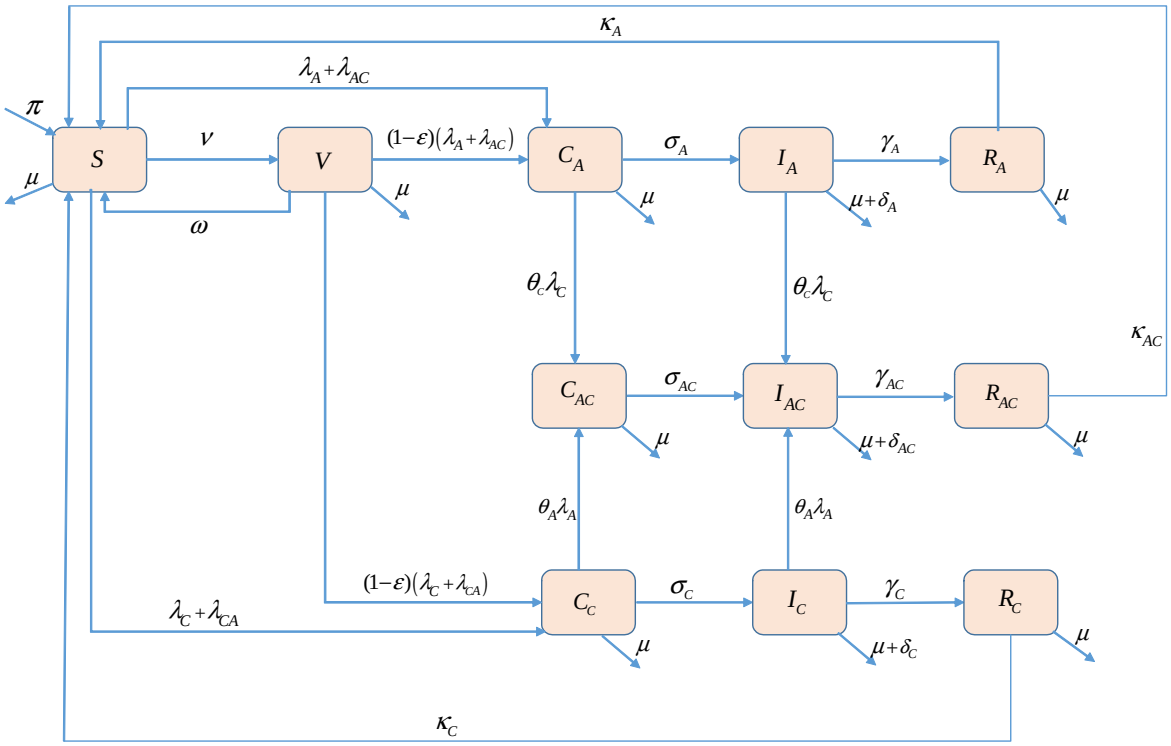

Figure 3.1: Schematic illustration of the full co-infection meningitis model (3.1).

3.2.2 Formulation of the sub-model without co-infection

In this section, we present a sub-model which assumed the absence of co-infected individuals with the two strains in the population. Hence, by setting the variables and parameters of the co-infected individuals to zero, the system of equation for the full model (3.1) reduces to the following system of equations:

$$\begin{aligned}
\frac{dS}{dt} &= \pi + \omega V + \kappa_A R_A + \kappa_C R_C - (\lambda_A + \lambda_C)S - (\nu + \mu)S \\
\frac{dV}{dt} &= \nu S - (1-\varepsilon)(\lambda_A + \lambda_C)V - (\omega + \mu)V \\
\frac{dC_A}{dt} &= \lambda_A S + (1-\varepsilon)\lambda_A V - (\sigma_A + \mu)C_A \\
\frac{dI_A}{dt} &= \sigma_A C_A - (\gamma_A + \mu + \delta_A)I_A \\
\frac{dR_A}{dt} &= \gamma_A I_A - (\kappa_A + \mu)R_A \\
\frac{dC_C}{dt} &= \lambda_C S + (1-\varepsilon)\lambda_C V - (\sigma_C + \mu)C_C \\
\frac{dI_C}{dt} &= \sigma_C C_C - (\gamma_C + \mu + \delta_C)I_C \\
\frac{dR_C}{dt} &= \gamma_C I_C - (\kappa_C + \mu)R_C
\end{aligned} \tag{3.2}$$

The schematic flow diagram of the model (3.2) is depicted in Figure 3.2.

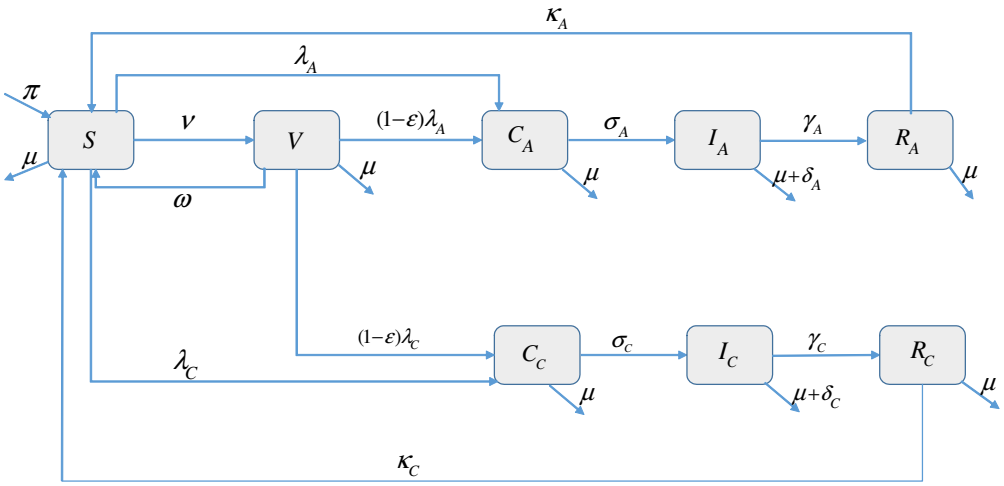

Figure 3.2: Schematic illustration of the meningitis sub-model without co-infection. The full model is reduced to (3.2) when there are no individuals that are infected with both strains of the disease.

3.3 Analysis of the full meningitis model with co-infection

3.3.1 Basic qualitative properties of the full model

In this section, the basic qualitative properties of the model (3.1) will be explored.

Positivity and Boundedness of Solutions

For the meningitis model (3.1) to be epidemiologically meaningful, it is important to prove that all its state variables are non-negative for all time $t \geq 0$. In other words, solutions of the model system (3.1) with non-negative initial data will remain non-negative for all time $t > 0$.

Lemma 3 *Let the initial data* $S(0) > 0$, $V(0) \geq 0$, $C_A(0) \geq 0$, $I_A(0) \geq 0$, $R_A(0) \geq 0$, $C_C(0) \geq 0$, $I_C(0) \geq 0$, $R_C(0) \geq 0$, $C_{AC}(0) \geq 0$, $I_{AC}(0) \geq 0$, *and* $R_{AC}(0) \geq 0$. *Then, the solu-*

tions $(S(t), V(t), C_A(t), I_A(t), R_A(t), C_C(t), I_C(t), R_C(t), C_{AC}(t), I_{AC}(t), R_{AC}(t))$ *of the meningitis model* (3.1) *are non-negative for all* $t > 0$. *Furthermore*

$$\lim_{t\to\infty} \sup N(t) \leq \frac{\pi}{\mu}.$$

Proof. Let $t_1 = \sup\{t > 0 : S(t) > 0, V(t) > 0, C_A(t) > 0, I_A(t) > 0, R_A(t) > 0, C_C(t) > 0, I_C(t) > 0, R_C(t) > 0, C_{AC}(t) > 0, I_{AC}(t) > 0, R_{AC}(t) > 0 \in [0, t]\}$. Thus, $t_1 > 0$. It follows from the first equation of the system (3.1), that

$$\begin{aligned} \frac{dS}{dt} &= \pi + \omega V + \kappa_A R_A + \kappa_C R_C + \kappa_{AC} R_{AC} - (\lambda_A + \lambda_C + \lambda_{AC} + \lambda_{CA} + \nu + \mu)S \\ &\geq -(\lambda_A + \lambda_C + \lambda_{AC} + \lambda_{CA} + \nu + \mu) \end{aligned}$$

So that,

$$\frac{dS}{dt} + (\lambda_A + \lambda_C + \lambda_{AC} + \lambda_{CA} + \nu_A + \mu)\, S \geq 0$$

Multiplying by Integrating factor I.F, $exp\left\{\int_0^{t_1} [\lambda_A(\psi) + \lambda_C(\psi) + \lambda_{AC}(\psi) + \lambda_{CA}(\psi)]\, d\psi + (\nu + \mu)t\right\}$, gives

$$\frac{d}{dt}\left[S(t) exp\left\{\int_0^{t_1} [\lambda_A(\psi) + \lambda_C(\psi) + \lambda_{AC}(\psi) + \lambda_{CA}(\psi)]\, d\psi + (\nu + \mu)t\right\}\right] \geq 0 \quad (3.3)$$

Integrating both sides of inequalitiy (3.3) gives

$$S(t) exp\left\{\int_0^{t_1} [\lambda_A(\psi) + \lambda_C(\psi) + \lambda_{AC}(\psi) + \lambda_{CA}(\psi)]\, d\psi + (\nu + \mu)t\right\} \geq C$$

Note that for the value of C, at $t = 0$ gives $S(0)$. Thus,

$$S(t) \geq S(0) exp\left\{-(\nu + \mu)t - \int_0^{t_1} [\lambda_A(\psi) + \lambda_C(\psi) + \lambda_{AC}(\psi) + \lambda_{CA}(\psi)]\, d\psi\right\} > 0.$$

It can similarly be shown that $V(t) > 0, C_A(t) > 0, I_A(t) > 0, R_A(t) > 0, C_C(t) > 0, I_C(t) > 0, R_C(t) > 0, C_{AC}(t) > 0, I_{AC}(t) > 0, R_{AC}(t) > 0$ for all $t > 0$.

Invariant region

Consider the biological feasible region

$$\mathcal{D} = \{(S, V, C_A, I_A, R_A, C_C, I_C, R_C, C_{AC}, I_{AC}, R_{AC}) \in \mathcal{R}_+^{11}; N \leq \frac{\pi}{\mu}\} \tag{3.4}$$

Lemma 4 *The region $\mathcal{D}$ defined by* (3.4) *is positively-invariant and attracting for model* (3.1) *with non-negative initial conditions in $\mathcal{R}_+^{11}$.*

Proof. Let $[S(t), V(t), C_A(t), I_A(t), R_A(t), C_C(t), I_C(t), R_C(t), C_{AC}(t), I_{AC}(t), R_{AC}(t)] \in \mathcal{R}_+^{11}$, be the solution of model (3.1) with non-negative initial conditions. The rate of change of the total population is obtained by adding up the compartments of the system (3.1) to give

$$\frac{dN}{dt} = \pi - \mu N - \delta_A I_A - \delta_c I_C - \delta_{AC} I_{AC} \leq \pi - \mu N \tag{3.5}$$

Since, $\frac{dN}{dt} \leq \pi - \mu N$, it follows that $\frac{dN}{dt} \leq 0$ if $N(t) \geq \frac{\pi}{\mu}$. Considering,

$$\frac{dN}{dt} + \mu N = \pi \tag{3.6}$$

Using the integrating factor method, so that equation (3.6) can be written as

$$d(Ne^{\mu t}) = \pi e^{\mu t} dt$$

Integrating both sides by the limit $0 < t$

$$\int_0^t d(Ne^{\mu t}) = \int_0^t \pi e^{\mu t} dt$$

$$N(t)e^{\mu t} - N(0) = \frac{\pi}{\mu}\left[e^{\mu t}\right]_0^t$$

$$N(t)e^{\mu t} - N(0) = \frac{\pi}{\mu}\left[e^{\mu t} - 1\right]$$

Hence,

$$N(t) = N(0)e^{-\mu t} + \frac{\pi}{\mu}\left[1 - e^{-\mu t}\right].$$

In particular, $N(t) \leq \frac{\pi}{\mu}$, if $N(0) \leq \frac{\pi}{\mu}$. Thus, every solution of the model (3.1) with initial conditions in $\mathcal{D}$ remains there for $t > 0$. Thus, $\mathcal{D}$ is a positive-invariant. Hence, it is sufficient to consider the dynamics of the flow generated by (3.1) in $\mathcal{D}$. In this region, the model is said to be mathematically and epidemiologically well posed (Hethcote, 2000). Thus, every solution of the meningitis model (3.1) with initial conditions in $\mathcal{D}$ remains in $\mathcal{D}$ for all $t > 0$.

3.3.2 Stability of the disease free equilibrium (DFE)

The meningitis model (3.1) has a disease free equilibrium obtained by setting the right-hand sides of the equations in the model to zero and solving at $C_A = C_C = C_{AC} = I_A = I_C = I_{AC} = 0$. Thus, the disease free equilibrium is given by

$$\begin{aligned}\mathcal{E}_0 &= (S^*, V^*, C_A^*, I_A^*, R_A^*, C_C^*, I_C^*, R_C^*, C_{AC}^*, I_{AC}^*, R_{AC}^*) \\ &= \left(\frac{\pi(\omega+\mu)}{\mu(\nu+\mu+\omega)}, \frac{\pi\nu}{\mu(\nu+\mu+\omega)}, 0, 0, 0, 0, 0, 0, 0, 0, 0\right) \qquad (3.7)\end{aligned}$$

The linear stability of $\mathcal{E}_0$ can be established using the next generation operator method. Using the infected compartment, matrices F and V, for the transmission matrix (new infec-

tion) and the transition matrix (remaining transfer terms) are given respectively by

$$F = \begin{pmatrix} \frac{\beta_A \eta}{N^*} P & \frac{\beta_A}{N^*} P & 0 & 0 & \frac{\beta_{AC} \eta}{N^*} P & \frac{\beta_{AC}}{N^*} P \\ 0 & 0 & 0 & 0 & 0 & 0 \\ 0 & 0 & \frac{\beta_C \eta}{N^*} P & \frac{\beta_C}{N^*} P & \frac{\beta_{CA} \eta}{N^*} P & \frac{\beta_{CA} \eta}{N^*} P \\ 0 & 0 & 0 & 0 & 0 & 0 \\ 0 & 0 & 0 & 0 & 0 & 0 \\ 0 & 0 & 0 & 0 & 0 & 0 \end{pmatrix} \tag{3.8}$$

and

$$V = \begin{pmatrix} k_3 & 0 & 0 & 0 & 0 & 0 \\ -\sigma_A & k_4 & 0 & 0 & 0 & 0 \\ 0 & 0 & k_6 & 0 & 0 & 0 \\ 0 & 0 & -\sigma_C & k_7 & 0 & 0 \\ 0 & 0 & 0 & 0 & k_9 & 0 \\ 0 & 0 & 0 & 0 & -\sigma_{AC} & k_{10} \end{pmatrix} \tag{3.9}$$

Where $k_3 = \sigma_A + \mu$, $k_4 = \gamma_A + \mu + \delta_A$, $k_6 = \sigma_C + \mu$, $k_7 = \gamma_C + \mu + \delta_C$, $k_9 = \sigma_{AC} + \mu$, $k_{10} = \gamma_{AC} + \mu + \delta_{AC}$ and $P = S^* + (1 - \varepsilon)V^*$. It follows that the reproduction number of the meningitis model (3.1) is given by

$$\begin{aligned} \mathcal{R}_0 &= \rho(FV^{-1}) \\ &= max \left\{ \frac{\beta_A(\eta k_4 + \sigma_A)[S^* + (1-\varepsilon)V^*]}{k_3 k_4 N^*}, \qquad \frac{\beta_C(\eta k_7 + \sigma_C)[S^* + (1-\varepsilon)V^*]}{k_6 k_7 N^*} \right\} \end{aligned} \tag{3.10}$$

where ρ is the spectral radius (highest eigenvalue) of the matrix FV^{-1} and $N^* = S^* + V^*$. The above threshold quantity (basic reproduction number) is defined as

$$\mathcal{R}_0 = max \left\{ \mathcal{R}_{0A}, \quad \mathcal{R}_{0C} \right\}$$

where $\mathcal{R}_{0A}$ and $\mathcal{R}_{0C}$ are the associated reproduction numbers for strain A and strain C respectively, given by

$$\mathcal{R}_{0A} = \frac{\beta_A(\eta k_4 + \sigma_A)[S^* + (1-\varepsilon)V^*]}{k_3 k_4 N^*}, \qquad \mathcal{R}_{0C} = \frac{\beta_C(\eta k_7 + \sigma_C)[S^* + (1-\varepsilon)V^*]}{k_6 k_7 N^*} \quad (3.11)$$

Theorem 4 *The meningitis model* (3.1) *disease-free equilibrium* $\mathcal{E}_0$ *is locally-asymptotically stable (LAS) if* $\mathcal{R}_0 < 1$ *and unstable if* $\mathcal{R}_0 > 1$.

The basic reproduction number $\mathcal{R}_0$ measures the average number of new infections generated by a single infected person during his or her infectious period in a population that is fully susceptible. Thus, the epidemiological implication of Theorem 4 above is that meningitis will be controlled in the population whenever $\mathcal{R}_0 < 1$ if the initial sizes of the population of the model are in the basin of attraction of the DFE ($\mathcal{E}_0$).

3.3.3 Existence and Stability of Boundary Equilibria

Here, we will explore the possible equilibria of the model. There are two possible single-strain infection equilibria $\mathcal{E}_1 = (S^{**}, V^{**}, C_A^{**}, I_A^{**}, R_A^{**})$ and $\mathcal{E}_2 = (S^{**}, V^{**}, C_C^{**}, I_C^{**}, R_C^{**})$ for existence of strain A and C respectively. Also, the model (3.1) has a double strain infection equilibrium $\mathcal{E}_3 = (S^{**}, V^{**}, C_A^{**}, I_A^{**}, R_A^{**}, C_C^{**}, I_C^{**}, R_C^{**}, C_{AC}^{**}, I_{AC}^{**}, R_{AC}^{**})$.

Strain A-only Boundary Equilibrium ($\mathcal{E}_1$)

Here we will establish the conditions for the existence of an equilibrium for which strain A-only is endemic in the population. The meningitis model (3.1) with strain A-only in the

absence of strain C reduces to the system of equations below,

$$\begin{aligned}
\frac{dS}{dt} &= \pi + \omega V + \kappa_A R_A - \lambda_A S - k_1 S \\
\frac{dV}{dt} &= \nu S - p\lambda_A V - k_2 V \\
\frac{dC_A}{dt} &= \lambda_A S + p\lambda_A V - k_3 C_A \\
\frac{dI_A}{dt} &= \sigma_A C_A - k_4 I_A \\
\frac{dR_A}{dt} &= \gamma_A I_A - k_5 R_A
\end{aligned} \tag{3.12}$$

where $k_1 = \nu + \mu$, $k_2 = \omega + \mu$, $k_3 = \sigma_A + \mu$, $k_4 = \gamma_A + \mu + \delta_A$, $k_5 = \kappa_A + \mu$, $p = 1 - \varepsilon$. The infection equilibrium of the strain A-only system (3.12) in terms of the force of infection (λ_A^{**}) is given as $\mathcal{E}_1 = (S^{**}, V^{**}, C_A^{**}, I_A^{**}, R_A^{**})$ where,

$$\begin{aligned}
S^{**} &= \frac{\pi k_3 k_4 k_5 (p\lambda_A^{**} + k_2)}{k_3 k_4 k_5 (\lambda_A^{**} + k_1)(p\lambda_A^{**} + k_2) - k_3 k_4 k_5 \omega\nu - \lambda_A^{**}\kappa_A\gamma_A(p\lambda_A^{**} + k_2 + p\nu)}, \\
V^{**} &= \frac{\nu\pi k_3 k_4 k_5}{k_3 k_4 k_5 (\lambda_A^{**} + k_1)(p\lambda_A^{**} + k_2) - k_3 k_4 k_5 \omega\nu - \lambda_A^{**}\kappa_A\gamma_A(p\lambda_A^{**} + k_2 + p\nu)}, \\
C_A^{**} &= \frac{\lambda_A^{**}\pi k_4 k_5 (p\lambda_A^{**} + k_2 + p\nu)}{k_3 k_4 k_5 (\lambda_A^{**} + k_1)(p\lambda_A^{**} + k_2) - k_3 k_4 k_5 \omega\nu - \lambda_A^{**}\kappa_A\gamma_A(p\lambda_A^{**} + k_2 + p\nu)}, \\
I_A^{**} &= \frac{\lambda_A^{**}\pi\sigma_A k_5 (p\lambda_A^{**} + k_2 + p\nu)}{k_3 k_4 k_5 (\lambda_A^{**} + k_1)(p\lambda_A^{**} + k_2) - k_3 k_4 k_5 \omega\nu - \lambda_A^{**}\kappa_A\gamma_A(p\lambda_A^{**} + k_2 + p\nu)}, \\
R^{**} &= \frac{\lambda_A^{**}\pi\gamma_A\sigma_A (p\lambda_A^{**} + k_2 + p\nu)}{k_3 k_4 k_5 (\lambda_A^{**} + k_1)(p\lambda_A^{**} + k_2) - k_3 k_4 k_5 \omega\nu - \lambda_A^{**}\kappa_A\gamma_A(p\lambda_A^{**} + k_2 + p\nu)}
\end{aligned} \tag{3.13}$$

The force of infection (λ_A^{**}) is given as

$$\lambda_A^{**} = \frac{\beta_A(\eta C_A^{**} + I_A^{**})}{N^{**}} \tag{3.14}$$

The total population is obtained by summing up the sub-populations as below

$$\begin{aligned} N^{**} &= S^{**} + V^{**} + C_A^{**} + I_A^{**} + R_A^{**} \\ &= \frac{\pi k_3 k_4 k_5 (p\lambda_A^{**} + k_2 + \nu) + (\lambda_A^{**}\pi k_4 k_5 + \lambda_A^{**}\pi\sigma_A k_5 + \lambda_A^{**}\pi\gamma_A\sigma_A)\,(p\lambda_A^{**} + k_2 + p\nu)}{k_3 k_4 k_5(\lambda_A^{**} + k_1)(p\lambda_A^{**} + k_2) - k_3 k_4 k_5 \omega\nu - \lambda_A^{**}\kappa_A\gamma_A(p\lambda_A^{**} + k_2 + p\nu)} \end{aligned} \tag{3.15}$$

Substituting equation (3.13) amd (3.15) into (3.14) gives,

$$\lambda_A^{**} = \frac{\lambda_A^{**}\beta_A(\eta\pi k_4 k_5 + \pi\sigma_A k_5)(p\lambda_A^{**} + k_2 + p\nu)}{\pi k_3 k_4 k_5 (p\lambda_A^{**} + k_2 + \nu) + (\lambda_A^{**}\pi k_4 k_5 + \lambda_A^{**}\pi\sigma_A k_5 + \lambda_A^{**}\pi\gamma_A\sigma_A)\,(p\lambda_A^{**} + k_2 + p\nu)} \tag{3.16}$$

Further simplification of (3.16) shows that the positive equilibria of the model (3.12) satisfy the following quadratic equation below (in terms of λ_A^{**})

$$a_0\lambda_A^{**2} + b_0\lambda_A^{**} + c_0 = 0 \tag{3.17}$$

where

$$\begin{aligned} a_0 &= \pi k_4 k_5 p + \pi k_5\sigma_A p + \pi\gamma_A\sigma_A p \\ b_0 &= \pi k_2 k_4 k_5 + \pi k_3 k_4 k_5 p + \pi k_4 k_5 p\nu + \pi k_2 k_5\sigma_A + \pi k_5\sigma_A p\nu + \pi\gamma_A\sigma_A k_2 \\ &\quad -\beta_A\eta\pi k_4 k_5 p - \beta_A\pi k_5\sigma_A p \\ c_0 &= \pi k_2 k_3 k_4 k_5 + \pi k_3 k_4 k_5\nu - \beta_A\eta\pi k_2 k_4 k_5 - \beta_A\eta\pi k_4 k_5 p\nu - \beta_A\pi k_2 k_5\sigma_A - \beta_A\pi k_5\sigma_A p\nu \end{aligned} \tag{3.18}$$

In order to write the expression of c_0 in form of $\mathcal{R}_{0A}$, we set $c_0 > 0$, then

$$\begin{aligned} \pi k_2 k_3 k_4 k_5 + \pi k_3 k_4 k_5\nu &> \beta_A\eta\pi k_2 k_4 k_5 + \beta_A\eta\pi k_4 k_5 p\nu + \beta_A\pi k_2 k_5\sigma_A + \beta_A\pi k_5\sigma_A p\nu \\ k_2 k_3 k_4 k_5 + k_3 k_4 k_5\nu &> \beta_A\eta k_2 k_4 k_5 + \beta_A\eta k_4 k_5 p\nu + \beta_A k_2 k_5\sigma_A + \beta_A k_5\sigma_A p\nu \end{aligned}$$

Substituting $k_2 = \omega + \mu$ results to,

$$k_3k_4(\omega + \mu + \nu) > \beta_A(\eta k_4 + \sigma_A)(\omega + \mu + p\nu) \tag{3.19}$$

So that

$$\mathcal{R}_{0A} = \frac{\beta_A(\omega + \mu + p\nu)(\eta k_4 + \sigma_A)}{k_3k_4(\nu + \omega + \mu)} < 1$$

Hence,

$$c_0 \equiv k_3k_4(\nu + \omega + \mu)(1 - \mathcal{R}_{0A})$$

Thus, the positive endemic equilibria of the meningitis strain A-only model are obtained by solving the quadratic equation (3.17) and substituting the results (positive values of λ_A^{**}) into equation (3.13). Using the quadratic formula in solving (3.17), we obtain

$$\lambda_A^{**} = \frac{-b_0 \pm \sqrt{b_0^2 - 4a_0c_0}}{2a_0} \tag{3.20}$$

where a_0, b_0, c_0 are defined as in equation (3.18) above.

The quadratic equation (3.17) above can be analyzed for the possibility of multiple endemic equilibria whenever $\mathcal{R}_{0A} < 1$. It should be noted that the coefficient a_0 of the quadratic equation (3.17) is always positive; and the constant term c_0 is negative (positive) whenever $\mathcal{R}_{0A}$ is greater (less) than unity. Hence, the following result is established.

Theorem 5 *The meningitis strain A-only model* (3.12) *has:*

(i) a unique endemic equilibrium if $c_0 < 0 \iff \mathcal{R}_{0A} > 1$*;*

(ii) a unique endemic equilibrium if ($b_0 < 0$ *and* $c_0 = 0$*) or* $b_0^2 - 4a_0c_0 = 0$*;*

(iii) two endemic equilibria if $c_0 > 0$*,* $b_0 < 0$ *and* $b_0^2 - 4a_0c_0 > 0$*;*

(iv) no endemic equilibrium otherwise.

Thus, it is clear from case (i) of Theorem 5 that the meningitis strain A-only model (3.12) has a unique EEP (of the form $\mathcal{E}_1$) whenever $\mathcal{R}_{0A} > 1$. Furthermore, case (iii) of Theorem 5 indicates the possibility of backward bifurcation, where a LAS DFE co-exists with a LAS endemic equilibrium when the associated reproduction number R_{0A} is less than unity ($R_{0A} < 1$). To check for the possibility of backward bifurcation in the meningitis strain A-only model (3.12), the discriminant $b_0^2 - 4a_0c_0$ of quadratic (3.17), is set to zero and the result solved for the critical value of R_{0A} (denoted by $R_{0A^*} < 1$). This gives;

$$R_{0A^*} = 1 - \frac{b_0^2}{4a_0k_3k_4(\nu + \omega + \mu)} \tag{3.21}$$

for which it can be shown that backward bifurcation occurs for values of R_{0A^*} such that $R_{0A^*} < R_{0A} < 1$. The epidemiological importance of the phenomenon of backward bifurcation is that, the requirement of having $R_{0A} < 1$ is necessary, but not sufficient for disease elimination.

Bifurcation analysis for meningitis strain A-only model

Following the above results, we will explore the possibility of backward bifurcation for the Meningitis strain A-only model. The phenomenon of backward bifurcation which has been observed in numerous disease transmission dynamics is totally characterized by the co-existence of a stable disease-free equilibrium and a stable endemic equilibrium when the associated reproduction number is less than unity. Here, we will employ the Centre Manifold theory (Carr, 1981), as described by Castillo-Chavez & Song (2004) to investigate the existence of backward bifurcation. We claim the following result (the proof is given in Appendix B.1)

Theorem 6 *The meningitis strain A-only model* (3.12) *undergoes a backward bifurcation at* $\mathcal{R}_{0A} = 1$ *whenever the coefficient "a", given in Appendix B.1 equation* (B.5) *is positive.*

The proof of Theorem 6 is given in Appendix B.1. Using the baseline parameter values

(except for $\beta_A = 0.6690, \omega = 0.100$), the bifucation paramters *"a"* and *"b"* given in Appendix B.1 are obtained as $a = 0.024353 > 0$ and $b = 183.500426 > 0$ respectively. The implication of backward bifurcation phenomenon is that the classical epidemiology requirement of having the reproduction number less than unity, while necessary, is no longer sufficient for the effective control of the disease in the population. Hence, the effective control of meningitis strain A in the population is difficult, since disease control when $\mathcal{R}_{0A} < 1$ is dependent on the initial sizes of the sub-populations of the model (3.12).

Global stability of meningitis strain A-only for special case $\varepsilon = 0$

Theorem 7 *The disease free equilibrium, $\hat{\mathcal{E}}_1$ of the meningitis strain A-only sub-model* (3.12)*, for special case $\varepsilon = 0$ is globally asymptotically stable whenever $\mathcal{R}_{0A} \leq 1$. The disease free equilibrium, $\hat{\mathcal{E}}_1 = \left(\frac{\pi(\omega+\mu)}{\mu(\nu+\mu+\omega)}, \frac{\pi\nu}{\mu(\nu+\mu+\omega)}, 0, 0, 0\right)$*

Proof: Consider the following Lyapunov function

$$L = b_1 C_A + b_2 I_A$$

with Lyapunov derivate (where dots represents differentiation with respect to time t).

$$\begin{aligned} \dot{L} &= b_1 \dot{C}_A + b_2 \dot{I}_A \\ &= b_1(\lambda_A S + \lambda_A V - k_3 C_A) + b_2(\sigma_A C_A - k_4 I_A) \end{aligned} \tag{3.22}$$

Lyapunov equation (3.22) can be further written as

$$\begin{aligned} \dot{L} &= b_1 \lambda_A S \\ &\quad - C_A(b_1 k_3 - b_2 \sigma_A) \\ &\quad - I_A(b_2 k_4) \end{aligned} \tag{3.23}$$

In order to obtain the value of b_1 and b_2 respectively, a small perturbation of equation (3.23)

with the reproduction number of meningitis strain A-only gives $b_1 = (\eta k_4 + \sigma_A)$ and $b_2 = k_3$. Substituting back the value of b_1 and b_2 above into equation (3.23) yields:

$$\begin{aligned}
\dot{L} &= (\eta k_4 + \sigma_A)\lambda_A S - C_A[(\eta k_4 + \sigma_A)k_3 - k_3\sigma_A] - I_A k_3 k_4 \\
&= (\eta k_4 + \sigma_A)\beta_A(\eta C_A + I_A)\frac{S}{N} - k_3 k_4(\eta C_A + I_A)
\end{aligned}$$

Since $S \leq N$ in the domain $\mathcal{D}$

$$\begin{aligned}
\dot{L} &\leq (\eta k_4 + \sigma_A)\beta_A(\eta C_A + I_A) - k_3 k_4(\eta C_A + I_A) \\
&\leq (\eta C_A + I_A)\left[\beta_A(\eta k_4 + \sigma_A) - k_3 k_4\right] \\
&\leq k_3 k_4(\eta C_A + I_A)\left[\frac{\beta_A(\eta k_4 + \sigma_A)}{k_3 k_4} - 1\right] \\
&= k_3 k_4(\eta C_A + I_A)(\mathcal{R}_{0A} - 1) \leq 0. \qquad (3.24)
\end{aligned}$$

Since all model parameters are non-negative, it follows that $\dot{L} \leq 0$ for $\mathcal{R}_{0A} \leq 1$ with $\dot{L} = 0$ if and only if $C_A = I_A = 0$. Thus, by LaSalle's Invariance Theorem, every solution to the equation of the model (3.12), with initial conditions in the domain $\mathcal{D}$, approaches $\mathcal{D}_0$ as $t \longrightarrow \infty$, whenever $\mathcal{R}_{0A} \leq 1$.

Strain C-only boundary equilibrium ($\mathcal{E}_2$)

Here we will establish the conditions for the existence of an equilibrium for which strain C-only is endemic in the population. The meningitis model (3.1) with strain C-only in the absence of strain A reduces to the system of equations below,

$$\begin{aligned}
\frac{dS}{dt} &= \pi + \omega V + \kappa_C R_C - \lambda_C S - k_1 S \\
\frac{dV}{dt} &= \nu S - p\lambda_C V - k_2 V \\
\frac{dC_C}{dt} &= \lambda_C S + p\lambda_C V - k_6 C_C \\
\frac{dI_C}{dt} &= \sigma_C C_C - k_7 I_C \\
\frac{dR_C}{dt} &= \gamma_C I_C - k_8 R_C
\end{aligned} \tag{3.25}$$

where: $k_1 = \nu + \mu$, $k_2 = \omega + \mu$, $k_6 = \sigma_C + \mu$, $k_7 = \gamma_C + \mu + \delta_C$, $k_8 = \kappa_C + \mu$, $p = 1 - \varepsilon$.

Let $\mathcal{E}_2 = (S^{**}, V^{**}, C_C^{**}, I_C^{**}, R_C^{**})$ be the infection equilibrium of the meningitis model with strain C-only system (3.25). The expression of the equilibrium $\mathcal{E}_2$ is given in Appendix B.2. For the strain C-only system (3.25), we present the following results

Theorem 8 *The meningitis strain C-only model* (3.25) *has:*

(i) a unique endemic equilibrium if $c_1 < 0 \Longleftrightarrow \mathcal{R}_{0C} > 1$*;*

(ii) a unique endemic equilibrium if ($b_1 < 0$ *and* $c_1 = 0$) *or* $b_1^2 - 4a_1c_1 = 0$*;*

(iii) two endemic equilibrium if $c_1 > 0$, $b_1 < 0$ *and* $b_1^2 - 4a_1c_1 > 0$*;*

(iv) no endemic equilibrium otherwise.

The proof of Theorem 8 is given in Appendix B.2. Thus, it is clear from case (i) of Theorem 8 that the meningitis strain C-only model (3.25) has a unique EEP (of the form $\mathcal{E}_2$) whenever $\mathcal{R}_{0C} > 1$. Furthermore, case (iii) of Theorem 8 indicates the possibility of backward bifurcation, where a LAS DFE co-exists with a LAS endemic equilibrium when the associated reproduction number R_{0C} is less than unity ($R_{0C} < 1$). To check for the possibility of backward bifurcation in the meningitis strain C-only model (3.25), the discriminant $b_1^2 - 4a_1c_1$ of

quadratic (B.12), is set to zero and the result solved for the critical value of R_{0C} (denoted by $R_{0C^*} < 1$). This gives;

$$R_{0C^*} = 1 - \frac{b_1^2}{4a_1k_6k_7(\nu+\omega+\mu)} \tag{3.26}$$

for which it can be shown that backward bifurcation occurs for values of R_{0C^*} such that $R_{0C^*} < R_{0C} < 1$. The epidemiological importance of the phenomenon of backward bifurcation is that, the requirement of having $R_{0C} < 1$ is necessary, but not sufficient for disease elimination. In this case, disease elimination will depend upon the initial sizes of the sub-populations of the model.

Theorem 9 *The disease free equilibrium, $\hat{\mathcal{E}}_2$ of the meningitis strain C-only sub-model* (3.25)*, for special case $\varepsilon = 0$ is globally asymptotically stable whenever $\mathcal{R}_{0C} \leq 1$. The disease free equilibrium is given as* $\hat{\mathcal{E}}_2 = \left(\frac{\pi(\omega+\mu)}{\mu(\nu+\mu+\omega)}, \frac{\pi\nu}{\mu(\nu+\mu+\omega)}, 0, 0, 0\right)$

We can prove Theorem 9 using the approach in Section 3.3.3.

The equilibrium ($\mathcal{E}_3$) of the full meningitis model (3.1)

Let

$$\mathcal{E}_3 = (S^{**}, V^{**}, C_A^{**}, I_A^{**}, R_A^{**}, C_C^{**}, I_C^{**}, R_C^{**}, C_{AC}^{**}, I_{AC}^{**}, R_{AC}^{**})$$

be the infection equilibrium of the full meningitis model (3.1). In this section, we present some results of this equilibrium. First we show the existence of this equilibrium $\mathcal{E}_3$. We can numerically show the existence of an equilibrium $\mathcal{E}_3$; however, for mathematical tractability we make the following transformation, set $\beta = max\{\beta_A, \beta_C, \beta_{AC}, \beta_{CA}\}$, $\sigma = min\{\sigma_A, \sigma_C, \sigma_{AC}\}$, $\delta = min\{\delta_A, \delta_C, \delta_{AC}\}$, $\gamma = min\{\gamma_A, \gamma_C, \gamma_{AC}\}$, $\kappa = min\{\kappa_A, \kappa_C, \kappa_{AC}\}$, and let $C = (C_A + C_C + C_{AC})$, $I = (I_A + I_C + I_{AC})$, and $R = (R_A + R_C + R_{AC})$. Thus, we can show the existence of this transformed system. The forces of infection $\lambda_A = \frac{\beta_A(\eta C_A + I_A)}{N}, \lambda_C = \frac{\beta_C(\eta C_C + I_C)}{N}, \lambda_{AC} = \frac{\beta_{AC}(\eta C_{AC} + I_{AC})}{N}, \lambda_{CA} = \frac{\beta_{CA}(\eta C_{AC} + I_{AC})}{N}$ becomes $\lambda = \frac{\beta(\eta C + I)}{N}$.

Hence, the full meningitis model (3.1) reduces to the following.

$$\begin{aligned}
\frac{dS}{dt} &= \pi + \omega V + \kappa R - \lambda S - k_1 S \\
\frac{dV}{dt} &= \nu S - p\lambda V - k_2 V \\
\frac{dC}{dt} &= \lambda S + p\lambda V - k_3 C \\
\frac{dI}{dt} &= \sigma C - k_4 I \\
\frac{dR}{dt} &= \gamma I - k_5 R
\end{aligned} \tag{3.27}$$

where, $k_1 = \nu + \mu$, $k_2 = \omega + \mu$, $k_3 = \sigma + \mu$, $k_4 = \gamma + \mu + \delta$, $k_5 = \kappa + \mu$, $p = 1 - \varepsilon$.

Setting the right-hand-side of (3.27) to zero and solving the equations at steady state in terms of the force of infection (λ), we obtain the following solutions

$$\begin{aligned}
S^{**} &= \frac{\pi k_3 k_4 k_5 (p\lambda^{**} + k_2)}{k_3 k_4 k_5 (\lambda^{**} + k_1)(p\lambda^{**} + k_2) - k_3 k_4 k_5 \omega\nu - \lambda^{**}\kappa\gamma(p\lambda^{**} + k_2 + p\nu)}, \\
V^{**} &= \frac{\nu\pi k_3 k_4 k_5}{k_3 k_4 k_5 (\lambda^{**} + k_1)(p\lambda^{**} + k_2) - k_3 k_4 k_5 \omega\nu - \lambda^{**}\kappa\gamma(p\lambda^{**} + k_2 + p\nu)}, \\
C^{**} &= \frac{\lambda^{**}\pi k_4 k_5 (p\lambda^{**} + k_2 + p\nu)}{k_3 k_4 k_5 (\lambda^{**} + k_1)(p\lambda^{**} + k_2) - k_3 k_4 k_5 \omega\nu - \lambda^{**}\kappa\gamma(p\lambda^{**} + k_2 + p\nu)}, \\
I^{**} &= \frac{\lambda^{**}\pi\sigma k_5 (p\lambda^{**} + k_2 + p\nu)}{k_3 k_4 k_5 (\lambda^{**} + k_1)(p\lambda^{**} + k_2) - k_3 k_4 k_5 \omega\nu - \lambda^{**}\kappa\gamma(p\lambda^{**} + k_2 + p\nu)}, \\
R^{**} &= \frac{\lambda^{**}\pi\gamma\sigma (p\lambda^{**} + k_2 + p\nu)}{k_3 k_4 k_5 (\lambda^{**} + k_1)(p\lambda^{**} + k_2) - k_3 k_4 k_5 \omega\nu - \lambda^{**}\kappa\gamma(p\lambda_A^{**} + k_2 + p\nu)}
\end{aligned} \tag{3.28}$$

Substituting the solution (3.28) into the force of infection, $\lambda^{**} = \dfrac{\beta(\eta C^{**} + I^{**})}{N^{**}}$, we obtain the following polynomial

$$a_2 \lambda^{**2} + b_2 \lambda^{**} + c_2 = 0 \tag{3.29}$$

where

$$\begin{aligned} a_2 &= \pi k_4 k_5 p + \pi k_5 p\sigma + \pi\gamma p\sigma \\ b_2 &= \pi k_2 k_4 k_5 + \pi k_3 k_4 k_5 p + \pi k_4 k_5 p\nu + \pi k_2 k_5 \sigma + \pi k_5 p\sigma\nu + \pi\gamma\sigma_A k_2 \\ &\quad -\beta\eta\pi k_4 k_5 p - \beta\pi k_5 p\sigma \\ c_2 &= k_3 k_4(\nu+\omega+\mu)(1-\mathcal{R}_{0F}) \end{aligned} \tag{3.30}$$

and

$$\mathcal{R}_{0F} = \frac{\beta(\omega+\mu+p\nu)(\eta k_4+\sigma)}{k_3 k_4(\nu+\omega+\mu)}$$

Using the approach in Section 3.3.3 we can prove the following results

Theorem 10 *The meningitis model* (3.27) *has:*

(i) a unique endemic equilibrium if $c_2 < 0 \Longleftrightarrow \mathcal{R}_{0F} > 1$*;*

(ii) a unique endemic equilibrium if ($b_2 < 0$ *and* $c_2 = 0$) *or* $b_2^2 - 4a_2c_2 = 0$*;*

(iii) two endemic equilibrium if $c_2 > 0$, $b_2 < 0$ *and* $b_2^2 - 4a_2c_2 > 0$*;*

(iv) no endemic equilibrium otherwise.

Theorem 11 *The disease free equilibrium,* $\hat{\mathcal{E}}_3$ *of the meningitis model* (3.27)*, for special case* $\varepsilon = 0$ *is globally asymptotically stable whenever* $\mathcal{R}_{0F} \leq 1$*. The disease free equilibrium is given as* $\hat{\mathcal{E}}_3 = \left(\frac{\pi(\omega+\mu)}{\mu(\nu+\mu+\omega)}, \frac{\pi\nu}{\mu(\nu+\mu+\omega)}, 0, 0, 0\right)$.

3.4 Analysis of the sub-model without co-infection (3.2)

3.4.1 Basic qualitative properties

Positivity and boundedness of solutions

Lemma 5 *Let the initial data $S(0) > 0$, $V(0) \geq 0$, $C_A(0) \geq 0$, $I_A(0) \geq 0$, $R_A(0) \geq 0$, $C_C(0) \geq 0$, $I_C(0) \geq 0$, $R_C(0) \geq 0$. Then, the solutions $(S(t), V(t), C_A(t), I_A(t), R_A(t), C_C(t), I_C(t), R_C(t))$ of the meningitis model without co-infection (3.2) are non-negative for all $t > 0$. Furthermore*

$$\lim_{t\to\infty} \sup N(t) \leq \frac{\pi}{\mu}.$$

The proof of Lemma 5 is given in Appendix B.3.

Invariant region

Analysis of the meningitis model without co-infection (3.2) will be carried out in the biological feasible region

$$\hat{\mathcal{D}} = \{(S, V, C_A, I_A, R_A, C_C, I_C, R_C) \in \mathcal{R}_+^8; N \leq \frac{\pi}{\mu}\} \tag{3.31}$$

Lemma 6 *The region $\hat{\mathcal{D}}$ is positively-invariant and attracting for meningitis model without co-infection (3.2) with non-negative initial conditions in $\mathcal{R}_+^8$.*

The proof of Lemma 6 is given in Appendix B.3.

3.4.2 Stability of the DFE of the meningitis model without co-infection (3.2)

The meningitis model without co-infection (3.2) has a disease-free equilibrium obtained by setting the right-hand sides of the equations in the model to zero and solving at $C_A = C_C = I_A = I_C = 0$. Thus, the disease-free equilibrium is given by

$$\begin{aligned}\mathcal{E}_0^+ &= (S^+, V^+, C_A^+, I_A^+, R_A^+, C_C^+, I_C^+, R_C^+)\\ &= \left(\frac{\pi(\omega+\mu)}{\mu(\nu+\omega+\mu)}, \frac{\nu\pi}{\mu(\nu+\omega+\mu)}, 0, 0, 0, 0, 0, 0\right)\end{aligned}$$

Theorem 12 *The disease-free equilibrium $\mathcal{E}_0^+$ of the meningitis model without co-infection* (3.2) *is locally-asymptotically stable (LAS) if $\hat{\mathcal{R}}_0 < 1$ and unstable if $\hat{\mathcal{R}}_0 > 1$.*

The computation of the reproduction number $\hat{\mathcal{R}}_0$ is presented in Appendix B.4. The reproduction number $\hat{\mathcal{R}}_0$ measures the average number of new infections generated by a single infected person during his or her infectious period in a population that is fully susceptible. Thus, the epidemiological implication of Theorem 12 above is that meningitis will be controlled in the population without co-infection whenever $\hat{\mathcal{R}}_0 < 1$ if the initial sizes of the sub populations of the model are in the basin of attraction of the DFE ($\mathcal{E}_0^+$).

Following the approach used for the analyzes of the full meningitis model (3.1) with co-infection in Section 3.3 above, we can show the existence and stability of boundary equilibria, bifurcation analysis for strains A-only and C-only models, and their global stabilities for special case $\varepsilon = 0$. However, we do not show the proofs since their derivations are similar to those provided previously in Section 3.3.3.

3.5 Numerical Simulation and Discussion

In this section, we explore and analyze the full meningitis model (3.1) and the meningitis model without co-infection (3.2) numerically, in order to see the dynamical behavior of the solutions. In addition, we explore for the full meningitis model (3.1) two scenarios in which the transmission of strain A is stronger in co-infected individuals, and when the transmission of strain C is stronger in co-infected individuals. Using the baseline parameter values as presented in Agusto & Leite (2019), except otherwise stated, we determine the respective reproduction numbers $\mathcal{R}_{0A}$ and $\mathcal{R}_{0C}$ of each strain A and C.

3.5.1 Numerical simulation for the full meningitis model (3.1)

As discussed by Martcheva et al. (2007), when each strain can invade the other's equilibrium ($\mathcal{R}_{0A} > 1$ and $\mathcal{R}_{0C} > 1$), they are both expected to coexist in the population. However, for models that allows super-infection (which is the process of a strain occuring after or on top of an earlier infection by a different strain), strain replacement depends on the details of competitive outcomes at the within-host level. This depends on the existence of some difference in the mode of transmission between the two strains or within-host competitive advantage of one of the strains. As presented in Figure 3.3(a) - 3.4(b), we explore the effect of strain transmission probabilities of co-infected individuals (β_{AC} and β_{CA}), in the population where the disease reproduction number of the two strains are equal and at endemic ($\mathcal{R}_{0A} = \mathcal{R}_{0C} > 1$). Figure 3.3(a) depicts that, strain A will dominate in the population even when the two strains have equal reproduction numbers. This result can be traced to the transmission probability of strain A in co-infected individuals ($\beta_{AC} = 0.3345$, $\beta_{CA} = 0$), thus driving out strain C and reducing the number of co-infected individuals to zero. Similarly, in Figure 3.3(b), strain C dominates and drives out strain A and co-infected individuals in the population given that the transmission probability of strain C through co-infected individual is nonzero ($\beta_{CA} = 0.3345$). Hence, the model (3.1) exhibits competitive exclusion

(where by strain A drives out strain C, and vice-versa, at their equilibrium), due to exclusive transmission of either strain A or strain C from co-infected individuals.

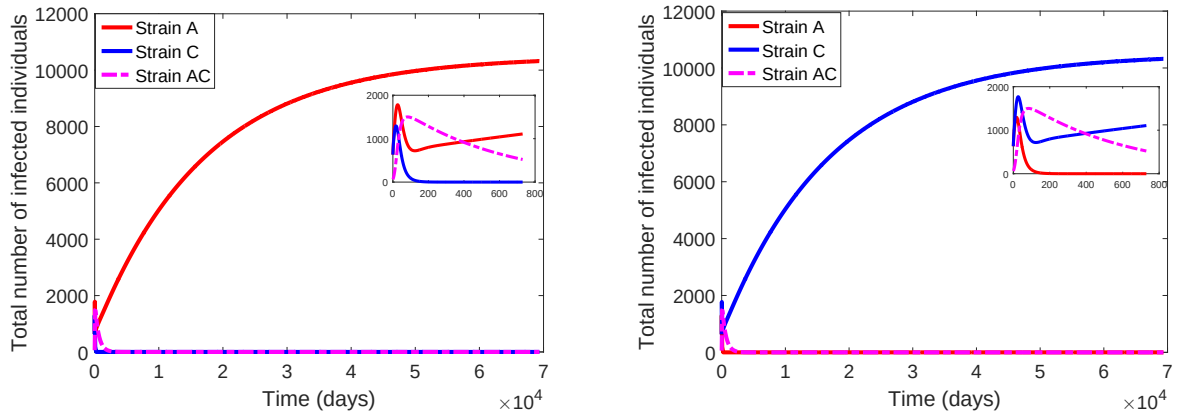

Figure 3.3: Simulation of the full model (3.1) showing total number of infected individuals when $\mathcal{R}_{0A} = \mathcal{R}_{0C} > 1$, with ($\mathcal{R}_{0A} = \mathcal{R}_{0C} = 4.20$). Parameters are at baseline values. (a) Strain A is transmitted in co-infected individuals, $\beta_{AC} > \beta_{CA}$, with ($\beta_{AC} = 0.3345$, $\beta_{CA} = 0$); (b) Strain C is transmitted in co-infected individuals, $\beta_{CA} > \beta_{AC}$, with ($\beta_{AC} = 0$, $\beta_{CA} = 0.3345$).

Allowing nonzero transmission probabilities for both strains in the co-infected individuals informs us of the dynamic of co-existence of the two strain in the population. As presented in Figure 3.4(a), a nonzero transmission probability of strain C in co-infected individuals β_{CA} enables its competition with strain A in the populace. Strain A dominates in the population but does not drive strain C to extinction. Similarly, Figure 3.4(b) depicts the co-existence of the two strains with strain C having the higher tranmission probability when both strains have nonzero transmission probabilities.

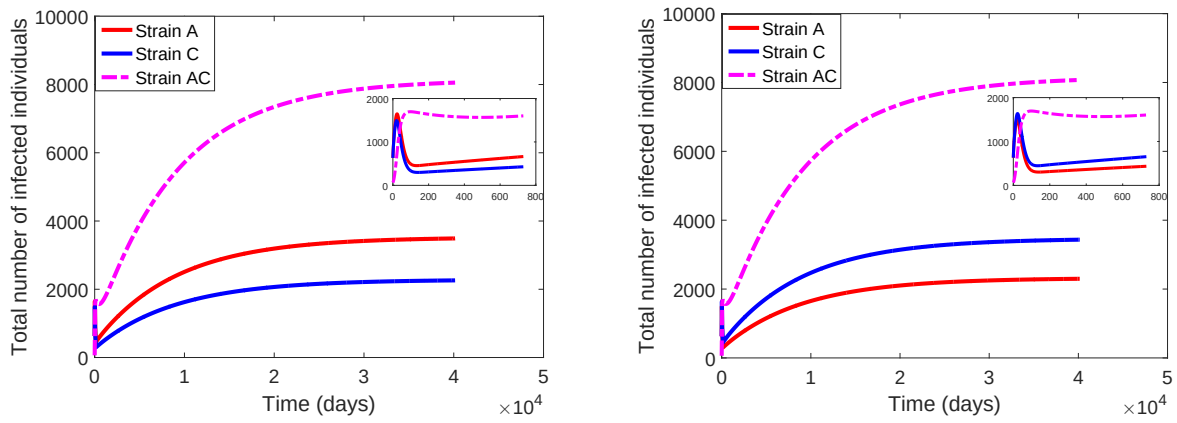

Figure 3.4: Simulation of the full model (3.1) showing total number of infected individuals when $\mathcal{R}_{0A} = \mathcal{R}_{0C} > 1$, with ($\mathcal{R}_{0A} = \mathcal{R}_{0C} = 4.20$). Parameters are at baseline values. (a) Strain A has higher transmission in co-infected individuals, than strain C $\beta_{AC} > \beta_{CA}$, with ($\beta_{AC} = 0.3345$, $\beta_{CA} = 0.2245$); (b) Strain C has higher transmission in co-infected individuals, than strain A $\beta_{CA} > \beta_{AC}$, with ($\beta_{AC} = 0.2245$, $\beta_{CA} = 0.3345$).

In order to answer the question of the possibilities of co-existence of the two strains in the population, we also explore cases when ($\mathcal{R}_{0A} > \mathcal{R}_{0C} > 1$ and $\mathcal{R}_{0C} > \mathcal{R}_{0A} > 1$) in Figure 3.5(a) through Figure 3.8(b). Figure 3.5(a) shows a similar result to Figure 3.3(a), where-by strain A dominates and drive strain C into extinction, due to the increase in the reproduction number of strain A and the only transmission probability in co-infected individuals (β_{AC}) leading to transmission of strain A. However, Figure 3.5(b) indicates a trade-off mechanism (the process whereby a strain with a lower reproduction number can co-exist with a strain with a higher reproduction number). Given that strain A has the highest reproduction number, the model exhibits a trade-off mechanism whereby strain A and C and co-infected individuals co-exist in the population. This mechanism occurs due to the transmission probabilities of strain A and C in co-infected individuals ($\beta_{AC} = 0$, $\beta_{CA} = 0.3345$), i.e. there is no possibilities of strain A been transmitted in the co-infected individuals. In other words, the model exhibits a trad-off mechanism when strain A has a between-host advantage in reproduction number, but strain C has a within-host advantage in

the co-infected individuals. This enables strain C to dominate in the population at endemic equilibrium.

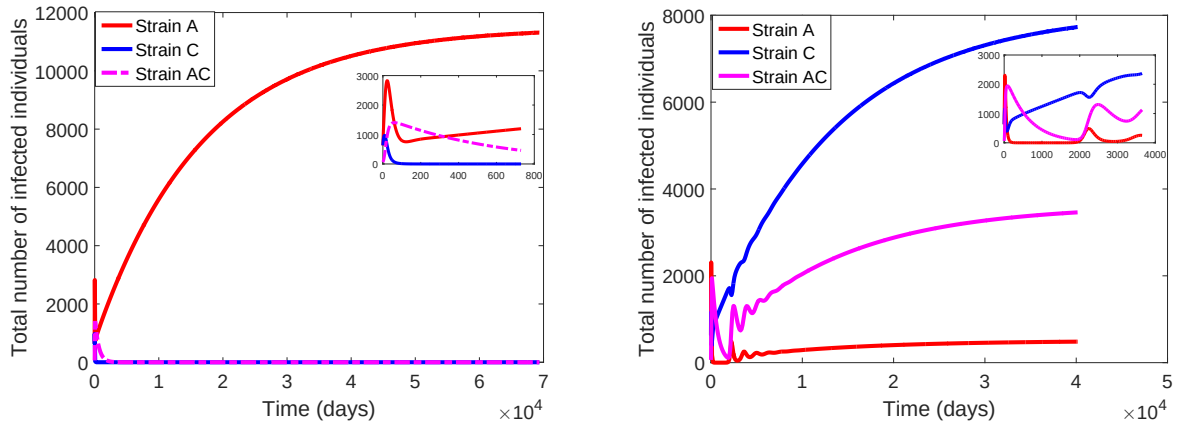

Figure 3.5: Simulation of the full model (3.1) showing total number of infected individuals when $\mathcal{R}_{0A} > \mathcal{R}_{0C} > 1$, with $(\mathcal{R}_{0A} = 6.72, \mathcal{R}_{0C} = 4.20)$. Parameters are at baseline values except for $\beta_A = 0.5345$. (a) Strain A is transmitted in co-infected individuals, $\beta_{AC} > \beta_{CA}$, with $(\beta_{AC} = 0.3345, \beta_{CA} = 0)$; (b) Strain C is transmitted in co-infected individuals, $\beta_{CA} > \beta_{AC}$, with $(\beta_{AC} = 0, \beta_{CA} = 0.3345)$.

In addition, increasing the transmission probabilities for the co-infected individuals changes the dynamics of the system. We observe a coexistence of the two strains, with the strain having the highest probability in co-infected individuals dominating but not driving the other strain into extinction. For example, as shown in Figure 3.6(b), the two strains co-exist while strain C is the dominant strain due to its high transmission probability $\beta_{CA} = 0.3345$ compare to $\beta_{AC} = 0.2245$.

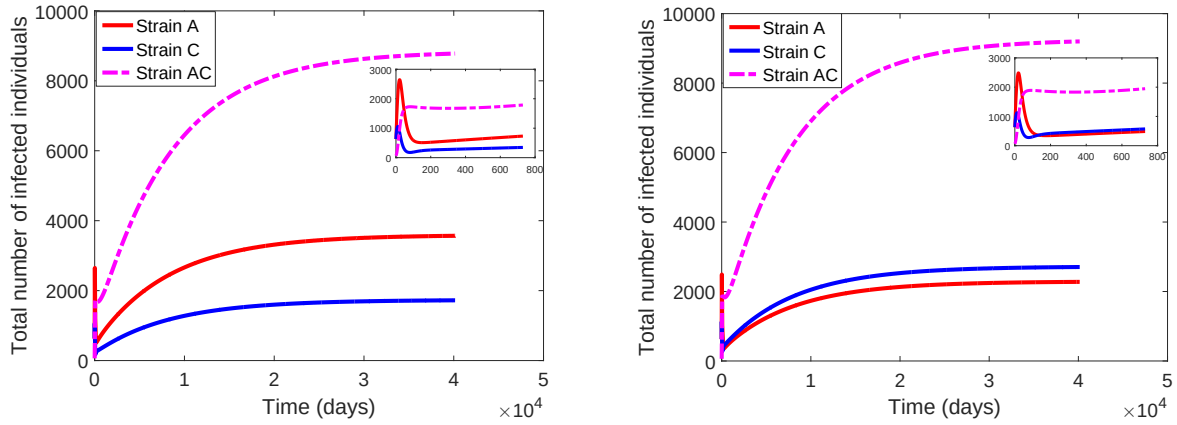

Figure 3.6: Simulation of the full model (3.1) showing total number of infected individuals when $\mathcal{R}_{0A} > \mathcal{R}_{0C} > 1$, with $(\mathcal{R}_{0A} = 6.72, \mathcal{R}_{0C} = 4.20)$. Parameters are at baseline values except for $\beta_A = 0.5345$. (a) Strain A has higher transmission than strain C in co-infected individuals, $\beta_{AC} > \beta_{CA}$, with ($\beta_{AC} = 0.3345$, $\beta_{CA} = 0.2245$); (b) Strain C has higher transmission than strain A in co-infected individuals, $\beta_{CA} > \beta_{AC}$, with ($\beta_{AC} = 0.2245$, $\beta_{CA} = 0.3345$).

Figure 3.7(a) - Figure 3.8(b) present a similar result in Figure 3.5(a) - Figure 3.6(b). In general, the transmission probabilities of the two strains in co-infected individuals has a greater impact in the competition and dominance of each strain in the population. In cases where one strain has the between-host advantage (reproduction number advantage) but it also has a zero transmission probability from co-infected hosts (within-host disadvantage), we see oscillatory behavior (Figure 3.5b and 3.7a).

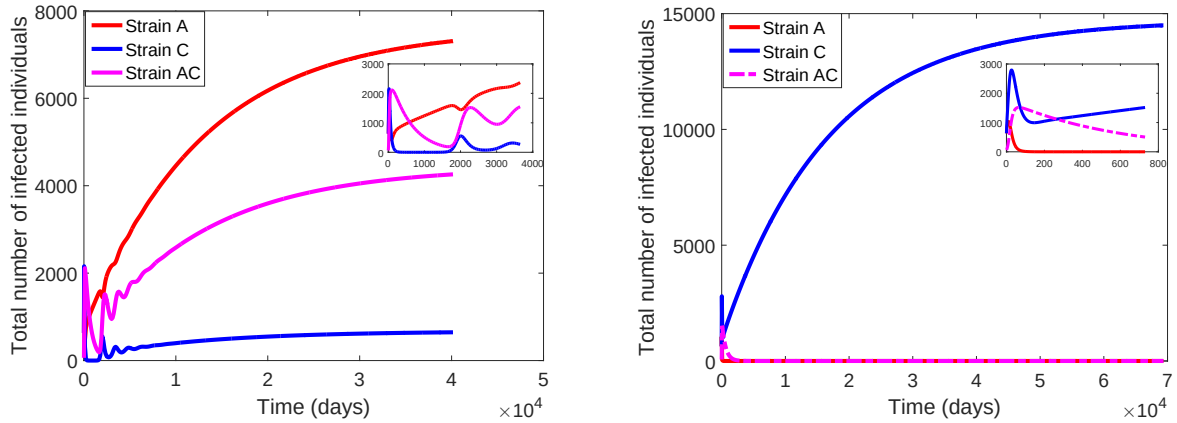

Figure 3.7: Simulation of the full model (3.1) showing total number of infected individuals when $\mathcal{R}_{0C} > \mathcal{R}_{0A} > 1$, with $(\mathcal{R}_{0A} = 4.20, \mathcal{R}_{0C} = 7.58)$. Parameters are at baseline values except for $\beta_C = 0.4683$ and $\sigma_C = 0.0313$. (a) Strain A is transmitted in co-infected individuals, $\beta_{AC} > \beta_{CA}$, with $(\beta_{AC} = 0.3345,\ \beta_{CA} = 0)$ (b) Strain C is transmitted in co-infected individuals, $\beta_{CA} > \beta_{AC}$, with $(\beta_{AC} = 0,\ \beta_{CA} = 0.3345)$.

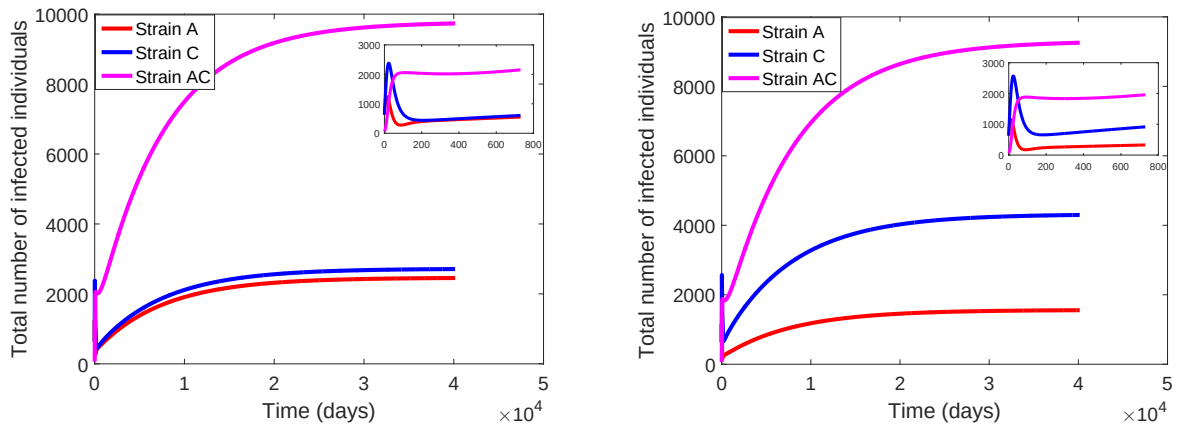

Figure 3.8: Simulation of the full model (3.1) showing total number of infected individuals when $\mathcal{R}_{0C} > \mathcal{R}_{0A} > 1$, with $(\mathcal{R}_{0A} = 4.20, \mathcal{R}_{0C} = 7.58)$. Parameters are at baseline values except for $\beta_C = 0.4683$ and $\sigma_C = 0.0313$. (a) Strain A has higher transmission than strain C in co-infected individuals, $\beta_{AC} > \beta_{CA}$, with $(\beta_{AC} = 0.3345,\ \beta_{CA} = 0.2245)$ (b) Strain C has higher transmission than strain A in co-infected individuals, $\beta_{CA} > \beta_{AC}$, with $(\beta_{AC} = 0.2245,\ \beta_{CA} = 0.3345)$.

3.5.2 Numerical simulation of the meningitis model without co-infection (3.2)

We also explore the dynamical behavior of the model without co-infection model as given in equation (3.2). For the case when $\mathcal{R}_{0A} > \mathcal{R}_{0C} > 1$, strain A dominates in the population while strain C is driven to extinction as shown in Figure 3.9(a). Similarly, Figure 3.9(b) depicts the extinction of strain A when $\mathcal{R}_{0C} > \mathcal{R}_{0A} > 1$. Hence, the model without co-infection will exhibit competitive exclusion when $\mathcal{R}_{0A} > \mathcal{R}_{0C} > 1$ (strain A drives out strain C) or when $\mathcal{R}_{0C} > \mathcal{R}_{0A} > 1$ (strain C drives out strain A). Thus, the dominance of a strain in the population depends on the strain with the highest reproduction number. However, in the case whereby the two strains have the same reproduction number at their endemic state, they are expected to both co-exist, hence, dominance of a strain will depend on the initial size of their population.

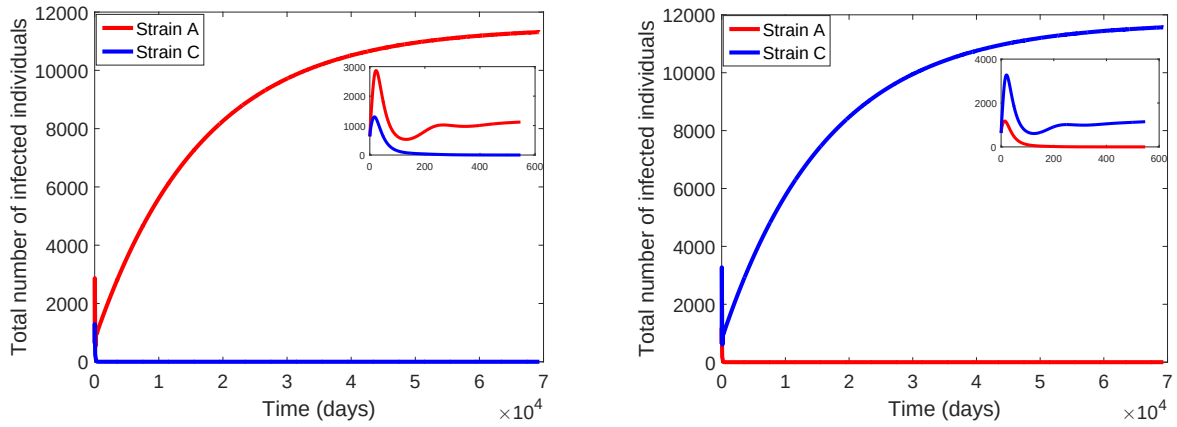

(a) (b)

Figure 3.9: Simulation of the model with no co-infection (3.2). (a) Total number of infected individuals when $\mathcal{R}_{0A} > \mathcal{R}_{0C} > 1$, with $(\mathcal{R}_{0A} = 6.72, \mathcal{R}_{0C} = 4.20)$. Parameters are at baseline values except for $\beta_A = 0.5345$ (b) Total number of infected individuals when $\mathcal{R}_{0C} > \mathcal{R}_{0A} > 1$, with $(\mathcal{R}_{0A} = 4.20, \mathcal{R}_{0C} = 7.98)$. Parameters are at baseline values except for $\beta_C = 0.6345$.

We simulate the dynamics of the model without co-infection, with equal reproduction number. Figure 3.10(a) shows that strain A dominates in the population due to its initial pop-

ulation size which is greater than strain C initial population size. Similarly, Figure 3.10(b) depicts strain C as the dominant strain, which is as a result of its initial population size.

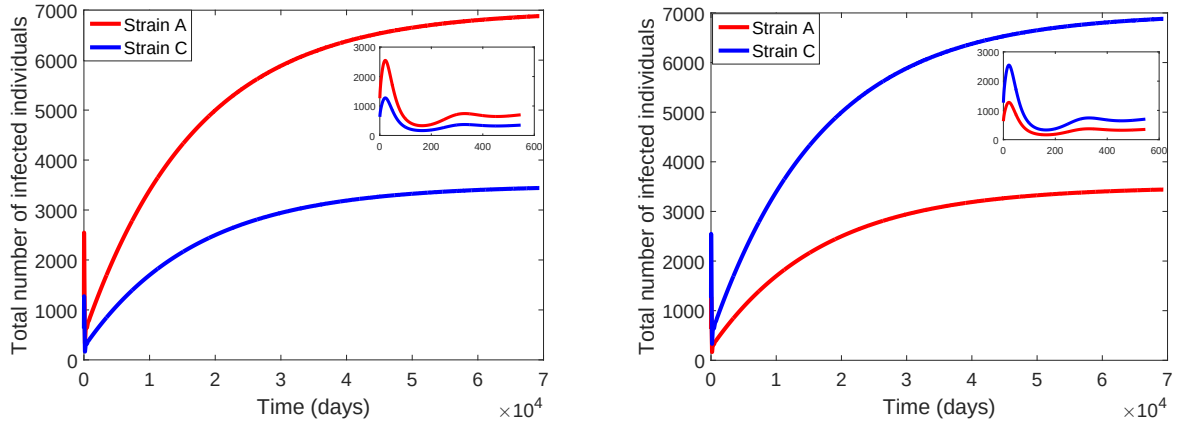

Figure 3.10: Simulation of the model without co-infection (3.2), when $\mathcal{R}_{0A} = \mathcal{R}_{0C} > 1$, with ($\mathcal{R}_{0A} = \mathcal{R}_{0C} = 4.20$). Parameters are at baseline values. (a) Showing total number of infected individuals when the initial population of strain A individuals is as twice as strain C population. (b) Showing total number of infected individuals when the initial population of strain C individuals is as twice as strain A population.

3.5.3 Conclusions

In this study, we developed a deterministic mathematical model to study the transmission dynamics of two strains of meningitis (strain A and strain C) in the population, using ordinary differential equations. We consider three different scenarios (i-ii. full model: when a particular strain is stronger in transmission than the other in co-infected individuals, iii. the model without co-infection). The main results obtained from the theoretical analysis and simulation are summarized below.

(i) The full meningitis model and the model without co-infection has a locally asymptotically stable disease-free equilibrium whenever $\mathcal{R}_0 < 1$ and unstable if $\mathcal{R}_0 > 1$ (i.e meningitis strain A can be curtailed when $\mathcal{R}_{0A} < 1$, similarly meningitis strain C can be curtailed when $\mathcal{R}_{0C} < 1$).

(ii) The meningitis strain A-only model exhibit backward bifurcation, where the stable disease-free equilibrium co-exists with a stable endemic equilibrium when reproduction number of strain A only is less than unity. The numerical values of the coefficients (a and b) are found.

(iii) The DFE of the meningitis strain A-only model with the special case $\varepsilon = 0$ (no vaccine efficacy) is globally asymptotically stable whenever the reproduction number $\mathcal{R}_{0A}$ is less than unity;

(iv) Numerical simulation shows that for the scenario where we set the transmission probability in co-infected individuals of a strain to zero, the co-infection model exhibit competitive exclusion (a strain driving out the other strain into extinction when both are at endemic), due to the relative transmission probabilities of the two strains in co-infected individuals. Biologically, this can be explained by the existence of some difference in the mode of transmission between the two strains or within-host competitive advantage of one of the strains. However, for the scenario where we set the transmission probability in co-infected individuals of a strain greater than the other (transmission probability of neither strain is equal to zero), we observed a trade-off mechanism which enables co-existence of the two strains. Regardless of the greatest reproduction number value of each strain, the strain with the highest transmission probability in co-infected individual will dominate in the population but not drive the other strain into extinction.

(v) The model without co-infection exhibits competitive exclusion when $\mathcal{R}_{0A} > \mathcal{R}_{0C} > 1$ (strain A drives out strain C) or when $\mathcal{R}_{0C} > \mathcal{R}_{0A} > 1$ (strain C drives out strain A). However, our results show that when the two strains have the same reproduction number at their endemic state, they are expected to both co-exist, but the dominance of a strain will depend on the initial size of their population.

Chapter 4

Conclusions

Bacterial meningitis remains a global public health challenge, with the highest burden being in the African meningitis belt. According to World Health Organization (WHO) (2018), vaccination is the most effective way of preventing the disease in the population. This study presents the formulation, analysis, and simulation of numerous, novel mathematical models to examine the effect of vaccination in controlling meningitis, specifically utilizing data from Nigeria to parameterize the models.

In Chapter 2, we present a non-impulsive model and an impulsive model to study the effect of constant and pulse vaccination in eradicating *Neisseria meningitidis* in the population. Overall, in this chapter, our results show that vaccinating with a lower rate slowly protects and prevent the disease transmission in contrast to when a high vaccination rate is used; this protect more people at a faster rate. Furthermore, our results depict that meningitis can be effectively controlled in the population using an imperfect vaccine with an efficacy greater than 75% and high vaccine coverage rate of at least 85%. In addition, numerical simulation of the impulsive model depict that final infected population size is lower when applying the impulsive vaccination strategy compare with the scenario without vaccination. Thus, disease burden in the population decreases with increasing vaccination pulses.

In the final chapter, we focus on the dynamics of meningitis A and meningitis C in the presence of vaccination under different scenarios. We present a full model with co-infection and also a sub-model without co-infection. For the scenario where we set the transmission probability of a strain from co-infected individuals to zero, our results depict that the co-

infection model exhibit competitive exclusion (a strain driving the other strain into extinction when both are at endemic), due to the difference in transmission probabilities of the two strains. Biologically, this can be explained by the existence of some difference in the mode of transmission between the two strains or within-host competitive advantage of one of the strains. However, for the scenario in which we set the transmission probability of a strain greater than the other (transmission probability of neither strain is equal to zero), we observed a trade-off mechanism which enables co-existence of the two strains. In this case, regardless of the greatest reproduction number value of each strain, the strain with the highest transmission probability in co-infected individual will dominate in the population but not drive the other strain into extinction.

The model without co-infection exhibit competitive exclusion when $\mathcal{R}_{0A} > \mathcal{R}_{0C} > 1$ (strain A drives out strain C) or when $\mathcal{R}_{0C} > \mathcal{R}_{0A} > 1$ (strain C drives out strain A). However, our results show that when the two strains have the same reproduction number at their endemic state, they are expected to both co-exist, but the dominance of a strain will depend on the initial size of their population.

Bibliography

Agier, L., Deroubaix, A., Martiny, N., Yaka, P., Djibo, A., & Broutin, H. (2013). Seasonality of meningitis in Africa and climate forcing: aerosols stand out. *Journal of the Royal Society Interface*, 10(79), 20120814.

Agier, L., Martiny, N., Thiongane, O., Mueller, J., Paireau, J., Watkins, E., Irving, T., Koutangni, T., & Broutin, H. (2017). Towards understanding the epidemiology of Neisseria meningitidis in the African meningitis belt: a multi-disciplinary overview. *International Journal of Infectious Diseases*, 54, 103–112.

Agur, Z., Cojocaru, L., Mazor, G., Anderson, R., & Danon, Y. (1993). Pulse mass measles vaccination across age cohorts. *Proceedings of the National Academy of Sciences*, 90(24), 11698–11702.

Agusto, F. & Leite, M. (2019). Optimal control and cost-effective analysis of the 2017 meningitis outbreak in Nigeria. *Infectious Disease Modelling*, 4, 161–187.

Agusto, F. B., Easley, S., Freeman, K., & Thomas, M. (2016). Mathematical model of three age-structured transmission dynamics of Chikungunya virus. *Computational and mathematical methods in medicine*, 2016.

Agyingi, E., Ngwa, M., & Wiandt, T. (2016). The dynamics of multiple species and strains of malaria. *Letters in Biomathematics*, 3(1), 29–40.

Ahn, K. W., Kosoy, M., & Chan, K.-S. (2014). An approach for modeling cross-immunity of two strains, with application to variants of Bartonella in terms of genetic similarity. *Epidemics*, 7, 7–12.

Aldila, D. & Agustin, M. R. (2018). A Mathematical Model Of Dengue-Chikungunya Co-Infection In A Closed Population. In *Journal of Physics: Conference Series*, volume 974 (pp. 012001).: IOP Publishing.

Asamoah, J. K. K., Nyabadza, F., Seidu, B., Chand, M., & Dutta, H. (2018). Mathematical Modelling of Bacterial Meningitis Transmission Dynamics with Control Measures. *Computational and mathematical methods in medicine*, 2018.

Awoke, T. & Kassa, S. (2018). Optimal Control Strategy for TB-HIV/AIDS Co-Infection Model in the Presence of Behaviour Modification. *Processes*, 6(5), 48.

Bainov, D. & Simeonov, P. (1995). *Impulsive differential equations: asymptotic properties of the solutions*, volume 28. World Scientific.

Bartlett, C., Smith, P., Berridge, V., Bradley, D., Coker, R., Fine, P., Geissler, P., Kovats, R., Wilkinson, P., et al. (2006). Foresight. Infectious Diseases: preparing for the future: Executive Summary.

Brauer, F., Castillo-Chavez, C., & Castillo-Chavez, C. (2001). *Mathematical models in population biology and epidemiology*, volume 40. Springer.

British Broascasting Cooperation (BBC) (2017). Nigeria meningitis: Vaccine cost cripples response to outbreak.
http://www.bbc.com/news/world-africa-39479097.

Broutin, H., Philippon, S., de Magny, G. C., Courel, M.-F., Sultan, B., & Guégan, J.-F. (2007). Comparative study of meningitis dynamics across nine African countries: a global perspective. *International Journal of Health Geographics*, 6(1), 29.

Brouwer, M. C., Tunkel, A. R., & van de Beek, D. (2010). Epidemiology, diagnosis, and antimicrobial treatment of acute bacterial meningitis. *Clinical microbiology reviews*, 23(3), 467–492.

Carr, J. (1981). Applications of centre manifold theory. springer.

Castillo-Chavez, C. & Song, B. (2004). Dynamical models of tuberculosis and their applications. *Mathematical biosciences and engineering*, 1(2), 361–404.

Centers for Disease Control and Prevention and others (2012). Meningococcal disease: epidemiology and prevention of vaccine-preventable diseases. *The Pink Book: Course Textbook.. 201212th ed. Atlanta, GA Centers for Disease Control and Prevention Available at: http://www. cdc. gov/vaccines/pubs/pinkbook/downloads/mening. pdf. Accessed April*, 26.

Centers for Disease Control and Prevention (CDC) (2017). Meningitis.

Centers for Disease Control and Prevention (CDC) (2019). Bacterial Meningitis.

Centre for Disease Control, N. (2019). Meningitis.

Chen, W. H., Neuzil, K. M., Boyce, C. R., Pasetti, M. F., Reymann, M. K., Martellet, L., Hosken, N., LaForce, F. M., Dhere, R. M., Pisal, S. S., et al. (2018). Safety and immunogenicity of a pentavalent meningococcal conjugate vaccine containing serogroups A, C, Y, W, and X in healthy adults: a phase 1, single-centre, double-blind, randomised, controlled study. *The Lancet Infectious Diseases*, 18(10), 1088–1096.

Coen, P., Cartwright, K., & Stuart, J. (2000). Mathematical modelling of infection and disease due to Neisseria meningitidis and Neisseria lactamica. *International Journal of Epidemiology*, 29(1), 180–188.

Del Valle, S. Y., Hyman, J. M., & Chitnis, N. (2013). Mathematical models of contact patterns between age groups for predicting the spread of infectious diseases. *Mathematical biosciences and engineering: MBE*, 10, 1475.

d'Onofrio, A. (2005). On pulse vaccination strategy in the SIR epidemic model with vertical transmission. *Applied Mathematics Letters*, 18(7), 729–732.

Forouzannia, F. & Gumel, A. B. (2014). Mathematical analysis of an age-structured model for malaria transmission dynamics. *Mathematical biosciences*, 247, 80–94.

Gao, S., Chen, L.and Nieto, J., & Torres, A. (2006a). Analysis of a delayed epidemic model with pulse vaccination and saturation incidence. *Vaccine*, 24(35-36), 6037–6045.

Gao, S. & Chen, L. (2005). The effect of seasonal harvesting on a single-species discrete population model with stage structure and birth pulses. *Chaos, Solitons & Fractals*, 24(4), 1013–1023.

Gao, S., Chen, L., Nieto, J. J., & Torres, A. (2006b). Analysis of a delayed epidemic model with pulse vaccination and saturation incidence. *Vaccine*, 24(35-36), 6037–6045.

Garmer, S., Lynn, R., Rossi, D., & Capaldi, A. (2015). Multistrain infections in metapopulations. *Spora: A Journal of Biomathematics*, 1(1), 4.

Ginsberg, L. (2004). Difficult and recurrent meningitis. *Journal of Neurology, Neurosurgery & Psychiatry*, 75(suppl 1), i16–i21.

Gleissner, B. & Chamberlain, M. (2006). Neoplastic meningitis. *The Lancet Neurology*, 5(5), 443–452.

Greenwood, B. (2006). 100 years of epidemic meningitis in West Africa–has anything changed? *Tropical medicine & international health*, 11(6), 773–780.

Hassan-King, M., Wall, R., & Greenwood, B. (1988). Meningococcal carriage, meningococcal disease and vaccination. *Journal of Infection*, 16(1), 55–59.

Hethcote, H. W. (2000). The mathematics of infectious diseases. *SIAM review*, 42(4), 599–653.

Hogan, A. B., Glass, K., Moore, H. C., & Anderssen, R. S. (2016). Age structures in mathematical models for infectious diseases, with a case study of respiratory syncytial virus. In *Applications+ Practical Conceptualization+ Mathematics= fruitful Innovation* (pp. 105–116). Springer.

Huppert, A. & Katriel, G. (2013). Mathematical modelling and prediction in infectious disease epidemiology. *Clinical Microbiology and Infection*, 19(11), 999–1005.

Irving, T., Blyuss, K., Colijn, C., & Trotter, C. (2012). Modelling meningococcal meningitis in the African meningitis belt. *Epidemiology & Infection*, 140(5), 897–905.

Kermack, W. O. & McKendrick, A. G. (1927). A contribution to the mathematical theory of epidemics. *Proceedings of the royal society of london. Series A, Containing papers of a mathematical and physical character*, 115(772), 700–721.

Kermack, W. O. & McKendrick, A. G. (1932). Contributions to the mathematical theory of epidemics. ii.—the problem of endemicity. *Proceedings of the Royal Society of London. Series A, containing papers of a mathematical and physical character*, 138(834), 55–83.

Kermack, W. O. & McKendrick, A. G. (1933). Contributions to the mathematical theory of epidemics. III.—Further studies of the problem of endemicity. *Proceedings of the Royal Society of London. Series A, Containing Papers of a Mathematical and Physical Character*, 141(843), 94–122.

LaForce, F., Konde, K.and Viviani, S., & Préziosi, M.-P. (2007). The meningitis vaccine project. *Vaccine*, 25, A97–A100.

Lakshmikantham, V., Simeonov, P., et al. (1989). *Theory of impulsive differential equations*, volume 6. World scientific.

Lambert, J. H. (1772). Beyträge zum Gebrauche der Mathematik und deren Anwendung Theil 3. *Beyträge zum Gebrauche der Mathematik und deren Anwendung*.

Laplace, P. (1812). Théorie analytique des probabilités. Courcier, Paris. *Oeuvres Complètes de Laplace*, 7.

Li, J. & Yang, Y. (2011). SIR-SVS epidemic models with continuous and impulsive vaccination strategies. *Journal of theoretical biology*, 280(1), 108–116.

Li, Y. & Cui, J. (2009). The effect of constant and pulse vaccination on SIS epidemic models incorporating media coverage. *Communications in Nonlinear Science and Numerical Simulation*, 14(5), 2353–2365.

Martcheva, M., Bolker, B. M., & Holt, R. D. (2007). Vaccine-induced pathogen strain replacement: what are the mechanisms? *Journal of the Royal Society Interface*, 5(18), 3–13.

Martcheva, M. & Crispino-O'Connell, G. (2003). The transmission of meningococcal infection: a mathematical study. *Journal of mathematical analysis and applications*, 283(1), 251–275.

Maseno, K. (2011). Mathematical model for malaria and meningitis co-infection among children. *Applied Mathematical Sciences*, 5(47), 2337–2359.

May, R. M. (2004). Uses and abuses of mathematics in biology. *Science*, 303(5659), 790–793.

Mayo Clinic (2018). Meningitis.

McLeod, R., Brewster, J., Gumel, A., & Slonowsky, A. (2006). Sensitivity and uncertainty analyses for a SARS model with time-varying inputs and outputs. *Mathematical Biosciences and Engineering*, 3(3), 527.

Merck Manual (Accessed October17, 2018). Introduction to Meningitis. *https://www.merckmanuals.com/home/brain,-spinal-cord,-and-nerve-disorders/meningitis/introduction-to-meningitistarget*.

Miller, M. A. & Shahab, C. K. (2005). Review of the cost effectiveness of immunisation strategies for the control of epidemic meningococcal meningitis. *Pharmacoeconomics*, 23(4), 333–343.

Molesworth, A., Thomson, M., Connor, S., Cresswell, M., Morse, A., Shears, P., Hart, C., & Cuevas, L. (2002). Where is the meningitis belt? Defining an area at risk of epidemic meningitis in Africa. *Transactions of the royal society of tropical medicine and hygiene*, 96(3), 242–249.

Moneim, I. A. & Greenhalgh, D. (2005). Use of a periodic vaccination strategy to control the spread of epidemics with seasonally varying contact rate. *Math. Biosci. Eng*, 2(3), 591–611.

Moore, P. (1992). Meningococcal meningitis in sub-Saharan Africa: a model for the epidemic process. *Clinical Infectious Diseases*, 14(2), 515–525.

Mutua, J. M., Wang, F.-B., & Vaidya, N. K. (2015). Modeling malaria and typhoid fever co-infection dynamics. *Mathematical biosciences*, 264, 128–144.

News24 (2017). Vaccine shortage for Nigeria meningitis outbreak. *https://www.news24.com/Africa/News/vaccine-shortage-for-nigeria-meningitis-outbreak-20170330-2*.

Nigeria Centre for Disease Control (2017). Meningitis Outbreak in Nigeria affects five States. *http://www.ncdc.gov.ng/news/67/meningitis-outbreak-in-nigeria-affects-five-states*.

Nigeria Centre for Disease Control (NCDC) (2017). Weekly Epidemiological Report. *http://www.ncdc.gov.ng/reports/96/2017-november-week-47*.

Nokes, D. J. & Swinton, J. (1995). The control of childhood viral infections by pulse vaccination. *Mathematical Medicine and Biology*, 12(1), 29–53.

Nokes, D. J. & Swinton, J. (1997). Vaccination in pulses: a strategy for global eradication of measles and polio? *Trends in microbiology*, 5(1), 14–19.

Oordt-Speets, A. M., Bolijn, R., van Hoorn, R. C., Bhavsar, A., & Kyaw, M. H. (2018). Global etiology of bacterial meningitis: A systematic review and meta-analysis. *PloS one*, 13(6), e0198772.

Orwa, T. O., Mbogo, R. W., & Luboobi, L. S. (2019). Multiple-Strain Malaria Infection and Its Impacts on Plasmodium falciparum Resistance to Antimalarial Therapy: A Mathematical Modelling Perspective. *Computational and Mathematical Methods in Medicine*, 2019.

Osman, S. & Makinde, O. D. (2018). A mathematical model for coinfection of listeriosis and anthrax diseases. *International Journal of Mathematics and Mathematical Sciences*, 2018.

P. Van den Driessche and J. Watmough (2002). Reproduction numbers and sub-threshold endemic equilibria for compartmental models of disease transmission. *Mathematical Biosciences*, 180(1), 29 – 48.

Peterson, M. E., Li, Y., Bita, A., Moureau, A., Nair, H., Kyaw, M. H., Abad, R., Bailey, F., de la Fuente Garcia, I., Decheva, A., et al. (2019). Meningococcal serogroups and surveillance: a systematic review and survey. *Journal of global health*, 9(1).

Qiu, Z., Kong, Q., Li, X., & Martcheva, M. (2013). The vector–host epidemic model with multiple strains in a patchy environment. *Journal of Mathematical Analysis and Applications*, 405(1), 12–36.

Ramsay, M., Gay, N., Miller, E., Rush, M., White, J., Morgan-Capner, P., & Brown, D. (1994). The epidemiology of measles in England and Wales: rationale for the 1994 national vaccination campaign. *Communicable disease report. CDR review*, 4(12), R141–6.

Reingold, A., Hightower, A., Bolan, G., Jones, E., Tiendrebeogo, H., Broome, C., Ajello, G., Adamsbaum, C., Phillips, C., & Yada, A. (1985). Age-specific differences in duration of clinical protection after vaccination with meningococcal polysaccharide A vaccine. *The Lancet*, 326(8447), 114–118.

Röst, G. & Vizi, Z. (2014). Backward bifurcation for pulse vaccination. *Nonlinear Analysis: Hybrid Systems*, 14, 99–113.

Rouphael, N. & Stephens, D. (2012). Neisseria meningitidis: biology, microbiology, and epidemiology. In *Neisseria meningitidis* (pp. 1–20). Springer.

Sabin, A. (1991). Measles, killer of millions in developing countries: strategy for rapid elimination and continuing control. *European journal of epidemiology*, 7(1), 1–22.

Sáez-Llorens, X. & McCracken Jr, G. (2003). Bacterial meningitis in children. *The lancet*, 361(9375), 2139–2148.

Shulgin, B., Stone, L., & Agur, Z. (1998). Pulse vaccination strategy in the SIR epidemic model. *Bulletin of mathematical biology*, 60(6), 1123–1148.

Siettos, C. I. & Russo, L. (2013). Mathematical modeling of infectious disease dynamics. *Virulence*, 4(4), 295–306.

Slater, H. C., Gambhir, M., Parham, P. E., & Michael, E. (2013). Modelling co-infection with malaria and lymphatic filariasis. *PLoS computational biology*, 9(6), e1003096.

Smith, D. L., Battle, K. E., Hay, S. I., Barker, C. M., Scott, T. W., & McKenzie, F. E. (2012). Ross, Macdonald, and a theory for the dynamics and control of mosquito-transmitted pathogens. *PLoS pathogens*, 8(4), e1002588.

Smith, R., Hogan, A., & Mercer, G. (2017). Unexpected Infection Spikes in a Model of Respiratory Syncytial Virus Vaccination. *Vaccines*, 5(2), 12.

Stone, L., Shulgin, B., & Agur, Z. (2000). Theoretical examination of the pulse vaccination policy in the SIR epidemic model. *Mathematical and computer modelling*, 31(4-5), 207–215.

Tartof, S., Cohn, A.and Tarbangdo, F. D. M., Messonnier, N., Clark, T., Kambou, J., Novak, R., Diomandé, F., Medah, I., et al. (2013). Identifying optimal vaccination strategies for serogroup A Neisseria meningitidis conjugate vaccine in the African meningitis belt. *PloS one*, 8(5), e63605.

United Nations Children's Fund (UNICEF) (2017). West Africa on alert for meningitis epidemic.
https://www.unicef.org/wcaro/english/4501_4872.html.

Van de Beek, D., de Gans, J., Tunkel, A., & Wijdicks, E. (2006). Community-acquired bacterial meningitis in adults. *New England Journal of Medicine*, 354(1), 44–53.

Voice of America (VOA) (2017). Nigeria Tackles Deadly Meningitis Outbreak Amid Vaccine Scarcity.
https://www.voanews.com/a/nigeria-tackles-deadly-meningitis-outbreak-amid-vaccine-scarcity/3806872.html.

Weston, D., Hauck, K., & Amlôt, R. (2018). Infection prevention behaviour and infectious disease modelling: a review of the literature and recommendations for the future. *BMC public health*, 18(1), 336.

Wikipedia (Assess October 15, 2019). Demographics of Nigeria. *https://en.wikipedia.org/wiki/Demographics_of_Nigeria#Population_projections*.

Williams, P. J. & Hull, H. F. (1983). Status of measles in the Gambia, 1981. *Reviews of infectious diseases*, 5(3), 391–394.

Wiratsudakul, A., Direksin, K., Phommasichan, S., Nopwinyoowong, S., Nakthong, C., Homat, T., Poltep, K., Wongwadhunyoo, W., Pamonsupornvichit, S., Ketchim, N., et al. (2016). Basic concepts and the construction of compartmental models in zoonotic disease epidemiology in Thailand. *Journal of Applied Animal Science*, 9(2), 9–18.

World Health Organization (Accessed October17, 2018a). Infectious diseases. *https://www.who.int/topics/infectiousdiseases/en/*.

World Health Organization (Accessed October17, 2018b). Meningococcal Meningitis Emergencies. *https://www.who.int/emergencies/diseases/meningitis/en/*.

World Health Organization (WHO) (2017). WHO and partners provide vaccines to control meningitis C in Nigeria.
http://www.who.int/emergencies/nigeria/meningitis-c/en/.

World Health Organization (WHO) (2018). Meningococcal Meningitis.

World Health Organization (WHO) (2019b). Meningococcal meningitis.

World Health Organization (WHO) (Accessed 2019a). Meningococcal disease in other countries:-weekly epidemiological report.
https://www.who.int/wer/2016/wer9116.pdf?ua=1.

Xu, X., Xiao, Y., & Cheke, R. (2015). Models of impulsive culling of mosquitoes to interrupt transmission of West Nile virus to birds. *Applied Mathematical Modelling*, 39(13), 3549–3568.

Zibolenová, J., Ševcovic, D., BAŠKA, T., & HUDECKOVÁ, H. (2016). Quantitative analysis of the age structured mathematical model of varicella spread in Slovakia. In *Proceedings of ALGORITMY* (pp. 285–291).

Zou, Q., Gao, S., & Zhong, Q. (2009). Pulse vaccination strategy in an epidemic model with time delays and nonlinear incidence. *Advanced Studies in Biology*, 1(7), 307–321.

Appendix A

A.1 Coefficients of polynomial (2.12)

$$
\begin{aligned}
A_7 &= \delta^5\beta^2\eta^2 EE \\
A_6 &= (-\eta\beta\delta^4(\eta\beta k_4 EE + \eta\beta k_2 EE + 2EE\sigma\beta - \delta EE\sigma - \sigma\delta + 3\eta\beta EE k_3)) \\
A_5 &= (-\delta^3(-\sigma^2\delta^2 + \delta\eta\beta k_2\sigma + \delta\eta\beta k_4\sigma + \delta\eta\beta EE\sigma\pi + \delta\eta\beta k_2 EE\sigma + \delta\eta\beta k_1\sigma \\
&\quad +\delta\eta\beta EE\sigma\nu + 2\delta\eta\beta EE\sigma k_3 + 2\delta\eta\beta\sigma k_3 + \delta\beta EE\sigma^2 + \delta\beta\sigma^2 + \delta\eta\beta k_4 EE\sigma - 3\eta^2\beta^2 k_4 EE k_3 \\
&\quad -3\eta^2\beta^2 k_3^2 EE + \eta^2\beta^2\kappa\gamma_C EE - \eta^2\beta^2 k_2 k_4 EE - 3\eta^2\beta^2 k_2 EE k_3 - 2\eta\beta^2 k_4 EE\sigma - 2\eta\beta^2 k_2 EE\sigma \\
&\quad -EE\sigma^2\beta^2 - 4\eta\beta^2 EE\sigma k_3)) \\
A_4 &= (-\delta^2(-\eta^2\beta^2\kappa\gamma_I\sigma EE + \delta\eta\beta\kappa\gamma_C\sigma - 3\eta^2\beta^2 k_3\kappa\gamma_C EE - 2\eta\beta^2\kappa\gamma_C EE\sigma \\
&\quad +\delta^2 k_4\sigma^2 + \beta^2 k_4 EE\sigma^2 + \delta^2\nu\sigma^2 - \delta\beta k_4\sigma^2 - \delta\eta\beta k_3^2\sigma - \delta\beta\sigma^2 k_3 + \delta^2\sigma^2 k_3 \\
&\quad +\delta^2 k_1\sigma^2 + \delta^2 k_2\sigma^2 - \delta\eta\beta k_4 k_1\sigma - \delta\eta\beta k_3^2 EE\sigma - \delta\eta\beta k_2 k_4 EE\sigma - \delta\eta\beta k_2 EE\sigma\nu \\
&\quad -\delta\beta k_4 EE\sigma^2 + \delta^2\sigma^2\pi + \beta^2 k_2 EE\sigma^2 + 3\eta^2\beta^2 k_3^2 k_4 EE + \beta^2 EE\sigma^2 k_3 + \eta^2\beta^2 k_3^3 EE + 4\eta\beta^2 k_2 EE\sigma k_3 \\
&\quad +3\eta^2\beta^2 k_2 k_4 EE k_3 + 3\eta^2\beta^2 k_2 k_3^2 EE + 2\eta\beta^2 k_3^2 EE\sigma + 4\eta\beta^2 k_4 EE\sigma k_3 + 2\eta\beta^2 k_2 k_4 EE\sigma + \delta\eta^2\beta^2 EE\sigma\pi \\
&\quad -2\delta\eta\beta EE\pi\sigma k_3 - \delta\beta EE\sigma^2\pi - \delta\eta\beta k_4 EE\sigma\pi - \delta\eta\beta k_2 EE\sigma\pi - \delta\beta EE\sigma^2\nu - \delta\beta k_2 EE\sigma^2 \\
&\quad -\delta\beta EE\sigma^2 k_3 - 2\delta\eta\beta k_2 EE\sigma k_3 - 2\delta\eta\beta k_1\sigma k_3 - \delta\eta\beta k_2 k_1\sigma - \delta\eta\beta k_2 k_4\sigma - \delta\eta\beta k_4 EE\sigma\nu \\
&\quad -2\delta\eta\beta k_4 EE\sigma k_3 - 2\delta\eta\beta EE\nu\sigma k_3 - 2\delta\eta\beta k_4\sigma k_3 - \delta\beta k_1\sigma^2 - \delta\beta k_2\sigma^2 - 2\delta\eta\beta k_2\sigma k_3)) \\
A_3 &= (\delta(-\delta\beta EE\sigma^2\pi k_3 + \delta\beta\kappa\gamma_C\sigma^2 + 2\delta\eta\beta k_3\kappa\gamma_C sigma + \delta\eta\beta\kappa\gamma_C k_1\sigma - 4\eta\beta^2 k_3\kappa\gamma_C EE\sigma \\
&\quad -beta^2\kappa\gamma_C EE\sigma^2 - \delta\beta k_4 EE\pi\sigma^2 - 2\eta^2\beta^2 k_3\kappa\gamma_I\sigma EE - \delta^2\eta\beta\sigma^2\pi + \delta\eta^2\beta^2 k_4 EE\sigma\pi \\
&\quad -\delta\eta\beta k_3^2 EE\sigma\pi + 2\delta\eta^2\beta^2 EE\pi\sigma k_3 + \delta^2 k_4\sigma^2\pi + \delta^2 k_1\sigma^2\pi + \delta^2 k_2\sigma^2\pi - 2\delta\eta\beta k_4 EE\pi\sigma k_3 \\
&\quad -\delta\eta\beta k_2 k_3^2 EE\sigma + \delta^2 k_1\sigma^2 k_3 + \delta^2 k_4 k_1\sigma^2 + \delta^2 k_2\sigma^2 k_3 + \delta^2 k_1\sigma^2\nu + \delta^2 k_2 k_1\sigma^2 + \delta^2 k_3\sigma^2\nu \\
&\quad +\delta^2 k_4\sigma^2\nu + \delta^2 k_4\sigma^2 k_3 + \delta^2 k_2\sigma^2\nu + \delta^2 k_2 k_4\sigma^2 - \delta^2\nu\sigma^2\omega - \delta\beta k_4 EE\sigma^2 k_3 - 2\delta\eta\beta k_4 k_1\sigma k_3 \\
&\quad -\delta\eta\beta k_3^2 k_4 EE\sigma - \delta\beta k_2 k_1\sigma^2 - \delta\beta k_4 k_1\sigma^2 - \delta\beta k_1\sigma^2 k_3 - \delta\beta k_2 k_4\sigma^2 - \delta\beta k_4\sigma^2 k_3 \\
&\quad -\delta\beta k_2\sigma^2 k_3 - 2\delta\eta\beta k_2 k_4\sigma k_3 - \delta\eta\beta k_2 k_3^2\sigma - \delta\eta\beta k_3^2 k_4\sigma - \delta\beta k_2 EE\sigma^2\nu - \delta\beta k_2 EE\sigma^2 k_3 \\
&\quad -2\delta\eta\beta k_2 k_4 EE\sigma k_3 - \delta\beta EE\sigma^2\nu k_3 - \delta\beta k_2 k_4 EE\sigma^2 - \delta\beta k_4 EE\nu\sigma^2 + \beta^2 k_2 k_4 EE\sigma^2 + \beta^2 k_2 EE\sigma^2 k_3 \\
&\quad -2\delta\eta\beta k_4 EE\nu\sigma k_3 - \delta\eta\beta k_3^2 EE\sigma\nu - \delta\eta\beta k_2 k_4 k_1\sigma - \delta\eta\beta k_3^2 k_1\sigma - \delta\eta\beta k_2 k_4 EE\sigma\nu \\
&\quad -2\delta\eta\beta k_2 EE\nu\sigma k_3 - 2\delta\eta\beta k_2 k_1\sigma k_3 + 3\eta^2\beta^2 k_2 k_3^2 k_4 EE + \eta^2\beta^2 k_2 k_3^3 EE + \beta^2 k_4 EE\sigma^2 k_3 + \eta^2\beta^2 k_3^3 k_4 EE \\
&\quad +4\eta\beta^2 k_2 k_4 EE\sigma k_3 + 2\eta\beta^2 k_3^2 k_4 EE\sigma + 2\eta\beta^2 k_2 k_3^2 EE\sigma - \delta\eta\beta k_2 k_4 EE\sigma\pi - 2\delta\eta\beta k_2 EE\pi\sigma k_3 \\
&\quad +\delta^2\sigma^2\pi k_3 + \delta\eta\beta\kappa\gamma_C EE\nu\sigma + 2\delta\eta\beta^2 EE\sigma^2\pi - 3\eta^2\beta^2 k_3^2\kappa\gamma_C EE - 2\eta\beta^2\kappa\gamma_I\sigma^2 EE \\
&\quad -\delta\beta k_2 EE\sigma^2\pi + \delta\eta\beta\kappa\gamma_I\sigma^2))
\end{aligned}
$$

$$
\begin{aligned}
A_2 &= (-k_2\delta^2\pi\sigma^2k_1 - \eta^2k_3^2\pi\sigma\delta EE\beta^2 - 2\eta k_3\pi\sigma^2\delta EE\beta^2 - 2\eta^2k_3\pi\sigma k_4EE\beta^2\delta + beta\eta\delta^2\pi\sigma^2k_1 \\
&\quad + nu\sigma^2EE\beta\eta\delta^2\pi + k_2k_3^2\delta\pi\sigma EE\beta\eta + k_2k_3\delta\pi\sigma^2EE\beta + k_2\delta k_4\pi\sigma^2EE\beta + \delta k_3^2k_4\pi\sigma EE\beta\eta \\
&\quad - delta^2k_4\pi\sigma^2k_1 + beta\eta k_3\pi\sigma^2\delta^2 - \pi\sigma^3\delta EE\beta^2 + 2k_2k_3k_4\pi\sigma EE\beta\eta\delta - k_2k_3\delta^2\pi\sigma^2 \\
&\quad - 2\eta\delta\pi\sigma^2k_4EE\beta^2 - \delta^2k_3k_4\pi\sigma^2 - delta^2k_3\pi\sigma^2k_1 - \delta^2k_4\nu\sigma^2k_1 + \delta k_3k_4\pi\sigma^2EE\beta \\
&\quad + \beta\eta\delta^2\pi\sigma^2k_4 - k_2\delta^2k_4\pi\sigma^2 - k_2k_3^3k_4\beta^2\eta^2EE - k_2k_3k_4\beta^2\sigma^2EE + 2k_2k_3k_4\beta\eta\delta k_1\sigma \\
&\quad + 2k_2k_3k_4\nu\sigma EE\beta\eta\delta - k_2k_3k_4\sigma^2\delta^2 - k_2k_3\delta^2\sigma^2k_1 - k_2k_3\delta^2\nu\sigma^2 + k_2k_3^2\delta\beta\eta k_1\sigma \\
&\quad + k_2k_3k_4\sigma^2\delta EE\beta + k_2k_3^2k_4\beta\eta\delta\sigma + k_2k_3k_4\beta\sigma^2\delta - 2k_2k_3^2k_4\beta^2\eta EE\sigma + k_2k_3\delta\beta\sigma^2k_1 \\
&\quad + k_2k_3^2\delta\nu\sigma EE\beta\eta + k_2k_3\delta\nu\sigma^2EE\beta - k_2\delta^2k_4\sigma^2k_1 - k_2\delta^2k_4\nu\sigma^2 + \delta^2k_3\omega\sigma^2\nu + k_2\delta k_4\beta\sigma^2k_1 \\
&\quad + k_2\delta k_4\nu\sigma^2EE\beta + k_2k_3^2k_4\sigma\delta EE\beta\eta - \delta^2k_3k_4\nu\sigma^2 + \delta k_3^2k_4\beta\eta k_1\sigma + \delta k_3k_4\beta\sigma^2k_1 \\
&\quad + \delta k_3^2k_4\nu\sigma EE\beta\eta + \delta k_3k_4\nu\sigma^2EE\beta - \delta^2k_3k_4\sigma^2k_1 + k_2\delta^2\omega\sigma^2\nu - k_2\delta^2\nu\sigma^2k_1 - \delta^2k_3\nu\sigma^2k_1 \\
&\quad + \delta^2k_4\omega\sigma^2\nu + \beta\pi\sigma^3\delta^2 - \beta\kappa\gamma_I\sigma^3\delta - \beta\eta\delta\kappa\gamma_I\sigma^2k_1 + \eta^2k_3^3\kappa\gamma_CEE\beta^2 \\
&\quad + 2\eta k_3^2\kappa\gamma_CEE\beta^2\sigma - \beta\eta k_3^2\kappa\gamma_C\sigma\delta - 2\nu\sigma EE\beta\eta k_3\kappa\gamma_C\delta - \nu\sigma^2EE\beta\eta\delta\kappa\gamma_I \\
&\quad + \sigma^2\kappa\gamma_Ck_3EE\beta^2 - \beta\sigma^2\kappa\gamma_Ck_3\delta - \beta\sigma^2\kappa\gamma_C\delta k_1 + \kappa\gamma_I\sigma^3EE\beta^2 - 2\beta\eta k_3\kappa\gamma_C\delta k_1\sigma \\
&\quad + \eta^2k_3^2\kappa\gamma_I\sigma EE\beta^2 + 2\eta k_3\kappa\gamma_I\sigma^2EE\beta^2 - \beta\eta k_3\kappa\gamma_I\sigma^2\delta - nu\sigma^2EE\beta\kappa\gamma_C\delta) \\
A_1 &= (\sigma(\sigma\eta\beta k_3\kappa\gamma_IEE\nu + \sigma\beta k_3\kappa\gamma_Ck_1 + \eta\beta k_3^2\kappa\gamma_CEE\nu + \eta\beta k_3^2\kappa\gamma_Ck_1 - \sigma\beta k_2k_4EE\nu k_3 \\
&\quad + \sigma k_2\delta k_4k_1k_3 + \sigma\delta k_2k_4k_1\nu - \sigma\beta k_2k_4k_1k_3 - \sigma\delta k_4\nu\omega k_3 + \sigma\delta k_2k_1\nu k_3 + \sigma\delta k_2k_4\nu k_3 \\
&\quad + \sigma\delta k_4k_1\nu k_3 - \sigma\delta k_2k_4\nu\omega - \sigma\delta k_2\nu\omega k_3 - \sigma^2\beta\delta\pi EE\nu - \sigma^2\beta\delta k_1\pi - \sigma^2\beta\delta k_4\pi \\
&\quad + \sigma^2k_4\pi EE\beta^2 - \sigma\eta\beta\delta k_4\pi k_3 - \sigma\beta k_2k_4EE\pi k_3 + 2\sigma\eta k_4EE\pi k_3\beta^2 - \sigma\eta\beta\delta k_1\pi k_3 - \sigma\eta\beta\delta k_4\pi EE\nu \\
&\quad - \sigma\eta\beta\delta k_3\pi EE\nu + \sigma\delta k_2k_4k_1\pi + \sigma\delta k_2k_1\pi k_3 + \sigma\delta k_2k_4\pi k_3 - \sigma\eta\beta\delta k_4k_1\pi - \eta\beta k_2k_3^2k_4EE\pi \\
&\quad + k_3^2k_4EE\pi\beta^2\eta^2 + \sigma^2\beta\kappa\gamma_Ik_1 + \sigma^2\beta\kappa\gamma_IEE\nu + \sigma\eta\beta k_3\kappa\gamma_Ik_1 + \sigma\beta k_3\kappa\gamma_CEE\nu + \sigma\delta k_4k_1\pi k_3 \\
&\quad - \eta\beta k_2k_3^2k_4k_1 - \eta\beta k_2k_3^2k_4EE\nu)) \\
A_0 &= -k_4\sigma^2(1-\mathcal{R}_0),
\end{aligned}
$$

where $EE = 1 - \varepsilon$.

Appendix B

B.1 Proof of Theorem 6

To apply the Centre Manifold theory, it is convenient to carry out the following change of variables. Let $S = x_1, V = x_2, C_A = x_3, I_A = x_4$, and $R_A = x_5$. Thus, $N = x_1 + x_2 + x_3 + x_4 + x_5$. Furthermore, by using the notation $X = (x_1, x_2, x_3, x_4, x_5)^T$, the Meningitis strain A-only model (3.12) can be written in the form $\frac{dX}{dt} = F(X)$, with $(f_1, f_2, f_3, f_4, f_5)^T$ as follows:

$$\begin{aligned}
\frac{dx_1}{dt} &= f_1 = \pi + \omega x_2 + k_A x_5 - \lambda_A x_1 - k_1 x_1 \\
\frac{dx_2}{dt} &= f_2 = \nu x_1 - p\lambda_A x_2 - k_2 x_2 \\
\frac{dx_3}{dt} &= f_3 = \lambda_A x_1 + p\lambda_A x_2 - k_3 x_3 \\
\frac{dx_4}{dt} &= f_4 = \sigma_A x_3 - k_4 x_4 \\
\frac{dx_5}{dt} &= f_5 = \gamma_A x_4 - k_5 x_5
\end{aligned} \tag{B.1}$$

with the associated force of infection given by:

$$\lambda_A = \frac{\beta_A(\eta x_3 + x_4)}{x_1 + x_2 + x_3 + x_4 + x_5} \tag{B.2}$$

Considering the case when $\mathcal{R}_{0A} = 1$. Suppose that β_A^* is chosen as the bifurcation parameter (obtained by solving for $\beta_A = \beta_A^*$ from $\mathcal{R}_{0A} = 1$) given below as:

$$\beta_A^* = \frac{k_3 k_4(\nu + \omega + \mu)}{(p\nu + \omega + \mu)(\eta k_4 + \sigma_A)} \tag{B.3}$$

The jacobian of the system (B.1), evaluated at disease-free $(\mathcal{E}_0) = (x_1^*, x_2^*, 0, 0, 0)$ with $\beta_A = \beta_A^*$

denoted by $\mathcal{J}(\mathcal{E}_0, \beta_A^*)$, is given by:

$$\mathcal{J}(\mathcal{E}_0, \beta_A^*) = \begin{pmatrix} -k_1 & \omega & -\frac{\beta_A^* \eta x_1^*}{x_1^*+x_2^*} & -\frac{\beta_A^* x_1^*}{x_1^*+x_2^*} & k_A \\ \nu & -k_2 & -\frac{p\beta_A^* \eta x_2^*}{x_1^*+x_2^*} & -\frac{p\beta_A^* x_2^*}{x_1^*+x_2^*} & 0 \\ 0 & 0 & \frac{\beta_A^* \eta x_1^*}{x_1^*+x_2^*} + \frac{p\beta_A^* \eta x_2^*}{x_1^*+x_2^*} - k_3 & \frac{\beta_A^* x_1^*}{x_1^*+x_2^*} + \frac{p\beta_A^* x_2^*}{x_1^*+x_2^*} & 0 \\ 0 & 0 & \sigma_A & -k_4 & 0 \\ 0 & 0 & 0 & \gamma_A & -k_5 \end{pmatrix} \tag{B.4}$$

Eigenvectors of $\mathcal{J}(\mathcal{E}_0, \beta_A^*)$

The Jacobian of (B.1), evaluated at the DFE ($\mathcal{E}_0$) with $\beta_A = \beta_A^*$ denoted by $\mathcal{J}(\mathcal{E}_0, \beta_A^*)$ has a right eigenvector (associated with the zero eigenvalue) given by $\mathbf{w} = (w_1, w_1, w_2, w_3, w_4, w_5)^T$, where;

$w_4 = \frac{\sigma_A w_3}{k_4}$, $\quad w_3 > 0$, $\quad w_5 = \frac{\gamma_A \sigma_A w_3}{k_4 k_5}$, $\quad w_1 = \left[\frac{\omega K_3 + \omega \sigma_A K_4 + k_2 k_5 K_4 \sigma_A + \kappa_A k_2 K_1 K_5 - \kappa_A k_2 \gamma_A \sigma_A}{k_4 k_5 (\omega \nu - k_1 k_2)}\right] w_3$,

$w_2 = \frac{1}{k_2}\left[\nu w_1 - \left(\frac{K_3 + \sigma_A K_4}{k_4}\right) w_3\right]$.

Similarly, the matrix $\mathcal{J}(\mathcal{E}_0, \beta_A^*)$ has a left eigenvector $\mathbf{v} = (v_1, v_1, v_2, v_3, v_4, v_5)^T$, where;

$v_1 = \frac{\nu v_2}{k_1}$, $\quad v_2 > 0$, $\quad v_5 = \frac{\nu \kappa_A v_2}{k_1 k_5}$, $\quad v_4 = -\frac{v_2(+\nu K_5 \gamma_A \kappa_A - \nu K_1 K_6 k_5 - K_3 K_6 k_1 k_5 - K_4 K_5 k_1 k_5 - \nu K_5 k_2)}{k_1 k_5 (K_6 \sigma_A - K_5 k_4)}$,

$v_3 = \frac{\sigma_A v_4 k_1 - K_1 \nu v_2 - K_3 v_2 k_1}{k_1 k_5}$.

Computation of bifurcation coefficient a and b

It can be shown, by computing the associated non-zero partial derivative of $F(X)$ (evaluated at the DFE $\mathcal{E}_0$) that

$$\begin{aligned} a &= \sum_{k,i,j=1}^{5} v_k w_i w_j \frac{\partial^2 f_k}{\partial x_i \partial x_j}(0,0), \\ &= \frac{2\beta_A^*}{(x_1^* + x_2^*)}(\eta w_3 + w_4) Q \end{aligned} \tag{B.5}$$

where;

$$Q = p(v_2 - v_3)(w_1 x_2 + w_3 x_2 + w_4 x_2 + w_5 x_2 - w_2 x_1) + (v_1 - v_3)(w_2 x_1 + w_3 x_2 + w_4 x_1 + w_5 x_1 - w_1 x_2)$$

Furthermore, it can be shown that the bifurcation coefficient b is obtained as follows

$$\begin{aligned} b &= \sum_{k,i=1}^{5} v_k w_i \frac{\partial^2 f_k}{\partial x_i \partial \beta_A^*}(0,0), \\ &= \frac{(p v_3 x_2^* + v_3 x_1^* - v_1 x_1^* - p v_2 x_2^*)(\eta w_3 + w_4)}{x_1^* + x_2^*} > 0 \end{aligned} \tag{B.6}$$

The inequality (B.6) holds if $(pv_3x_2^* + v_3x_1^*) > (v_1x_1^* + pv_2x_2^*)$. Since the coefficient b is always positive, it follows that the meningitis strain A-only (3.12) will undergo backward bifurcation if the coefficient a, given by (B.5) is positive.

B.2 Strain C-only Boundary Equilibrium ($\mathcal{E}_2$)

Here we will establish the conditions for the existence of an equilibrium for which strain C-only is endemic in the population. At the infection equilibria $\mathcal{E}_2 = (S^{**}, V^{**}, C_C^{**}, I_C^{**}, R_C^{**})$ the meningitis model (3.1) is reduced to the system of equation below,

$$\begin{aligned}
\frac{dS}{dt} &= \pi + \omega V + \kappa_C R_C - \lambda_C S - k_1 S \\
\frac{dV}{dt} &= \nu S - p\lambda_C V - k_2 V \\
\frac{dC_C}{dt} &= \lambda_C S + p\lambda_C V - k_6 C_C \\
\frac{dI_C}{dt} &= \sigma_C C_C - k_7 I_C \\
\frac{dR_C}{dt} &= \gamma_C I_C - k_8 R_C
\end{aligned} \tag{B.7}$$

where: $k_1 = \nu + \mu$, $k_2 = \omega + \mu$, $k_6 = \sigma_C + \mu$, $k_7 = \gamma_C + \mu + \delta_C$, $k_8 = \kappa_C + \mu$, $p = 1 - \varepsilon$.

The equations of the systems (B.7) are solved at steady state in term of the force of infection (λ_C^{**}), given by

$$\lambda_C^{**} = \frac{\beta_C(\eta C_C^{**} + I_C^{**})}{N^{**}} \tag{B.8}$$

Equating the right hand side of the equations in (B.7) to be zero and solving simultaneouly, we obtain the following:

$$\begin{aligned}
S^{**} &= \frac{\pi k_6 k_7 k_8 (p\lambda_C^{**} + k_2)}{k_6 k_7 k_8 (\lambda_C^{**} + k_1)(p\lambda_C^{**} + k_2) - k_6 k_7 k_8 \omega\nu - \lambda_C^{**}\kappa_C\gamma_C(p\lambda_C^{**} + k_2 + p\nu)}, \\
V^{**} &= \frac{\nu\pi k_6 k_7 k_8}{k_6 k_7 k_8 (\lambda_C^{**} + k_1)(p\lambda_C^{**} + k_2) - k_6 k_7 k_8 \omega\nu - \lambda_C^{**}\kappa_C\gamma_C(p\lambda_C^{**} + k_2 + p\nu)}, \\
C_C^{**} &= \frac{\lambda_C^{**}\pi k_7 k_8 (p\lambda_C^{**} + k_2 + p\nu)}{k_6 k_7 k_8 (\lambda_C^{**} + k_1)(p\lambda_C^{**} + k_2) - k_6 k_7 k_8 \omega\nu - \lambda_C^{**}\kappa_C\gamma_C(p\lambda_C^{**} + k_2 + p\nu)}, \\
I_C^{**} &= \frac{\lambda_C^{**}\pi\sigma_C k_8 (p\lambda_C^{**} + k_2 + p\nu)}{k_6 k_7 k_8 (\lambda_C^{**} + k_1)(p\lambda_C^{**} + k_2) - k_6 k_7 k_8 \omega\nu - \lambda_C^{**}\kappa_C\gamma_C(p\lambda_C^{**} + k_2 + p\nu)}, \\
R^{**} &= \frac{\lambda_C^{**}\pi\gamma_C\sigma_C (p\lambda_C^{**} + k_2 + p\nu)}{k_3 k_4 k_5 (\lambda_C^{**} + k_1)(p\lambda_C^{**} + k_2) - k_6 k_7 k_8 \omega\nu - \lambda_C^{**}\kappa_C\gamma_C(p\lambda_C^{**} + k_2 + p\nu)}
\end{aligned} \tag{B.9}$$

The total population is obtained by summing up the sub-population as below

$$\begin{aligned} N^{**} &= S^{**} + V^{**} + C_C^{**} + I_C^{**} + R_C^{**} \\ &= \frac{\pi k_6 k_7 k_8 (p\lambda_C^{**} + k_2 + \nu) + (\lambda_C^{**}\pi k_7 k_8 + \lambda_C^{**}\pi\sigma_C k_8 + \lambda_C^{**}\pi\gamma_C\sigma_C)(p\lambda_C^{**} + k_2 + p\nu)}{k_6 k_7 k_8(\lambda_C^{**} + k_1)(p\lambda_C^{**} + k_2) - k_6 k_7 k_8\omega\nu - \lambda_C^{**}\kappa_C\gamma_C(p\lambda_C^{**} + k_2 + p\nu)} \end{aligned} \tag{B.10}$$

Substituting equation (B.9) and (B.10) into (B.8) gives,

$$\lambda_C^{**} = \frac{\lambda_C^{**}\beta_C(\eta\pi k_7 k_8 + \pi\sigma_C k_8)(p\lambda_C^{**} + k_2 + p\nu)}{\pi k_6 k_7 k_8(p\lambda_C^{**} + k_2 + \nu) + \left(\lambda_C^{**}\pi k_7 k_8 + \lambda_C^{**}\pi\sigma_C k_8 + \lambda_C^{**}\pi\gamma_C\sigma_C\right)(p\lambda_C^{**} + k_2 + p\nu)} \tag{B.11}$$

Further simplification of (B.11) shows that the positive equilibria of the model (B.7) satisfy the following quadratic equation below (in terms of λ_C^{**})

$$a_1\lambda_C^{**2} + b_1\lambda_C^{**} + c_1 = 0 \tag{B.12}$$

where

$$\begin{aligned} a_1 &= \pi k_7 k_8 p + \pi k_8\sigma_C p + \pi\gamma_C\sigma_C p \\ b_1 &= \pi k_2 k_7 k_8 + \pi k_6 k_7 k_8 p + \pi k_7 k_8 p\nu + \pi k_2 k_8\sigma_C + \pi k_8\sigma_C p\nu + \pi\gamma_C\sigma_C k_2 \\ &\quad -\beta_C\eta\pi k_7 k_8 p - \beta_C\pi k_8\sigma_C p \\ c_1 &= \pi k_2 k_6 k_7 k_8 + \pi k_6 k_7 k_8\nu - \beta_C\eta\pi k_2 k_7 k_8 - \beta_C\eta\pi k_7 k_8 p\nu - \beta_C\pi k_2 k_8\sigma_C - \beta_C\pi k_8\sigma_C p\nu \end{aligned} \tag{B.13}$$

In order to write the expression of c_1 in form of $\mathcal{R}_{0C}$, we set $c_1 > 0$, then

$$\begin{aligned} \pi k_2 k_6 k_7 k_8 + \pi k_6 k_7 k_8\nu &> \beta_C\eta\pi k_2 k_7 k_8 + \beta_C\eta\pi k_7 k_8 p\nu + \beta_C\pi k_2 k_8\sigma_C + \beta_C\pi k_8\sigma_C p\nu \\ k_2 k_6 k_7 k_8 + k_6 k_7 k_8\nu &> \beta_C\eta k_2 k_7 k_8 + \beta_C\eta k_7 k_8 p\nu + \beta_C k_2 k_8\sigma_C + \beta_C k_8\sigma_C p\nu \end{aligned}$$

Substituting $k_2 = \omega + \mu$ results to,

$$k_6 k_7(\omega + \mu + \nu) > \beta_C(\eta k_7 + \sigma_C)(\omega + \mu + p\nu) \tag{B.14}$$

So that

$$\mathcal{R}_{0C} = \frac{\beta_C(\omega + \mu + p\nu)(\eta k_7 + \sigma_C)}{k_6 k_7(\nu + \omega + \mu)} < 1$$

Hence,

$$c_1 \equiv k_6 k_7(\nu + \omega + \mu)(1 - \mathcal{R}_{0C})$$

Thus, the positive endemic equilibria of the meningitis strain C-only model are obtained by solving the quadratic equation (B.12) and substituting the results (positive values of λ_C^{**}) into equation

(B.9). Using the quadratic formular in solving (B.12), we obtain

$$\lambda_C^{**} = \frac{-b_1 \pm \sqrt{b_1^2 - 4a_1c_1}}{2a_1} \tag{B.15}$$

where a_1, b_1, c_1 are defined as in equation (B.13) above.
The quadratic equation (B.12) above can be analyzed for the possibility of multiple endemic equilibria whenever $\mathcal{R}_{0C} < 1$. It should be noted that the coefficient a_1, of the quadratic equation (B.12) is always positive; and the constant term c_1, is negative (positive) whenever $\mathcal{R}_{0C}$ is greater (less) than unity.

B.3 Analysis of the meningitis model without co-infection (3.2)

B.3.1 Basic qualitative properties

We will explore the basic qualitative properties of the meningitis model without co-infection (3.2) in this section.

Positivity and boundedness of solutions

For the meningitis model without co-infection (3.2) to be epidemiologically meaningful, it is important to prove that all its state variables are non-negative for all time $t \geq 0$. In other words, solutions of the model system (3.2) with non-negative initial data will remain non-negative for all time $t > 0$.

Lemma 7 *Let the initial data $S(0) > 0$, $V(0) \geq 0$, $C_A(0) \geq 0$, $I_A(0) \geq 0$, $R_A(0) \geq 0$, $C_C(0) \geq 0$, $I_C(0) \geq 0$, $R_C(0) \geq 0$. Then, the solutions $(S(t), V(t), C_A(t), I_A(t), R_A(t), C_C(t), I_C(t), R_C(t))$ of the meningitis model without co-infection (3.2) are non-negative for all $t > 0$. Furthermore*

$$\lim_{t\to\infty} \sup N(t) \leq \frac{\pi}{\mu}$$

Proof. Let $t_2 = \sup\{t > 0 : S(t) > 0, V(t) > 0, C_A(t) > 0, I_A(t) > 0, R_A(t) > 0, C_C(t) > 0, I_C(t) > 0, R_C(t) > 0 \in [0, t]\}$. Thus, $t_2 > 0$. It follows from the first equation of the system (3.2), that

$$\frac{dS}{dt} = \pi + \omega V + \kappa_A R_A - (\lambda_A + \lambda_C + \nu + \mu)S \geq -(\lambda_A + \lambda_C + \nu + \mu)S$$

So that,

$$\frac{dS}{dt} + (\lambda_A + \lambda_C + \nu_A + \mu)S \geq 0$$

Multiplying by Integrating factor I.F, $exp\left\{\int_0^{t_2} [\lambda_A(\psi) + \lambda_C(\psi)]\, d\psi + (\nu + \mu)t\right\}$, gives

$$\frac{d}{dt}\left[S(t)exp\left\{\int_0^{t_2} [\lambda_A(\psi) + \lambda_C(\psi)]\, d\psi + (\nu + \mu)t\right\}\right] \geq 0 \tag{B.16}$$

Integrating both sides of inequalitiy (B.16) gives

$$S(t)exp\left\{\int_0^{t_2}\left[\lambda_A(\psi)+\lambda_C(\psi)\right]d\psi+(\nu+\mu)t\right\} \quad \geq \quad C$$

Note that for the value of C, at $t=0$ gives $S(0)$. Thus,

$$S(t) \quad \geq \quad S(0)exp\left\{-(\nu+\mu)t-\int_0^{t_2}\left[\lambda_A(\psi)+\lambda_C(\psi)\right]d\psi\right\}>0.$$

It can similarly be shown that $V(t)>0, C_A(t)>0, I_A(t)>0, R_A(t)>0, C_C(t)>0, I_C(t)>0, R_C(t)>0$ for all $t>0$.

Invariant region

Consider the biological feasible region

$$\hat{\mathcal{D}}=\{(S,V,C_A,I_A,R_A,C_C,I_C,R_C)\in\mathcal{R}_+^8; N\leq\frac{\pi}{\mu}\} \tag{B.17}$$

Lemma 8 *The region $\hat{\mathcal{D}}$ defined by* (B.17) *is positively-invariant and attracting for model* (3.2) *with non-negative initial conditions in $\mathcal{R}_+^8$.*

Proof. Let $[S(t),V(t),C_A(t),I_A(t),R_A(t),C_C(t),I_C(t),R_C(t)]\in\mathcal{R}_+^8$, be the solution of model (3.2) with non-negative initial conditions. The rate of change of the total population is obtained by adding up the compartment of the system (3.2) to give

$$\frac{dN}{dt} \quad = \quad \pi-\mu N-\delta_A I_A-\delta_c I_C\leq\pi-\mu N \tag{B.18}$$

Since, $\frac{dN}{dt}\leq\pi-\mu N$, it follows that $\frac{dN}{dt}\leq 0$ if $N(t)\geq\frac{\pi}{\mu}$.

Considering,

$$\frac{dN}{dt}+\mu N \quad = \quad \pi \tag{B.19}$$

Using the integrating factor method, so that equation (B.19) can be written as

$$d(Ne^{\mu t})=\pi e^{\mu t}dt$$

Integrating both sides by the limit $0<t$

$$\int_0^t d(Ne^{\mu t})=\int_0^t \pi e^{\mu t}dt$$

$$N(t)e^{\mu t} - N(0) = \frac{\pi}{\mu}\left[e^{\mu t}\right]_0^t$$

$$N(t)e^{\mu t} - N(0) = \frac{\pi}{\mu}\left[e^{\mu t} - 1\right]$$

Hence,

$$N(t) = N(0)e^{-\mu t} + \frac{\pi}{\mu}\left[1 - e^{-\mu t}\right].$$

In particular, $N(t) \leq \frac{\pi}{\mu}$, if $N(0) \leq \frac{\pi}{\mu}$. Thus, every solution of the model (3.2) with initial conditions in $\hat{\mathcal{D}}$ remains there for $t > 0$. Thus, $\hat{\mathcal{D}}$ is a positive-invariant. Hence, it is sufficient to consider the dynamics of the flow generated by (3.2) in $\hat{\mathcal{D}}$. In this region, the model is said to be mathematically and epidemiologically well posed (Hethcote, 2000). Thus, every solution of the meningitis model without co-infection (3.2) with initial conditions in $\hat{\mathcal{D}}$ remains in $\hat{\mathcal{D}}$ for all $t > 0$.

B.4 Stability of the DFE of the meningitis model without co-infection (3.2)

The linear stability of $\mathcal{E}_0^+$ can be established using the next generation operator method. Using the infected compartment, matrices F and V, for the transmission matrix (new infection) and the transition matrix (remaining transfer terms) are given respectively by

$$F = \begin{pmatrix} \frac{\beta_A \eta}{N^*}P^+ & \frac{\beta_A}{N^*}P^+ & 0 & 0 \\ 0 & 0 & 0 & 0 \\ 0 & 0 & \frac{\beta_C \eta}{N^*}P^+ & \frac{\beta_C}{N^*}P^+ \\ 0 & 0 & 0 & 0 \end{pmatrix} \tag{B.20}$$

and

$$V = \begin{pmatrix} k_3 & 0 & 0 & 0 \\ -\sigma_A & k_4 & 0 & 0 \\ 0 & 0 & k_6 & 0 \\ 0 & 0 & -\sigma_C & k_7 \end{pmatrix} \tag{B.21}$$

Where $k_3 = \sigma_A + \mu$, $k_4 = \gamma_A + \mu + \delta_A$, $k_6 = \sigma_C + \mu$, $k_7 = \gamma_C + \mu + \delta_C$ and $P^+ = S^+ + (1-\varepsilon)V^+$. It follows that the reproduction number of the meningitis model (3.2) is given by

$$\begin{aligned}\hat{\mathcal{R}}_0 &= \rho(FV^{-1}) \\ &= max\left\{\frac{\beta_A(\eta k_4+\sigma_A)[S^+ + (1-\varepsilon)V^+]}{k_3k_4N^+}, \qquad \frac{\beta_C(\eta k_7+\sigma_C)[S^+ + (1-\varepsilon)V^+]}{k_6k_7N^+}\right\} \quad \text{(B.22)}\end{aligned}$$

where ρ is the spectral radius (highest eigenvalue) of the matrix FV^{-1} and $N^+ = S^+ + V^+$. The above threshold quantity (basic reproduction number) is define as

$$\hat{\mathcal{R}}_0 = max\left\{\hat{\mathcal{R}}_{0A}, \quad \hat{\mathcal{R}}_{0C}\right\}$$

where $\hat{\mathcal{R}}_{0A}$ and $\hat{\mathcal{R}}_{0C}$ are the associated reproduction numbers for strain A and strain C respectively, given by

$$\hat{\mathcal{R}}_{0A} = \frac{\beta_A(\eta k_4+\sigma_A)[S^+ + (1-\varepsilon)V^+]}{k_3k_4N^+}, \qquad \hat{\mathcal{R}}_{0C} = \frac{\beta_C(\eta k_7+\sigma_C)[S^+ + (1-\varepsilon)V^+]}{k_6k_7N^+} \quad \text{(B.23)}$$